

**Middle Holocene SST record (6,200 +/- 80 to 4,760 +/- 90 yr
B.P.) based on corals from Cañada Honda, Dominican Republic**

by:

Ashlyann Arana Morales

Thesis submitted in partial fulfillment of the requirements for the degree of

MASTER OF SCIENCE

in

GEOLOGY

UNIVERSITY OF PUERTO RICO

MAYAGÜEZ CAMPUS

2018

Approved by:

Wilson R. Ramírez Martínez, Ph.D.
President of the Graduate Committee

Date

Amos Winter, Ph.D.
Member of the Graduate Committee

Date

Rafael Mendez Tejeda, Ph.D.
Member of the Graduate Committee

Date

Hernán Santos Mercado, Ph.D.
Member of the Graduate Committee

Date

Kurt A. Grove
Representative of Graduate Studies

Date

Lizzette Rodríguez Iglesias, Ph.D.
Chairperson of the Department of Geology

Date

Abstract

It is important to understand climate change in the past, present, and future. The Holocene was initially considered to have a relative stable climate, however, significant climate variations have been observed in several paleoclimate records studies. Previous studies have shown that coral proxy records can provide past archives of paleoclimate variations in the tropics. Using both Sr/Ca and $\delta^{18}\text{O}$ analysis should lead to a higher precision and resolution of the SST reconstruction. The subaerial exposure of the Cañada Honda fossil coral reef, located in the Enriquillo Valley of the Dominican Republic, provides remarkable well-preserved corals that lived in a shallow water reef environment during the Holocene. Although many coral species are present in the Cañada Honda reef, the *Orbicella sp.* corals are the main focus of this project. The U/Th dates from MZ facies range from 5152 ± 30 to 6833 ± 31 yr B.P. The average growth rate obtained for all MZ coral facies zone ranges from 4.43 ± 0.03 to 5.18 ± 0.04 mm/yr with an average value of 4.73 ± 0.03 mm/yr (n from 21 to 32 years). Based on the measurements of the corals the estimated sedimentation rate in the reef at the time of accretation was 6.29 ± 0.15 to 5.76 ± 0.15 mm/yr with an average value of 6.03 ± 0.15 mm/yr (n = 1 to 3 years). The presence of the expected aragonite XRD spectra and absence of all the possible calcite peaks in the diffractograms indicates the coral samples studied have retained the original aragonitic mineralogical composition. The Sr/Ca values obtained from coral samples range from 9.1 to 9.5 mmol/mol, similar to Holocene samples from the tropics. The $\delta^{18}\text{O}$ values obtained from the MZ *Orbicella sp.* in this study (6 kya B.P) range from -2.84 to -3.11 ‰. Having a more positive $\delta^{18}\text{O}$ from the fossil corals than modern corals is a result of the corals being exposed to a salinity environment. The Sr/Ca ratios measured in corals of the facies MZ resulted relatively higher than Sr/Ca measurements reported for modern corals but similar to Holocene samples from different locations. By measuring higher Sr/Ca ratios, the temperatures obtain were colder than anticipated.

Resumen

Es importante entender el cambio climático en el pasado, presente y futuro. Inicialmente, se consideró que el Holoceno tenía un clima relativamente estable, sin embargo, se han observado variaciones climáticas significativas en varios estudios de registros del paleoclima. Estudios previos han demostrado que los registros de coral pueden proporcionar archivos pasados de variaciones paleoclimáticas en los trópicos. El uso de análisis Sr/Ca y $\delta^{18}\text{O}$ debería resultar en una mayor precisión y resolución de la reconstrucción de SST. La exposición subaérea del arrecife de coral fósil Cañada Honda, ubicado en el Valle de Enriquillo en la República Dominicana, provee corales conservados que vivieron en un entorno de arrecifes de aguas poco profundas durante el Holoceno. Aunque muchas especies de coral están presentes en el arrecife Cañada Honda, el coral *Orbicella sp.* es el foco principal de este proyecto. Las fechas U/Th de la facie MZ varían de 5152 ± 30 a 6833 ± 31 años B.P. La tasa de crecimiento promedio obtenida para todas las zonas de facies de coral de MZ varía de 4.43 ± 0.03 a 5.18 ± 0.04 mm /yr con un valor promedio de 4.73 ± 0.03 mm /yr (n de 21 a 32 años). Basado en las medidas de los corales, la tasa de sedimentación estimada en el arrecife en el momento de la acreción fue de 6.29 ± 0.15 a 5.76 ± 0.15 mm/yr con un valor promedio de 6.03 ± 0.15 mm /yr (n = 1 a 3 años). La presencia del espectro esperado de aragonita en el XRD y la ausencia de todos los posibles picos de calcita en los difractogramas, indica que las muestras de coral estudiadas han conservado la composición mineralógica de aragonítica original. Los valores de Sr/Ca obtenidos de las muestras de coral varían de 9.1 a 9.5 mmol/mol, similar a las muestras del Holoceno de los trópicos. Los valores de $\delta^{18}\text{O}$ obtenidos en MZ con corales *Orbicella sp.* en este estudio (6 kya B.P) varían de -2.84 a -3.11 ‰. Obtener un $\delta^{18}\text{O}$ más positivo en los corales fósiles que en los corales modernos es el resultado de la exposición de los corales a un ambiente de salinidad. Las relaciones de Sr/Ca medidas en los corales de la facies MZ resultaron relativamente más altas que las medidas de Sr/Ca notificadas para los corales modernos, pero similares a las muestras del Holoceno de diferentes lugares. Al medir mayores relaciones de Sr/Ca, las temperaturas obtenidas fueron más frías de lo esperado.

Acknowledgments

I would like to take this opportunity to thank those who help in the process of completing this research and making it possible to achieve my degree. I am deeply grateful for my advisor Dr. Wilson Ramirez for his support and for always being present when I needed his help. I also would like to thank the members of my committee, Hernan Santos, Amos Winter and Rafael Mendez-Tejeda for being available and sharing their knowledge with me. I have to recognize those whose collaboration were essential for the completion of this investigation. First of all, the Servicio Geologico Nacional de la Republica Dominicana and Ministerio Educación Superior Ciencia y Tecnología for providing the permissions required for this investigation and the funding needed for the project. Additional thanks goes to Dr. Ivette Roche and her staff from San Antonio Hospital at Mayagüez, Puerto Rico for being available to help in the analysis. Also, Yelitsa Gonzalez lab technician in GASI Laboratory of the UPRM Geology Department who did part of the geochemical analysis. Dr. Ali Pourmand and his staff from Rosenstiel School of Marine and Atmosphere Science (RSMAS) in Miami since they took time from their work to analyze part of my samples. Plus, the technician Jose R. Almodovar from the UPRM Biological Department who was available and help complete a part of the research. It is crucial to mention the staff of the Department of Geology, Catherine Perez and Marsha Irizarry for always helping in any way that they could. I continue by saying thank you to my colleagues from the Geology Department in UPRM especially Yesenia Herrera, Victor Flores, Maria Figueroa.

Table of Contents

Abstract.....	ii
Resumen.....	iii
Acknowledgments.....	iv
Table of Contents.....	v
List of Tables.....	vii
List of Figures.....	viii
List of appendixes.....	ix
1. Introduction.....	1
2. Previous Work.....	6
2.1 Paleoclimate.....	6
2.2 Corals as proxies.....	7
3. Study Area.....	14
3.1 Location.....	14
3.2 Geological background.....	16
4. Methodology.....	19
4.1 General description of the methodology.....	19
4.2 Field Work.....	19
4.3 Mineralogical Analysis.....	24
4.3.1 XRD analysis.....	24
4.3.2 SEM.....	26
4.4 Growth Rates Measurements.....	26
4.4.1 X-Ray Radiographs.....	26
4.4.2 Coral-XDS software.....	26
4.5 Sedimentation rate estimates.....	27
4.6 Age of the Coral Skeleton.....	29
4.6.1 Radiogenic Dating.....	29
4.7 Paleoenvironmental Measurements.....	29
4.7.1 Microsampling.....	29
4.7.2 Trace Element Analysis.....	30
4.7.3 Stable Isotope Analysis.....	31
5. Results.....	33
5.1 Skeletal Average Growth rate.....	33
5.2 Skeletal Composition.....	36
5.2.1 XRD.....	36
5.2.2 Scanning Electron Microscope (SEM) Analysis.....	38
5.3 Growth Rate Estimates.....	39
5.4 Sedimentation Rate estimates.....	40
5.5 U/Th Radiogenic Dating.....	41
5.6 Paleoenvironmental Measurements.....	43
5.6.1 Sr/Ca Elemental Analysis.....	43
5.6.2 Stable Isotope Analysis.....	46
6. Discussion.....	49
6.1 Mineralogy Analysis.....	49
6.2 Growth Rate Measurements.....	50
6.3 Sedimentation Rate.....	53

6.4 Age of the Coral.....	55
6.5 Paleoenvironmental Parameters.....	56
6.5.1 Element analysis.....	56
6.5.2 Stable Isotope Analysis.....	57
6.5.3 SST from Sr/Ca.....	59
6.5.4 SST from Stable Isotopes.....	63
7. Conclusion	67
Reference.....	71
Appendix.....	78

List of Tables

Table 1: Average growth rate measurements for the coral samples selected.....	39
Table 2: Estimated sedimentation rate calculations for the coral samples selected.....	40
Table 3: Estimated sedimentation rate calculations for the coral samples selected using equation 3 to compare to modern corals.....	40
Table 4: Summary of U/Th dates analysis for samples selected.....	41
Table 5: Summary of Sr/Ca ratio calculations for samples selected.....	43
Table 6: Summary of $\delta^{18}\text{O}$ and $\delta^{13}\text{C}$ calculations for samples selected.....	46

List of Figures

Figure 1: Location of Cañada Honda in Dominican Republic.....	5
Figure 2: <i>Serpulid worm</i> mounds along the northern margin of the Enriquillo Lake Valley.....	10
Figure 3: Proxy relationships.....	11
Figure 4: Stratigraphic measurements (stratigraphic columns) along the Cañada Honda Reef exposure used to create a facies map of the reef.....	12
Figure 5: Cañada Honda Reef exposures facies map.....	13
Figure 6: Holocene sea level curve for the Caribbean.....	17
Figure 7: The majority of the corals are in growth position.....	18
Figure 8: Shape of the coral changes with the increasing of sedimentation.....	18
Figure 9: Cañada Honda Reef exposure facies map with the locations of the coral samples processed for this study.....	21
Figure 10: Example of the samples labeling and sample documentation.....	22
Figure 11: Cutting the sides of the coral.....	22
Figure 12: Cutting the coral heads.....	23
Figure 13: Example of a highly bioeroded coral skeleton sample.....	23
Figure 14: Example of powder diffraction spectra produced by an aragonitic sample. Courtesy of the University of Arizona Mineral Museum.....	25
Figure 15: Example of a foliated morphology from a coral in Cañada Honda.....	28
Figure 16: Annual extension rate (luminosity) analysis of coral samples.....	34-35
Figure 17: XRD analysis.....	37
Figure 18: SEM images of coral samples.....	38
Figure 19: Cañada Honda reef facies map with location and U/Th ages of each coral.....	42
Figure 20: Sr/Ca and $\delta^{18}\text{O}$ values vs. track length of coral sample.....	45
Figure 21a: $\delta^{18}\text{O}$ and $\delta^{13}\text{C}$ record for sample MZ 165.9-0.3.....	48
Figure 21b: $\delta^{18}\text{O}$ and $\delta^{13}\text{C}$ values for coral sample MZ 148.8-3.3.....	48
Figure 22: Growth Rate vs. Stratigraphic Height for coral samples.....	51
Figure 23: Growth Rate vs. Age for coral samples.....	52
Figure 24: Growth Rate data for all Cañada Honda facies.....	52
Figure 25: Sedimentation Rate vs. Stratigraphic Height for coral samples.....	54
Figure 26: Sedimentation Rate compared to other studies.....	54
Figure 27: Age and Stratigraphic Height vs. Distance for coral samples.....	55
Figure 28: Sr/Ca-SST for coral samples.....	61
Figure 29: Sr/Ca/SST from this study compared to previous studies.....	62
Figure 30: SST-Anomaly.....	62
Figure 31: SST obtained from $\delta^{18}\text{O}$	65
Figure 32: $\delta^{18}\text{O}$ -SST compared to other studies.....	66
Figure 33: Mean seawater $\delta^{18}\text{O}$	66

Appendix

Appendix 1: Selected transect and densitometry analysis of sample MZ 148.8-3.3 part a.....	78
Appendix 2: Selected transect and densitometry analysis of sample MZ 148.8-3.3 part b.....	79
Appendix 3: Selected transect and densitometry analysis of sample MZ 148.8-3.3 part c.....	80
Appendix 4: Selected transect and densitometry analysis of sample MZ 165.9-0.3.....	81
Appendix 5: Selected transect and densitometry analysis of sample MZ 154.7-2.3.....	82
Appendix 6: Selected transect and densitometry analysis of sample MZ 198.4-0.9.....	83
Appendix 7: Selected transect and densitometry analysis of sample MZ 118.6-2.1.....	84
Appendix 8: Selected transect and densitometry analysis of sample MZ 164.1-1.2.....	85
Appendix 9: Selected transect and densitometry analysis of sample MZ 202.4-2.7.....	86
Appendix 10: XRD analysis for sample MZ 148.8-3.3.....	87
Appendix 11: XRD analysis for sample MZ 165.9-0.3.....	88
Appendix 12: XRD analysis for sample MZ 154.7-2.3.....	89
Appendix 13: XRD analysis for sample MZ 198.4-0.9.....	90
Appendix 14: XRD analysis for sample MZ 118.6-2.1.....	91
Appendix 15: XRD analysis for sample MZ 164.1-1.2.....	92
Appendix 16: XRD analysis for sample MZ 202.4-2.7.....	93
Appendix 17: SEM analysis for sample MZ 148.8-3.3.....	94
Appendix 18: SEM analysis for sample MZ 165.9-0.3.....	94
Appendix 19: SEM analysis for sample MZ 154.7-2.3.....	95
Appendix 20: SEM analysis for sample MZ 198.4-0.9.....	95
Appendix 21: SEM analysis for sample MZ 118.6-2.1.....	96
Appendix 22: SEM analysis for sample MZ 164.1-1.2.....	96
Appendix 23: SEM analysis for sample MZ 202.4-2.7.....	97
Appendix 24: $\delta^{18}\text{O}$ and $\delta^{13}\text{C}$ plot for MZ 154.7-2.3.....	98
Appendix 25: $\delta^{18}\text{O}$ and $\delta^{13}\text{C}$ plot for MZ 198.4-0.9.....	99
Appendix 26: $\delta^{18}\text{O}$ and $\delta^{13}\text{C}$ plot for MZ 118.6-2.1.....	100
Appendix 27: $\delta^{18}\text{O}$ and $\delta^{13}\text{C}$ plot for MZ 202.4-2.7.....	101
Appendix 28: $\delta^{18}\text{O}$ and $\delta^{13}\text{C}$ plot for MZ 164.1-1.2.....	102
Appendix 29: Table for Sr/cr-SST equations for MZ 165.9-0.3.....	103
Appendix 30: Table for Sr/Ca-SST equations for MZ 148.8-3.3.....	103
Appendix 31: Table for residual variations for coral samples.....	104

1. Introduction

It is important to understand climate change in the past, present, and future. Chollet et al., (2012) indicated that global sea surface temperatures (SSTs) during the past 150 years have increased at an average of $0.04^{\circ}\text{C decade}^{-1}$. The Holocene was initially considered to have a relative stable climate (Goudeau et al., 2015), however, significant climate variations have been observed in several paleoclimate records studies (Lane et al., 2009). These climate variations have been more frequent and significant than previously recognized (Mayewski et al., 2004) and the changes seem to have occurred rapidly (centuries or decades) involving regional-scale changes in mean annual temperatures (Maslin et al., 2010). Studies have shown abrupt climate variations of tropical acidity, polar cooling and major atmospheric oscillations (Greer and Swart, 2006).

To document changes in SST during the Holocene, fossil corals are a very useful proxies, providing access to study past climates (Kilpatrick et al., 2015, Werner et al., 2015; Grottoli, 2001). Paleoclimate records derived from corals are studied based on three timescales: seasonal, interannual to decadal and long-term trends. The opportunity to compare these three time scales of past and present climate is attainable by using large corals that have records covering several decades to centuries. One of the limitations of this method is the high alteration potential of scleractinean coral skeletons that leads to uncertainties in the climate reconstructions (Sayani et al., 2011). This diagenesis occurs in the marine environment and also when corals are no longer in seawater. The original mineralogy of the corals is aragonitic, but this composition tends to be altered easily. The reason for this is that aragonite tends to be metastable in marine environments (Hendy et al., 2007). The alterations that occur as a result of diagenesis are the dissolution of primary coral aragonite, recrystallization of coral aragonite to calcite and infilling of skeletal porespace with secondary cements (Sayani et al., 2011). As a consequence of diagenesis, finding

pristine fossil corals can be quite challenging, even if they are a few thousand years old. A common problem with the method is the precipitation of secondary aragonite on the coral skeleton. When secondary aragonite is present, the geochemistry of the coralline matrix changes by removal or exchange of isotopes and trace elements of the coral (McGregor and Gagan, 2002). These can cause problems with the temperature products (Sayani et al., 2011; Müller et al., 200).

The subaerial exposure of the Cañada Honda fossil coral reef, located in the Enriquillo Valley of the Dominican Republic, provides remarkable well-preserved corals that lived in a shallow water reef environment during the Holocene (Fig. 1)(Cuevas et al., 2005). The relatively dry climate present in the area after the reef was exposed and the documented high sedimentation environment that produced a fast burial of these reefs during their accretion and after exposure resulted in an excellent preservation of the original aragonitic skeletal mineralogy of these fossil corals. The high sedimentation environment, produced by the high relief along the northern and southern boundaries of the embayment, documented by Cuevas et al (2005), is an important factor for the preservation of the corals. The original aragonitic composition of the coral skeletal carbonate at this location has been found to be pristine in most cases and has provided valuable information concerning the environment in which the corals grew (Morales, 2015; Greer and Swart, 2006).

A high-resolution archive of past climate is present in the geochemistry of the skeleton of the scleractinian coral (Brachert et al., 2006). Significant marine environment parameters during coral growth are reflected in the $\delta^{13}\text{C}$ and $\delta^{18}\text{O}$ isotopic values as well as trace elemental ratios (Greer and Swart, 2006). This project measured the $\delta^{18}\text{O}$ (oxygen isotopic values) and Sr/Ca (trace elemental concentrations) and integrated them into the chronology of the coral skeletons that is based on growth bands (X-ray images) and coral dating (U/Th). With this information, sea surface

temperature (SST) values and sea surface salinity (SSS) values were approximated. In addition, climate variability over a semi-continuous time interval of about one thousand years was addressed. Oxygen isotopic values ($\delta^{18}\text{O}$) in coral skeletons are affected by SST and SSS. In environments with absent or small salinity variations $\delta^{18}\text{O}$ values primarily reflect changes in SST (Grottoli, 2001). However, in environments with salinity variations, as the paleo-Enriquillo Bay was, $\delta^{18}\text{O}$ values will be affected by both SST and SSS parameters. The Cañada Honda reef exposure was located in a large embayment with high relief along the northern and southern margins. The lithology of the Sierra de Neiba and Sierra de Bahoruco mountain ranges is composed of porous limestone rocks of Oligocene and Miocene age (Mann et al., 1999). Today, due to the endorheic conditions of the basin, the salinity of the Enriquillo Lake has varied significantly during the past decades as documented by Rosado et al. (2016) and Delanoy and Mendez-Tejeda (2017). Since similar conditions are expected to have occurred during the Holocene in the area, the $\delta^{18}\text{O}$ values from the coral skeletons are probably influenced by salinity variations as well as large temperature variations.

Sr/Ca values in corals seem to be at equilibrium with the surrounding marine environment and seawater as the aragonitic coral grows (Grottoli, 2001). Temperature tracers require elemental concentrations in seawater to be stable through time (Corrège, 2006; Yu et al., 2005). Within the crystal structure, calcium ion (Ca^{+2}) can be substituted by various divalent trace ions such as magnesium (Mg^{+2}) and strontium (Sr^{+2}) present in marine water, preserving the chemical identity of the environment in the skeleton. Improved documentation of paleotemperatures has been possible by measuring Sr/Ca ratios in the coral skeleton since previous studies have found an inverse relationship with water temperatures and Sr with a precision better than 0.1% (Swart et al., 2002). Sr/Ca values are not influenced by changes in salinity (Smith, 2006) and thus are better at

recording SST than $\delta^{18}\text{O}$ (Swart et al., 2002). Sr/Ca is more stable in seawater than $\delta^{18}\text{O}$, which is influenced by precipitation/evaporation ratio (Corrège, 2006). The rate of SST variations during the last six thousand years produced by the corals Sr/Ca-T were compared to modern SST variations as an effort to assess the impact caused by natural causes and/or human influences in climate changes (Greer, 2001).

It is assumed that the incorporation of Sr/Ca into coral aragonite is the primary control on SST when using the coral Sr/Ca thermometer (Cohen et al., 2001). However, there are several factors that can challenge this assumption; 1) it is impossible to calculate absolute temperatures from fossil corals using modern calibration equations because there is considerable variation in the values obtained for Sr/Ca-SST calibration equations derived from different colonies of the same species, 2) slower growing coral colonies have higher Sr/Ca than faster growing corals of the same species at the same site (Cohen et al., 2001). These findings suggest that Sr/Ca ratios in corals are not only control by SST. Kinetic process linked to coral growth rates seem to affect the co-precipitation of strontium with aragonite during skeletogenesis (Cohen et al., 2001).

This research also studied the record of growth (sclerochronology) preserved in the high-low density bands present in the fossil coral skeletons. The thickness of growth bands in the coral skeleton was measured by image analysis to assess if changes in relative thickness of growth bands reveal climatic cycles, such as decadal cycles from sunspot activity of a constant 11-year cyclicity (Haigh, 2011). Changes in climate can be caused by sunspot cycles but the effects and magnitudes of these cycles are still unclear. The results acquired in this project may help improved our understanding of these cycles and the SST variations during the Early Holocene in the Caribbean.

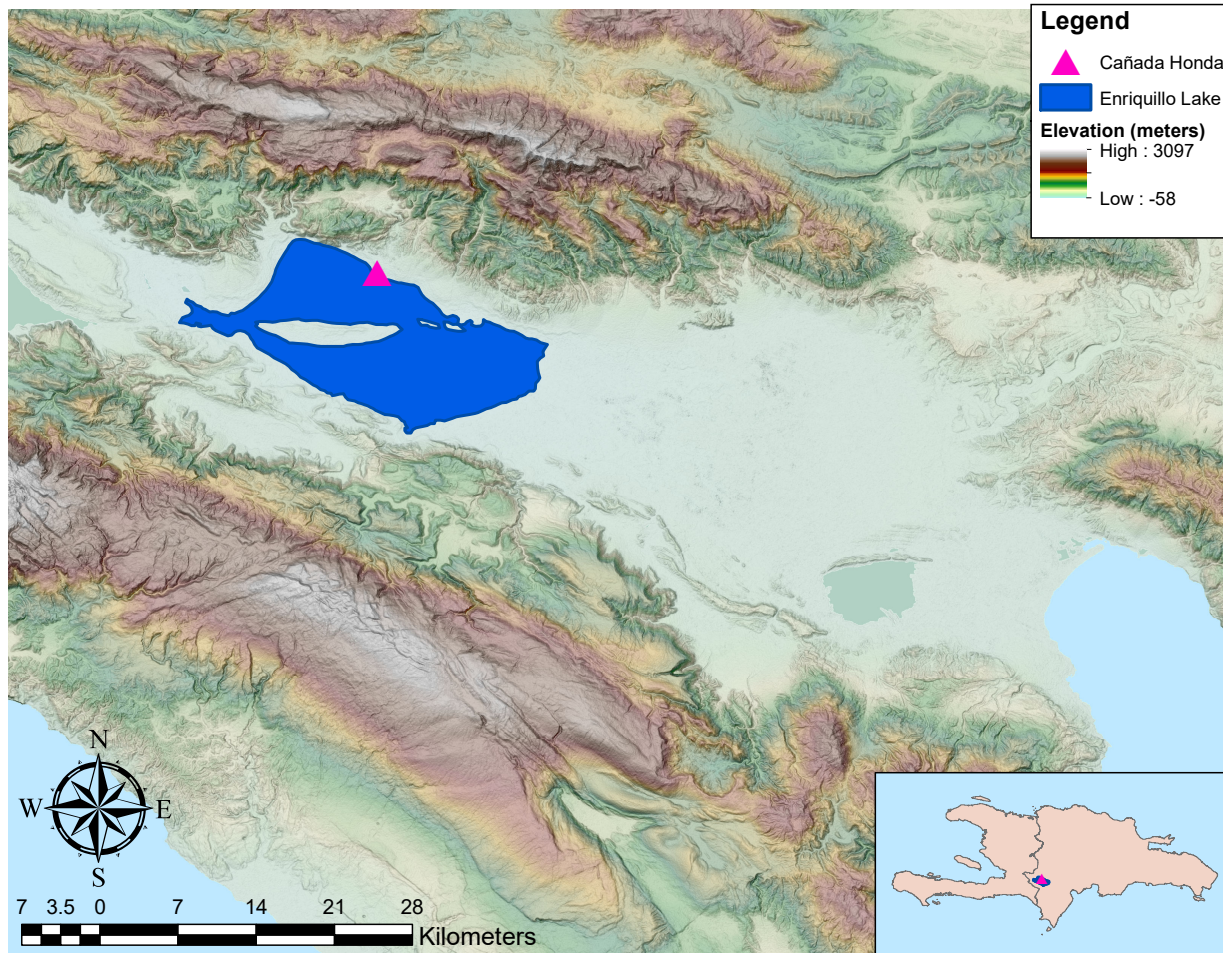


Figure 1: A) Location of Cañada Honda in Dominican Republic represented by the triangle
 B) Closer view of the Enriquillo Lake.

2. Previous work

2.1 Paleoclimate

The Holocene epoch represents an interglacial period that has experienced considerable changes in climate variations (Wanner et al., 2008). Possible forcing factors (Wanner et al., 2008) for the multi-century climate variations are changes in solar variability (Denton and Karlén, 1973), volcanic activity (Bryson and Goodman, 1980), orbital variations, land cover and greenhouse gases. To explain Holocene climate changes, Wanner et al. (2008) use selected proxy reconstructions of different climate variables from models such as general circulation models (GCMs) and earth system models of intermediate complexity (EMICs). Other studies have used ocean cores to provide information about the last glacial maximum as well as terrestrial pollen, lake levels and macrofossil data to characterize millennial-scale climate changes (Wanner et al., 2008).

El Niño Southern oscillation (ENSO) and the North Atlantic Oscillation (NAO) represent major modes of climate variability that could influence SST at a interannual timescales (Wanner et al., 2008; Giannini et al., 2001; Birgmark, 2014). ENSO affects the equatorial Pacific SST and atmospheric pressure (Birgmark, 2014). NAO affects the atmospheric pressure between the Icelandic low pressure and Azores high pressure. A positive phase of the NAO indicates a large pressure difference between Icelandic low and Azores high. Previous studies (Birgmark, 2014) have concluded that the combined effects of ENSO and NAO in the Caribbean are factors responsible for climate variability. Variations in SST can affect rainfall and the development of tropical storms (Birgmark, 2014). Studies done using on coral Sr/Ca records reveal that insolation changes on orbital timescales affect the Atlantic SST seasonality (Giry et al., 2012). Warm tropical Atlantic SST may be caused by a warm ENSO event and a negative phase of the NAO. The

strength of the trade winds in the Caribbean is affected by ENSO and NAO that influence the SST because of cooling due to evaporation. Nevertheless, the strength of ENSO and NAO is affected by locally driven phenomena such as seasonal changes and upwelling and advection making it hard to assess (Birgmark, 2014).

Major climate events have been reported globally during the Holocene. A event that created climate variations during the Holocene was the “5.2 ka event”. Paleoclimate records have recorded variations in both hemisphere between 5.6 to 5 ka (Roland et al., 2015). Previous studies have examined records that gave ages defining the onset of the event, resulting in an average of 5.23 ka, making this event known as the “5.2 ka event” (Magny et al., 2006). Wetter conditions were reported in the northern Europe and southern South America, while widespread cooling was accompanied by drier conditions in part of North America, central and eastern Asia, Africa and the Mediterranean (Roland et al., 2015). The reduction of solar activity, based on a modelling study, was a major driver of the 5.2 ka event through an expansion of sea ice that lead to cooling across the wider North Atlantic region (Renssen et al., 2006). The end of the early to mid-Holocene humid period in the lower latitude was mark by a long-term trend of increasing rainfall variability and aridification in tropical Africa, however some areas (e.g. Caribbean) become wetter (Mayewski et al., 2004).

2.2 Corals as proxies

Previous studies have shown that coral proxy records can provide past archives of paleoclimate variations in the tropics (Grottoli, 2001). Grottoli (2001) suggested that using both Sr/Ca and $\delta^{18}\text{O}$ analysis should lead to a higher precision and resolution of the SST reconstruction. Studies focused on trace elements have concluded that the most reliable proxy for paleotemperature is Sr/Ca since Mg/Ca and U/Ca are influenced by factors other than temperature

(Swart and Grottoli, 2003). Studies done by Swart et al. (2002), established a relationship between SST and Sr/Ca in the scleractinian coral *Orbicella annularis* (previously known as *Montastraea sp.* (Budd et al., 2012)). Their results showed an excellent correlation between temperature and Sr/Ca (Fig. 3).

The fossil coral skeletons that will be used in this project were collected from the Cañada Honda fossil reef exposure present along the northern flank of the Enriquillo Lake Valley. The Cañada Honda reef exposure was studied in detail by Hubbard et al. (2004) and was divided into several reef facies based on the coral species present, and their abundance (Fig. 4). These facies as named by Hubbard et al. (2004) are (Fig. 5); Massive Corals Facies 1 (M1), Massive Corals Facies 2 (M2), Mixing Zone Facies (MZ), and Massive Corals Facies 3 (M3). The M1 facies was described as the basal coral unit of the reef with abundant massive corals present including *Siderastrea sp.* and *Orbicella* Complex (Hubbard et al., 2004). The M2 facies was described with the similar characteristics as the M1 facies but the two facies, located at the base of the reef, are separated by a coral rubble deposit. This coral rubble layer is composed of abundant broken pieces of *Madracis sp.* corals with a matrix of calcareous mud and was interpreted as a storm deposit by Hubbard et al. (2004). A *Madracis sp.* corals fragment from this layer was dated (U/Th dating) providing an age of 9000 (+/- 200) ybp (Hubbard et al., 2004). The layer above the M2 facies, named the MZ facies, seem to have been deposited during a time of favorable environmental conditions, according to Hubbard et al. (2004). This is evidenced by the presence of several species of branching corals mixed with massive corals (Hubbard et al., 2004). Above the MZ facies, the M3 facies exhibits abundant massive corals (*Orbicella faveolata*, *Orbicella franksii*, *Montastraea cavernosa* and *Siderastrea sp.*) of considerable size and highly foliated morphology. At the northernmost part of the reef, probably close to the paleo-shore and above the M3 facies,

an ~11 meter thick unit with facies of *Acropora cervicornis* is present (Hubbard et al., 2004; Greer et al., 2009). At the top of the whole reef sequence *Serpulid worm* mounds (Greer and Swart, 2006) are present and they can be traced at this same stratigraphic level along many locations along the northern margin of the Enriquillo Lake Valley (Fig. 2). The *Serpulids* mounds features lined the embayment and lived in shallow brackish waters according to Greer and Swart (2006). They are a useful indicator of modern sea level since their elevation is within one meter of modern sea level (Greer and Swart, 2006)..

Another study that used coral skeletons from the Cañada Honda Reef location as climate proxies is by Greer and Swart (2006). They measured oxygen and carbon isotopes ($\delta^{18}\text{O}$ and $\delta^{13}\text{C}$) from the coral skeletons to document decadal-scale fluctuations in regional precipitation. They proposed that changes in salinity created by local precipitation events were the primary variable affecting the decadal oscillations observed in $\delta^{18}\text{O}$ and $\delta^{13}\text{C}$ measurements. Furthermore, they proposed that Sr/Ca from the coral skeletons would be an ideal proxy to document temperature variations in the area since Sr/Ca is not affected by the significant changes in salinity that probably occurred in the paleo-Enriquillo Bay.



Figure 2: *Serpulid worm* mounds along the northern margin of the Enriquillo Lake Valley. (Photo by: W. Ramírez, 2004).

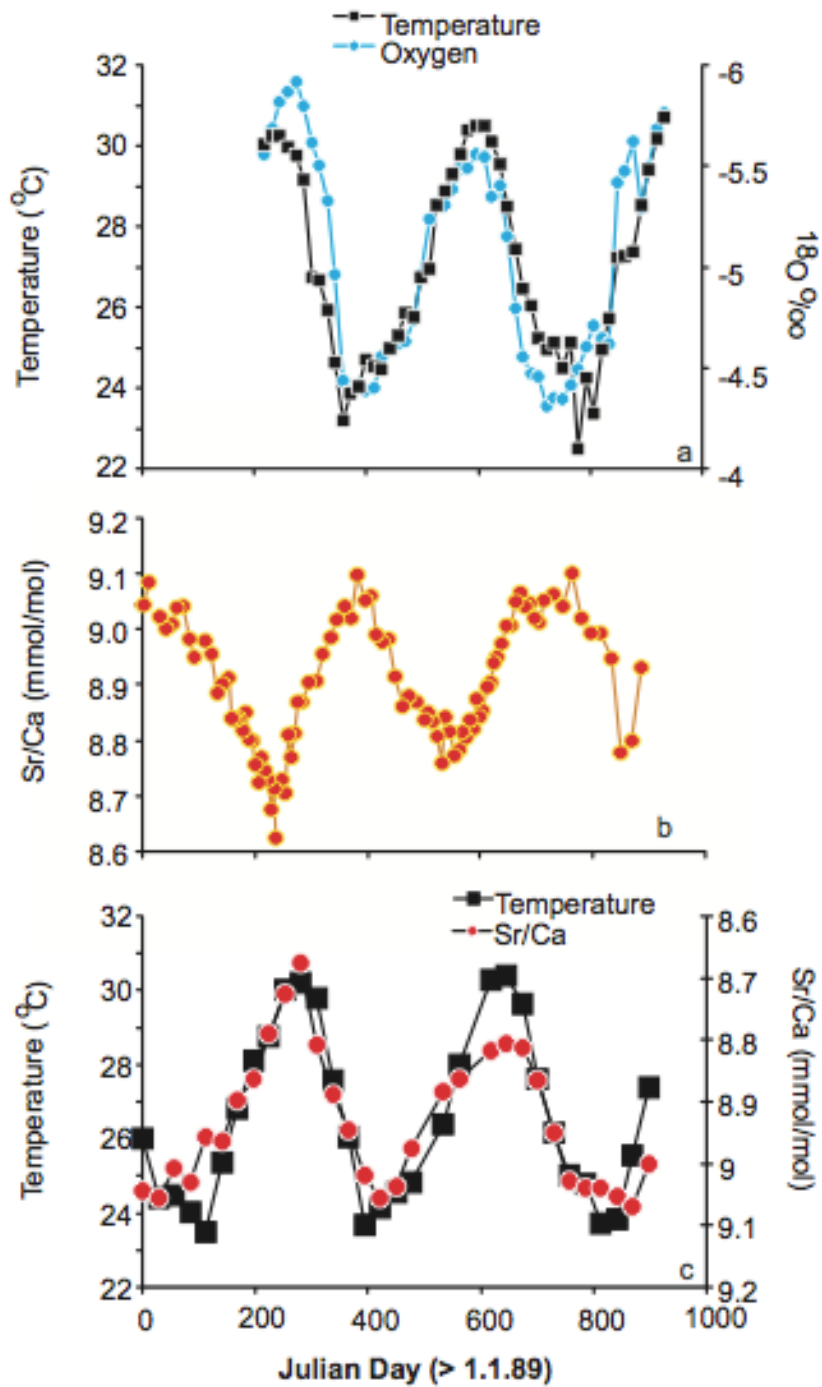


Figure 3: Proxy relationships: a) correlation between $\delta^{18}O$ and SST through Julian day since 1.1.89 b) Sr/Ca ratio as a function of time c) correlation between Sr/Ca ratio through time and SST. (Swart, 2002)

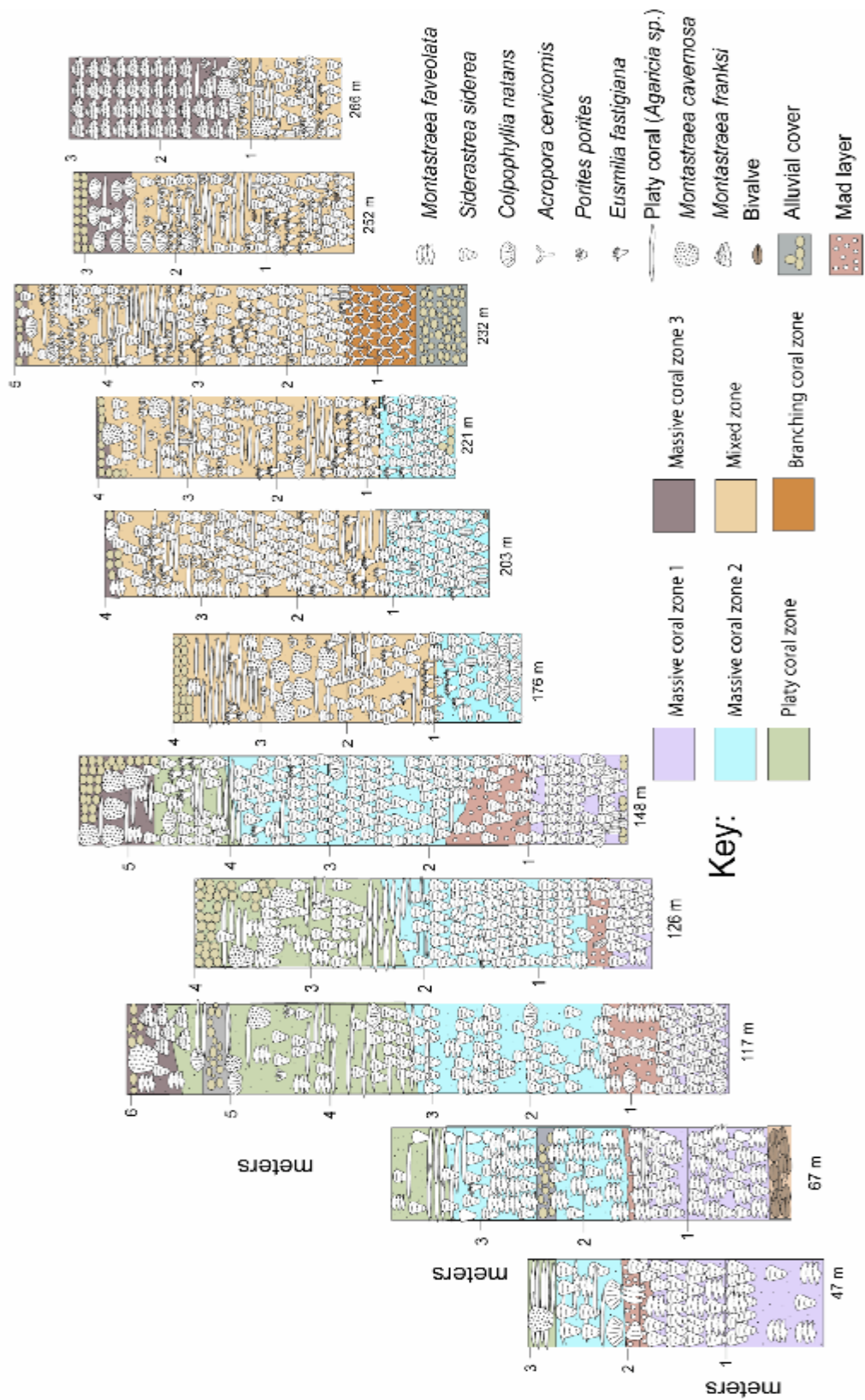


Figure 4: Stratigraphic measurements (stratigraphic columns) along the Cañada Honda Reef exposure used to create a facies map of the reef. (Cuevas et al., 2005)

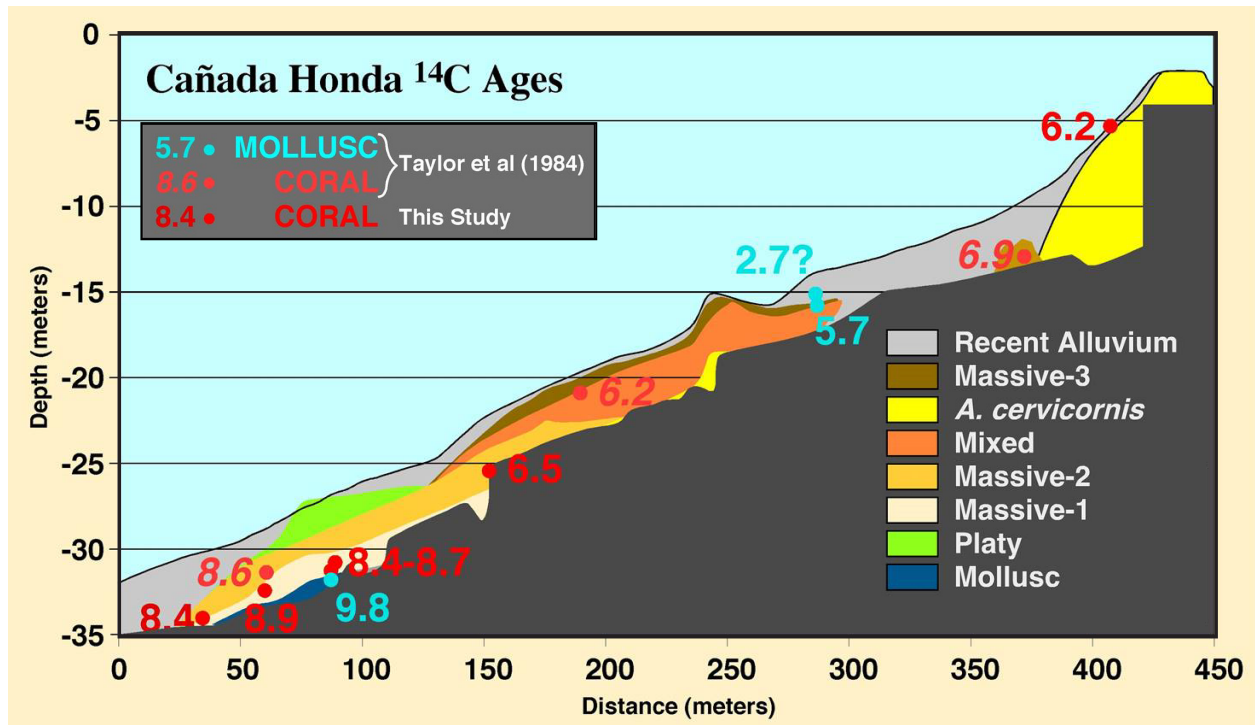


Figure 5: Cañada Honda Reef exposures facies map including ¹⁴C ages of corals located in each one of the proposed facies. Modified from Hubbard (2004).

3. Study Area

3.1 Location

This investigation was conducted in the Cañada Honda Reef exposure located along the northern flank of the Enriquillo Valley, in the western part of the Dominican Republic. The Enriquillo Valley consist of a fault bounded, east-west trending feature that resulted from a subsidence following north-south compression in which the Sierra de Neiba to the North and the Sierra de Bahoruco to the South were overthrust against the valley (Mann et al., 1984). Around 10 kyr BP a rapid sea level rise occurred flooding the valley and created a large bay open to the Caribbean Sea. The flooding occurred over previous transgressive deposits resulting in a shallowing upward sequence that was formed as rising sea level slowed (Fig. 6). Fluvial deposits from Yaque del Sur River together with minimal vertical uplift caused by left-lateral movement that occurred from 5.0 to about 4.0 kyr BP, isolated the previously large open bay until it was completely separated from the Caribbean Sea creating the Enriquillo Lake and Valley (Mann et al., 1984). Today the Enriquillo Lake covers the center of the valley and is the largest saltwater lake in the Caribbean area (Greer and Swart, 2006). Although the Holocene fossil reef upper surface is covered by alluvium material along most of its extension around the lake, gullies and ravines cut by sheet flow and arroyos flowing into the lake have created spectacular reef exposures (Mann et al., 1984; Cuevas et al., 2005).

Exposed Holocene reefs preserved above sea level with aragonitic corals in pristine conditions are very difficult to find and few if any examples of remarkable coral preservation have been reported in the Caribbean (Hubbard et al., 2004), with the exception of the Cañada Honda Reef exposure. Hence, acquiring paleoclimate information from Pleistocene fossil corals is difficult since most of the corals of that age available have been altered by diagenesis (Cuevas et

al., 2005). The Cañada Honda fossil reef exposure provides an exceptional opportunity to obtain detailed paleoclimate information due to the excellent coral skeleton preservation in its corals (Morales, 2015)(Fig. 7). Radiocarbon ages from fossil corals sampled at various stratigraphic levels established the reef age between ~9,000 to ~5,000 ybp. (Cuevas, 2010). Another important feature present in the Cañada Honda Holocene fossil coral reef is that most of the corals along the reef exposure are in growth position. Hubbard et al. (2004), Cuevas et al. (2005), Greer et al. (2009) and Cuevas (2010), all documented high percentages of corals in growth position that reached up to 63% in some cases (measured transects stratigraphic columns) by Cuevas (2010) along the wall of the reef exposure using a one-meter square quadrangles). Only *Orbicella sp.* corals were analyzed in this study and only samples oriented in growth position along the reef framework were sampled. *Siderastrea sp.* and *Orbicella sp.* are the most abundant corals in the reef (Cuevas et al., 2005). Although many coral species are present in the Cañada Honda reef, the *Orbicella sp.* corals are the main focus of this project since many investigations have used the skeletons of this species for paleoclimates studies producing Sr/Ca-SST and there are many calibration equations, from many locations, available to calculate and compared the SST values obtained (Leder et al., (1996); Swart et al., 2002).

Abundant *Acropora cervicornis* corals are present associated with the paleo-Enriquillo Bay shoreline instead of the expected *Acropora palmata*. Hubbard et al. (2004) proposed that this replacement of *Acropora cervicornis* for *Acropora palmata* is the result of an environment of high sedimentation (high relief) and low wave regime (large embayment) present in the paleo-Enriquillo Bay. Columnar foliated and cone shape corals were the most common morphologies surveyed along the reef (Fig. 8). Hubbard et al. (2008) proposed that these morphologies are the result of the corals adapting to the high sediment influx rate. According to Hubbard et al. (2008)

different coral species react in different ways depending on their tolerance to sedimentation. *Siderastrea sp.* tends to growth in a more conical shape since is a more sediment tolerant coral, while *Orbicella sp.* grows in a columnar shape.

3.2 Geologic Background

During the late Eocene, under-thrusting and accretion took place against the Hispaniola (Heubeck and Mann, 1991). Deep-water sediments were exposed during the formation of the Peralta Belt, which is now deposited in the Southern Hispaniola. Oblique movement of the Oceanic plate during the early Miocene caused transpressional uplift and thrusting of the Peralta Belt. Evidence of the tectonic events that occurred during the Miocene are recorded in the geologic structures of the region that created many of the geomorphic features present today in Southern Hispaniola.

Southern Hispaniola is dominated by synclinal valleys and young anticlinal mountains. Active transpression is reflected in this geomorphology that affects the Hispaniola segment of the North America-Caribbean plate boundary zone (Mann et al., 2008). The structure of Southern Hispaniola is dominated by intervening mountain ranges and topographically lows that represent fault-bounded Neogene basins (Mann and Lawrence, 1991). During the Late Pliocene, Sierra de Bahoruco and Sierra de Neiba steep mountain ranges were surrounded by undergoing thrusting and ramping in the area (Mann, 1999). After the last interglacial period flooding formed a gulf called Enriquillo Bay (Mann et al., 1999). According to Mann et al., (1995), active tectonism has not substantially affect the Enriquillo Basin during the Holocene. Based on these assumptions, reconstructions of the reef paleodepth and the interpretations of variations of coral growth rates measurements (corals grow at different rates in different depths) are possible.

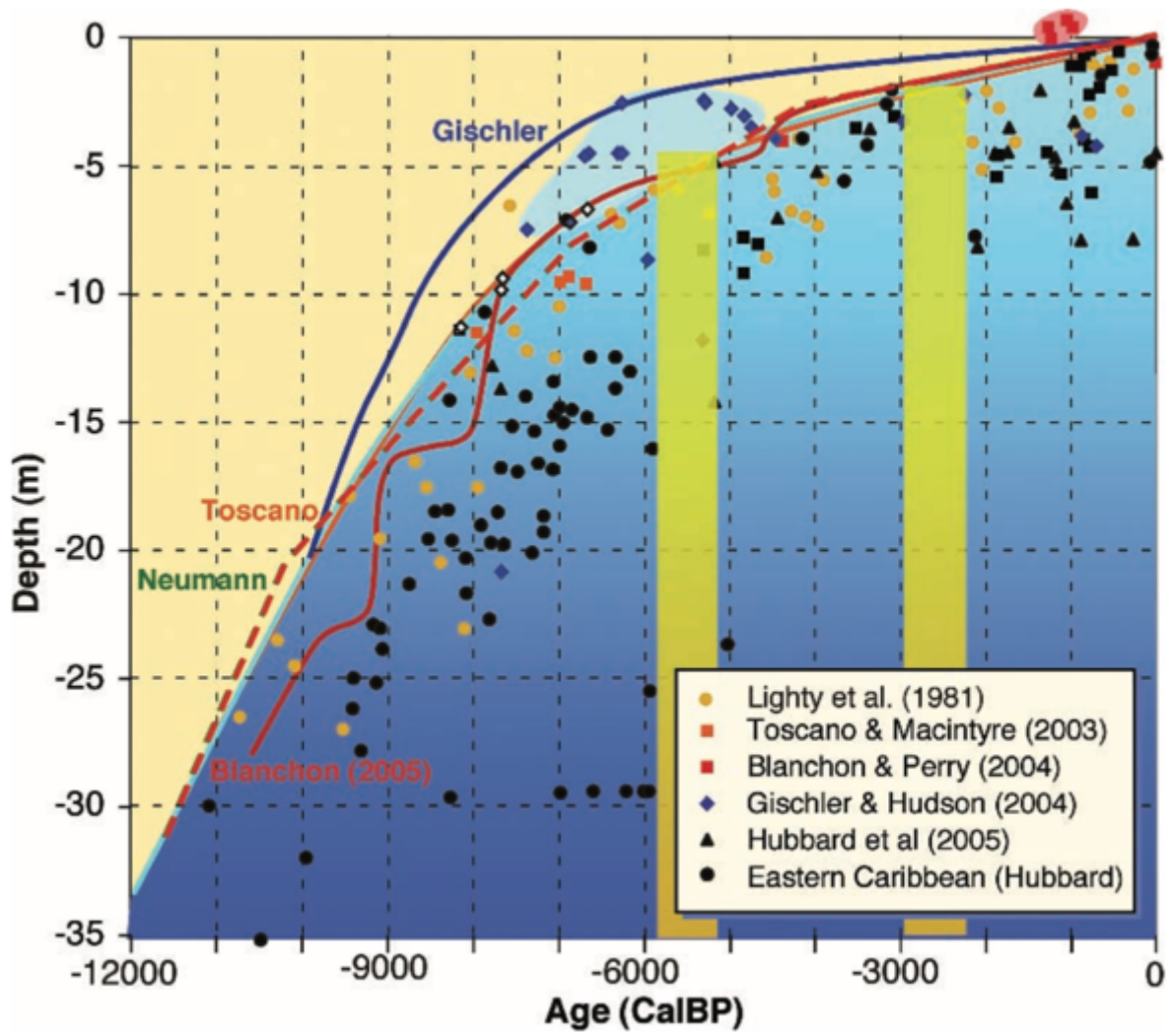


Figure 6: Holocene sea level curve for the Caribbean (Hubbard et al., 2008).



Figure 7: The majority of the corals are in growth position. Photo by: W. Ramírez (2004).

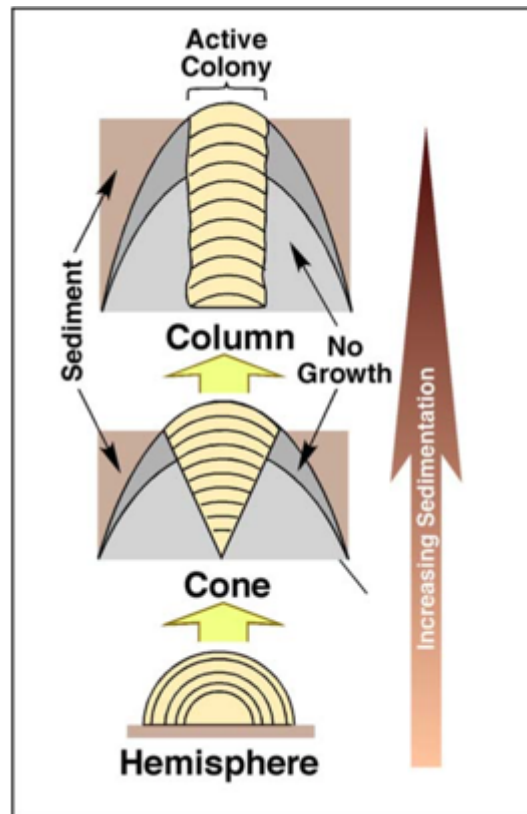


Figure 8: Interpretation of how the shape of the coral changes with the increasing of sedimentation (Hubbard et al., 2008).

4. Methodology

4.1 General description of the methodology

Orbicella sp. corals were collected in the field (Cañada Honda Reef Exposure), where their geographic and stratigraphy location was recorded. The coral samples were cut into 5mm slabs in the laboratory. The cut slabs were X-rayed in the San Antonio Hospital in Mayagüez. The changes in skeleton density visible in the X-ray image were used to measure coral growth rates based on the linear extensions of the high and low density bands (one high + one low density band = 1 year) using the Coral XDS software that measures image changes in luminosity. Micromilling of the coral slab followed. The drilling was done in increments of one millimeter by millimeter (approximately 100 samples for each coral). A Micromilling machine with a 1mm drill bit was used. The drilling was done following the growth axis along the wall of a single corallite visible on the Micromill Microscope apparatus. Oxygen isotopic ($\delta^{18}\text{O}$) and Sr/Ca concentrations (Sr/Ca) from the coral skeletons were measured in a Mass Spectrometer (UPRM-GASI Lab) and used as proxy's records for temperatures (SST) and salinity (SSS) variations. The SST and SSS measurements were assembled within a chronologic context based on the coral skeleton growth measurements (density bands) and dating (U/Th) of the coral colonies. Local changes in SST and SSS were compared to modern values and to the available paleoclimate records of similar time intervals during the Holocene.

4.2 Field Work

Samples of *Orbicella sp.* coral samples were collected by Wilson R. Ramírez, Elson Core and Kevin Velez during the summer of 2014. The area was visited the following summer by this author for a detailed inspection of the field location and to study the specific areas of samples collection. The samples of *Orbicella sp.* analyzed in this investigation were collected from the

Mixed Coral Zone (MZ). Figure 9 shows the Cañada Honda reef facies map and the specific locations along the reef from where the samples were collected. Prior to this sampling, previous surveys done by Hubbard et al. (2004), Cuevas et al. (2005), and Cuevas (2010) measured and described the exposure in detail. The features described and the stratigraphy developed by these previous studies was evaluated and used in the field to make the sampling decisions. During the sampling the attitude (growth position), taphonomy and morphology of the fossil corals were evaluated to select the most adequate samples. These characteristics are important since the analysis requires that the location and geochemistry of the fossil coral has not changed since the aragonite skeleton was precipitated. Some of the samples were big coral heads and had to be cut into smaller pieces that were labeled by adding lowercase letters, from bottom to top, to the sample name. Each individual coral was photographed in the outcrop before sampling to document its attitude and the general aspect of the area from where it was collected.

A total of seven *Orbicella* Complex corals skeletons were sampled (Fig. 9) for this study. Each coral was identified with a name that corresponds to the coordinates of the position it was sampled from. The first number describes the horizontal distance from the 2014 Enriquillo Lake shoreline (0) through the 450 meters of the measured outcrop towards the north. The second number corresponds to the elevation of the coral from the base of the reef exposure as it was at the time of the collection of the sample during the summer of 2014 (Fig. 10). Also, the location of the facies where the coral came from, as described by Hubbard et al. (2004), was documented. To facilitate transportation the edges of the coral colonies were cut leaving only the central growth axis of the coral sample (Fig. 11). This was done using a portable Nakita Doc 7301 cutting machine (Fig. 12). After cutting them, the samples were cleaned to remove dust and external sediment from the cutting machine, labeled, and photographed. This procedure was done to reduce

the volume and weight of the coral sample, to inspect the degree of preservation of the skeleton, and to determine the degree of bioerosion of the internal parts of the coral in the field, eliminating the possibility of collecting highly bioeroded corals that could not be used for the analysis (Fig. 13). The processed coral samples were then transported from the Enriquillo Valley to the Geology Department of the University of Puerto Rico, Mayagüez Campus (UPRM).

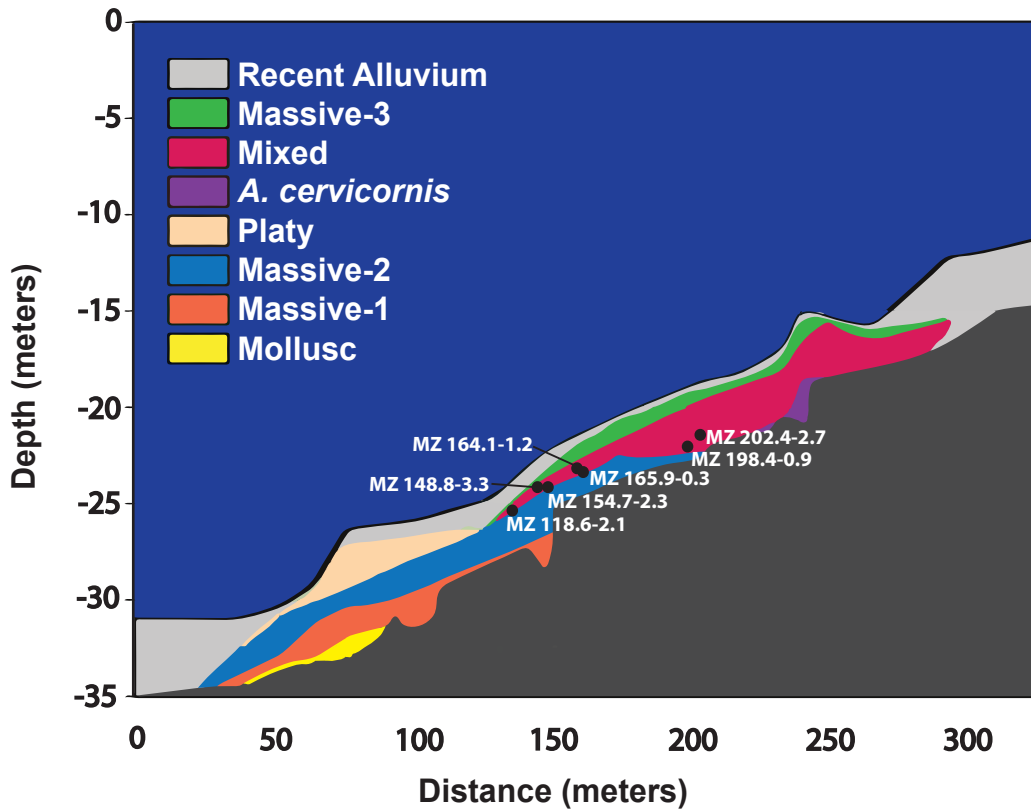


Figure 9: Cañada Honda Reef exposure facies map with the locations of the coral samples processed for this study. Modified from Hubbard (2004).



Figure 10: Example of the samples labeling and sample documentation of each coral while still in the outcrop. (Photo by: W. Ramirez, 2014).



Figure 11: Cutting the sides of the coral with a portable saw and leaving a central core of the skeleton managed to volume and weight of the coral sample. The red arrows shows examples of processed coral samples. (Photo by: W. Ramirez, 2014).



Figure 12: Cutting the coral heads with the portable saw at Cañada Honda. Large amounts of water were carried to the field to assist in the process. (Photo by: W. Ramirez, 2014)



Figure 13: Example of a highly bioeroded coral skeleton sample. Most of the bioerosion in the coral skeletons was produced by the boring clam *Lithophaga* sp. Cutting the samples in the field was important to identify highly bioeroded samples. Extensive boring of the coral skeletons has been reported in previous studies (Cuevas et al., 2005; Hubbard et al., 2004). (Photo by: W. Ramirez, 2014)

4.3 Mineralogical Analysis

Preservation of the original aragonitic composition and absence of secondary aragonite is a major requirement for the samples processed in this study. Two independent analyses were done to assess the problem.

4.3.1 XRD analysis

The mineralogy of the corals skeleton was examined using a Siemens X-Ray Diffractometer (XRD) D500 from the UPRM Geology Department. To perform the analysis, a portion of the coral slab was pulverized using a mortar and pestle until a very fine texture was obtained. The pulverized sample was analyzed with a step of 0.02, time of 1 sec and range from 4-70 2-Theta scale. To confirm the aragonitic composition remains intact, the results obtained were compared to the aragonite XRD analysis done by Downs, (2006) (Fig. 14). Aragonite is expected to have peaks at 26.2° ($I_1=100\%$), 45.86° ($I_2=65\%$) and 27.2° ($I_3=52\%$). Calcite presence and dominance over aragonite can be considered by looking at possible peaks at 29.4° ($I_1=100\%$), 43.1° ($I_{2-3}=18\%$) and 39.4° ($I_{2-3}=18\%$). Since the same intensity percent (I) for calcite is found in peaks at 43.1° and 39.4°, it cannot be distinguished between I_2 or I_3 . The XRD has a calcite detection limit of 1-2% (Sayani et al., 2011; Reuter et al., 2005).

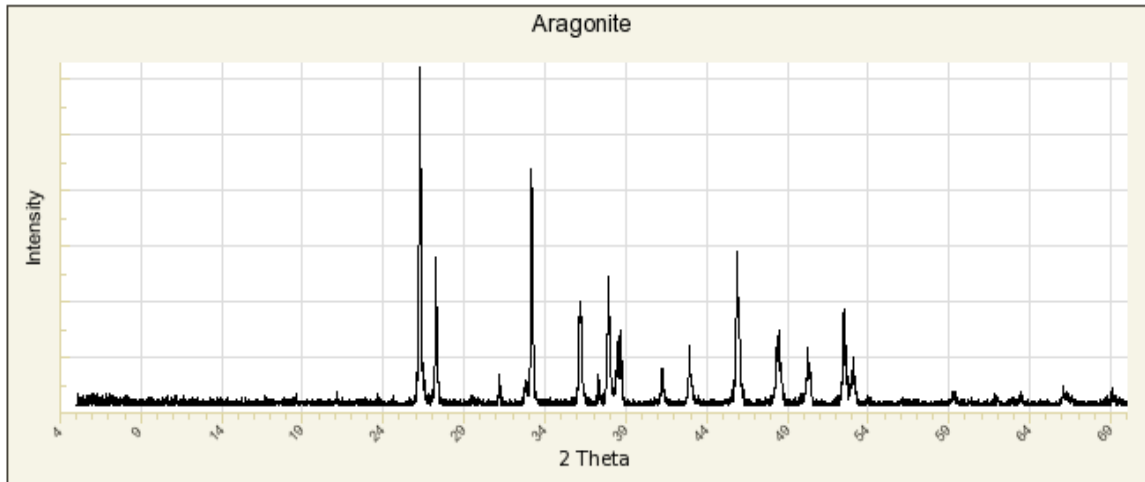


Figure 14: Example of powder diffraction spectra produced by an aragonitic sample. Courtesy of the University of Arizona Mineral Museum (Downs, 2006).

4.3.2 SEM

The coral skeletons surface was examined using a Scanning Electron Microscope (SEM) to observe if there is secondary aragonite in the interstices of the coral skeleton or along the coral skeleton surface. This analysis was performed in the UPRM Biological Department in a JSM-5410LV Scanning Microscope machine by the technician Jose R. Almodovar. To do the analysis, a section of the coral slab was cut into a 5 mm cube. Each coral cube was coated with a gold (Sputtering/Argon Coating) to increase the electrical conductivity of the samples. The coated samples were then viewed and photographed in the SEM.

4.4 Growth Rates Measurements

4.4.1 X-Ray Radiographs

A SMI Fulker DiMet C/149B masonry and concrete saw was used to cut the samples in longitudinal slabs to a thickness of 5 mm. To obtain the correct X-Ray exposure showing the changes in skeletal density (density bands) from the image, the slabs need to be 5 mm or less in thickness. Radiographies of the slabs were done in the San Antonio Hospital at Mayagüez, Puerto Rico by using a Toshiba Rotanode LX125 Collimator.

4.4.2 Coral-XDS software

The annual extension rates (growth rates) for the coral skeletons were determined by measuring the thickness of the combined high and low density bands using Coral X-radiograph densitometry system (Coral-XDS) software. Each couplet of high-low density bands is assumed to represent a year of skeletal growth (Winter et al., 2000). Counting the number of couplets present along the longitudinal section of the entire coral sample gives the total number of years represented on the coral skeleton (Winter et al., 2000). Greer and Swart (2006) proposed the high-density band is formed during the warmest seasonal SST, which occurs during August and

September in the Caribbean. During this season there is also an increase in regional precipitation. Other variations in density can result from changes in linear extension and/or changes in the coral calcification rate (Felis and Pätzold, 2004). Coral growth rates were calculated using Equation 1. The software generates a graph demonstrating the extension and luminance of the coral sample where the average maximum and minimum luminance points are detected. Some maximum and minimum points were selected manually within the software since some points were not detected by the software.

$$\text{Average Growth rate} = \frac{\text{coral growth extension (mm)}}{\text{number of couplets (yr)}} \quad (1)$$

4.5 Sedimentation rate estimates

The foliated morphology present in many of the corals of the Cañada Honda fossil reef (Fig. 14) was used to estimate sedimentation rates. This approximation was done by assuming that each foliation of the coral represents a period of growth after a specific sedimentation event covered the lower part of the coral (Hubbard et al., 2008). The extension of a particular foliation along its growth axis in relation to the growth bands is measured to do the estimation (Fig. 15). To estimate the sedimentation rates Equation 2 was used. To be able to compare the sedimentation rates obtained with modern sedimentation rates measured in modern environments at other studies equation 3 was used.

$$\text{sedimentation rate} = \frac{\text{pancake growth extension (mm)}}{\text{number of couplets (yr)}} \quad (2)$$

$$\text{Sedimentation rate} \left(\frac{mg}{cm^2d} \right) = \text{sedimentation rate} \left(\frac{cm}{d} \right) * \text{sedimentation density} \left(\frac{mg}{cm^3} \right) \quad (3)$$

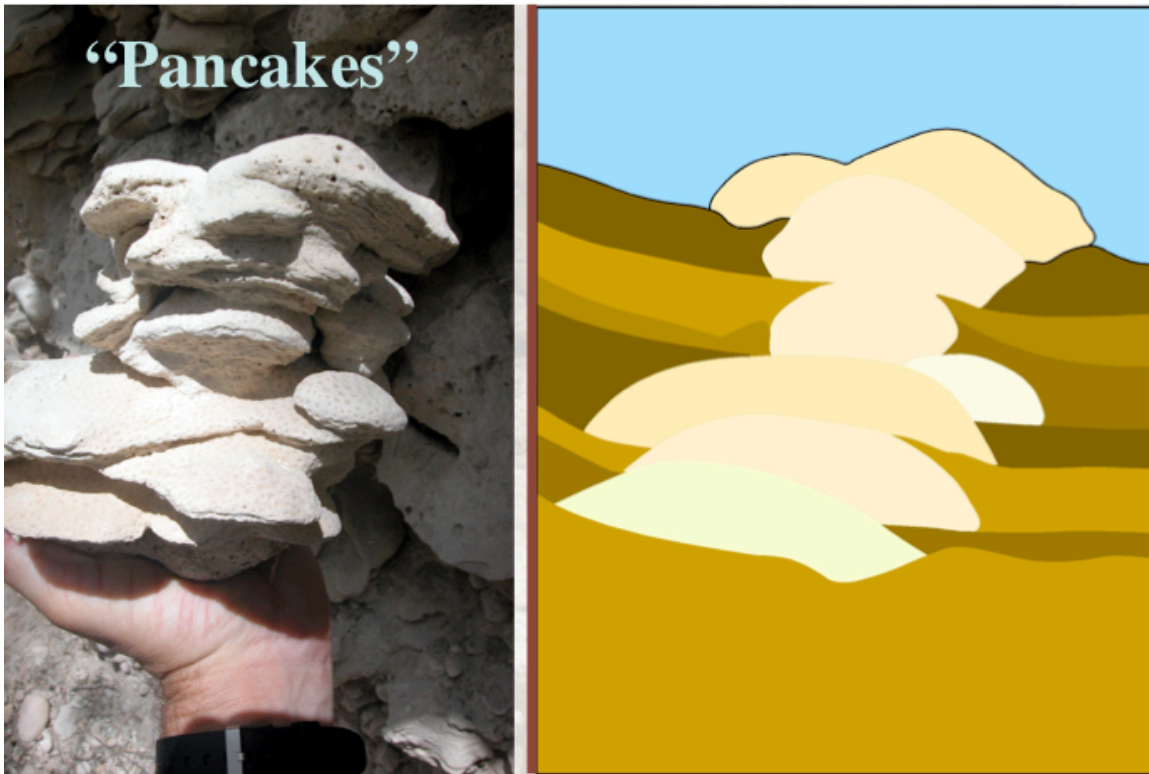


Figure 15: Example of a foliated morphology from a coral in Cañada Honda (Hubbard et al., 2004).

4.6 Age of the Coral Skeleton

4.6.1 Radiogenic Dating

Four coral samples were analyzed using uranium thorium radiogenic dating (U/Th). A sample of the skeleton (one gram) was collected close to the base of the coral. The integrity of the skeletons was inspected to make sure it was in pristine conditions. The sample for dating was collected as close as possible to the starting point of the microsampling transect (isotopic and trace elemental analyses). The radiogenic dating sampling location were documented in detail in each coral skeleton. U/Th analysis of the powdered samples was done at the multi-collector inductive coupled plasma mass spectrometer (MC-ICP-MS) available at the Rosenstiel School of Marine and Atmosphere Science (RSMAS) in Miami. The analysis were made by Dr. Ali Pourmand.

4.7 Paleoenvironmental Measurements

4.7.1 Microsampling

The sampling for isotope analysis and trace element analysis were done by microsampling. The drilling was done in increments of one millimeter (approximately 100 samples per coral). A Micromilling machine with a 1mm drill bit was used. The drilling was done following the growth axis along the wall of a single corallite visible in the Micromill Microscope apparatus. Each powdered sample should have generated a sub-annual resolution through a time-series along the coral covered cover decades.

Since the coral skeleton has a three-dimensional structure and the position of the transect line may change beneath the surface of the coral, some samples were not collected along the wall of a single corallite. This may introduce error into the analysis (Swart et al., 2002). When this problem is present sample material from different time periods could be sampled even though it may appear that a sample was drilled from a particular time increment in the skeleton (Swart et

al., 2002). The powder obtained from the micromilling sampling was collected and weighted using a Mettler UMT2 micro-balance. 300 to 600 μ g were collected for stable isotope analysis and 1,000-2,000 μ g for trace elemental analysis.

4.7.2 Trace Element Analysis

The Sr/Ca ratios present in the coral skeleton were measured using a ThermoFisher Neptune Plus, high performance Multi-Collector Inductively Coupled Plasma Mass Spectrometer (MC-ICP-MS) at Rosenstiel School of Marine and Atmosphere Science (RSMAS) in Miami (Professor Ali Pourmand). By using the Schrag (1999) nearest-neighbor correction method, the measurements produced an analytical precision of ± 0.08 - 0.24% (1σ). The Sr/Ca ratios were used to calculate SST (Figure 2). The ideal situation would be to have a Sr/Ca calibration from the same time and the same environment the corals were precipitated but that is not possible since the reef formed thousands of years in the past and in a semi-enclosed deep embayment environment that no longer exist (Hubbard et al., 2004; Cuevas et al., 2005; Mann et al., 2008). Due to this limitation several Sr/Ca-T calibrations produced by other authors will be used including one obtained from a modern coral sample collected from a reef in Barahona Bay that is ~ 67.5 kilometer from Cañada Honda and close to the mouth of Rio Yaque del Sur (i.e. similar high sedimentation environment as in the Cañada Honda Reef from the same river) by Jimenez (2018). The Sr/Ca-T equations used are the ones published by Swart et al. (2002) in Ball Buoy Reef, south Florida (Eq. 4), Smith (2006) in Dry Tortugas, Florida (Eq. 5), Flannery et al. (2013) in Dry Tortugas, Florida (Eq. 6) and Jimenez (2018) in Barahona, Dominican Republic (Eq. 7). From all the Sr/Ca-T calibration equations applied to our case the most adequate is the Barahona (Eq. 7) by Jimenez (2018) since it is the closest one to Cañada Honda. Plus, the corals collected in this area represent similar environmental conditions as the corals collected in this study. Barahona is also surrounded

by the same mountain ranges as Cañada Honda (Sierra de Neiba and Sierra Bahoruco), hence, the coral reef has the same sedimentation influx. The coral use to obtain Sr/Ca-T calibration (Eq. 7) is also influence by the discharge of Yaque del Sur River as Cañada Honda reef was. This implies that the coral collected in Barahona growth in an estuary environment similar as the corals collected in this study, since Paleo-Enriquillo Bay probably had estuary environment.

$$\text{Sr/Ca} = 10.165 - 0.0471 * \text{SST} \quad (4)$$

$$\text{Sr/Ca} = 9.962 - 0.0282 * \text{SST} \quad (5)$$

$$\text{Sr/Ca} = 10.205 - 0.0392 * \text{SST} \quad (6)$$

$$\text{Sr/Ca} = 10.786 - 0.0676 * \text{SST} \quad (7)$$

4.7.3 Stable Isotope Analysis

An IsoPrime JB079 Micromass Gas isotope ratio Mass Spectrometer (MS) with a gas precision of 0.02-0.03‰ and linearity of 0.03‰ NBS-19 Limestone (NBS-19) calibrated for Pee Dee Belemnite (PDB) values was used to analyze the $\delta^{18}\text{O}$ isotopic ratios. The machine is located in the GASI Laboratory of the UPRM Geology Department. The amount of aragonite powder collected for the analysis was 300-600 μg . The standard deviation was calculated for each analytical run using the standard (PDB) results that were obtained from the analysis. A curve was created with the data obtained that shows the fluctuations of stable isotope through time (Figure 2A). More reliable SST reconstructions are expected when $\delta^{18}\text{O}$ measurements are combined with Sr/Ca (Grottoli, 2001). Oxygen isotopic measurements ($\delta^{18}\text{O}$) from Greer and Swart (2006) in corals at the same location (Cañada Honda) and of similar ages (Holocene) than the ones analyzed

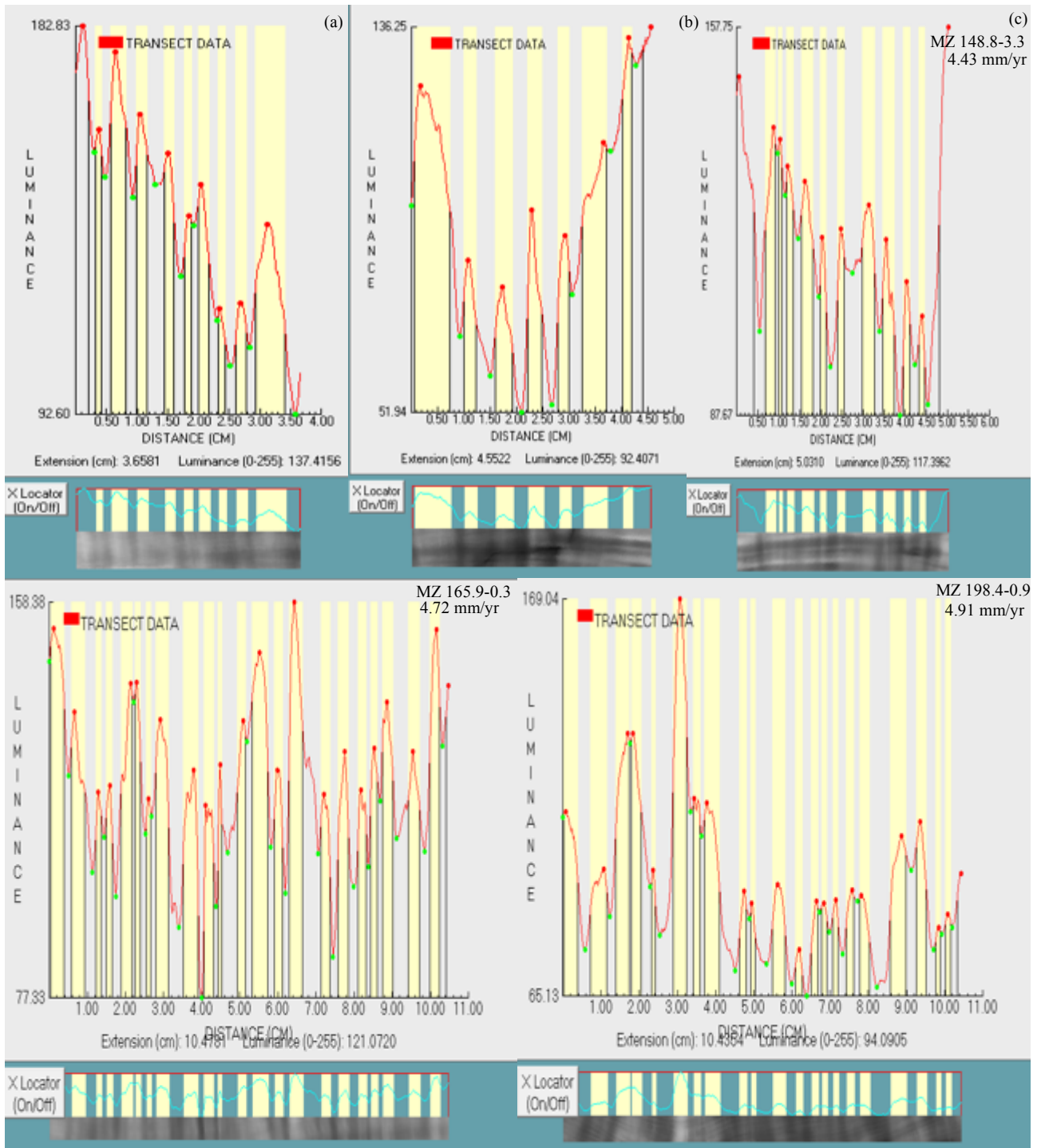
in this study were also used for comparisons. The calibration curve by Leder et al., (1996) was used to get SST from the $\delta^{18}\text{O}$ values (Eq. 8). This calculation is done by maintaining the oxygen isotope values of the water constant or $\delta^{18}\text{O}_w=0$. This helps to attribute the variations in $\delta^{18}\text{O}$ to changes in temperature due to fractionation of the isotopes and not to variations in $\delta^{18}\text{O}$ in the water (Greer and Swart, 2006). The comparison of SST values obtained from Sr/Ca with the SST values obtained from $\delta^{18}\text{O}$ will help to determine if the former assumption holds.

$$\text{SST} = 5.55 - 4.519 (\pm 19) * (\delta^{18}\text{O}_c - \delta^{18}\text{O}_w) \quad (8)$$

5.Results

5.1 Skeletal Average Growth rate

Annual average extension rates or growth rates are plotted in Figure 16 for samples MZ 148.8-3.3, MZ 165.9-0.3, MZ 154.7-2.3 and MZ 198.4-0.9. The X axis represents the extension length and Y axis the amount of luminance present in the X-ray image (see appendix for individual plots). Sample MZ 148.8-3.3 was divided into three segments to measure its average growth rate. The X-ray image from sample MZ 148.8-3.3 part (a) (3.6 cm extension) show a decreasing trend in luminance values from 0.5-3.5 cm extension length. Thinner growth bands are observed between 0.0-0.5 cm and 1.7-2.5 cm extension length. Part (b) of MZ 148.8-3.3 (4.5 cm extension) shows an increasing trend in the luminance from 2.0-4.7 cm in the X axis. The growth band thickness of this part of the sample is less dramatic than part a and b of the coral. MZ 148.8-3.3 part (c) (5.0 cm extension) demonstrates a decreased in luminance between 0.0-4.5 cm extension length, a similar trend as part (a). A thinner growth band is notice from 0.7-1.2 cm length. The change in growth thickness between 1.5-5.0 cm is not that noticeable. Sample MZ 165.9-0.3 (10.5 cm extension) shows increasing trend in luminance at 6.0-6.7 cm extension length and a thinner growth between 2.0-3.0 cm extension length. MZ 198.4-0.9 demonstrates an increased in luminance from 2.5-3.0 cm extension length, then a decreased from 3.5- 10.5 cm extension length. Growth thickness variations in this sample are less dramatic compare to samples MZ 148.8-3.3 part (a and b) and MZ 165.9-0.3. Sample MZ 154.7-2.3 (11.4 cm extension) shows decreasing trend in luminance values from 0.0-4.5 cm extension length then increases from 4.5-8.0 cm extension length. Growth band thickness variations is less dramatic in this sample than samples MZ 148.8-3.3, MZ 165.9-0.3 and MZ 198.4-0.9.



Continue in next page

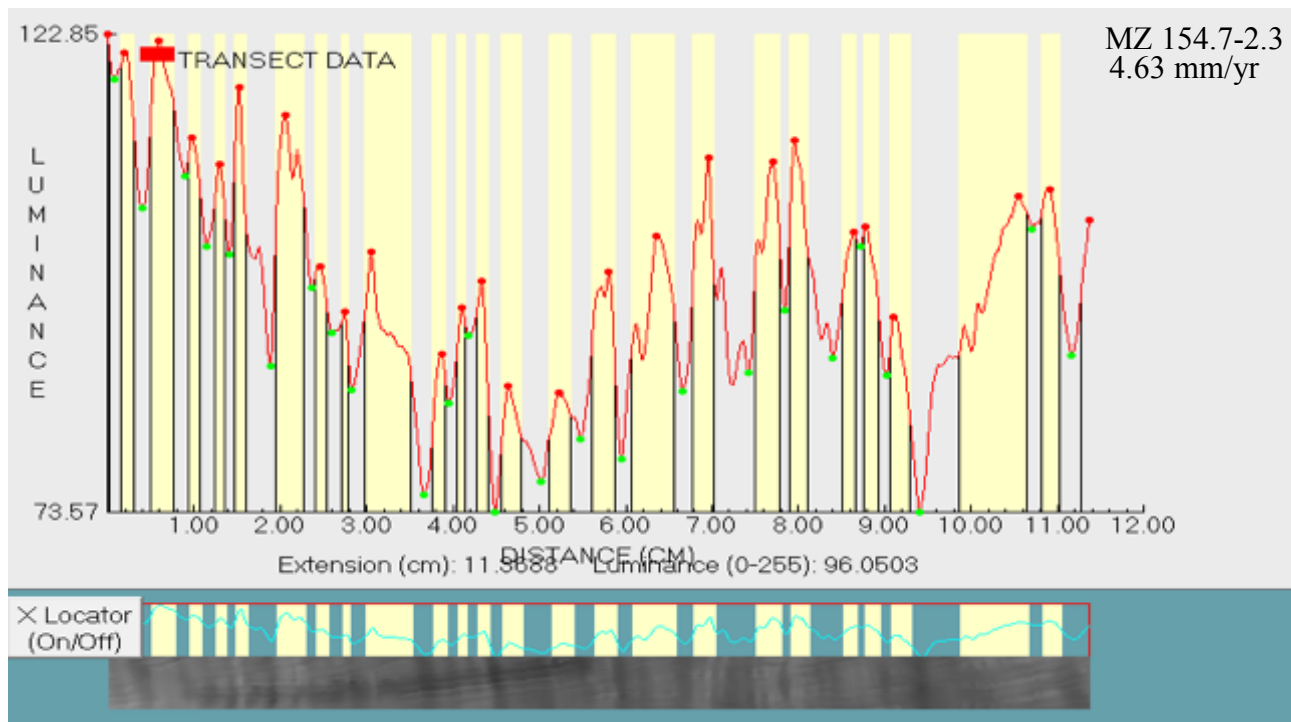


Figure 16: Annual extension rate (luminosity) analysis of samples MZ 148.8-3.3, MZ 165.9-0.3, MZ 154.7-2.3, and MZ 198.4-0.9 generated by Coral-XDS. In the bottom of the figure shows a transect for each sample. The estimated average growth rate is at the upper right side of the figure.

5.2 Skeletal Composition

5.2.1 XRD

Figure 17 shows the outcome produced by the XRD analysis with the 2theta in the X axis and intensity count in the Y axis (see appendix for all the plots). The figure shows that only aragonite peaks are present. The two most noticeable peaks are at 26.2° (160 - 270 counts) and 27.2° (110 - 160 counts), which corresponds to the aragonite peaks I_1 and I_3 respectively. Another peak can be observed at 46° (160 – 210 counts) matching the aragonite peak I_2 . The most notable calcite peak in XRD diffractograms, I_1 , calcite at 29.4° was not detected in any of the samples. However, the XRD has a calcite detection limitation of 1-2%. Thus, small amounts of calcite, less than 1-2%, could be present in the coral samples without being detected in the analysis.

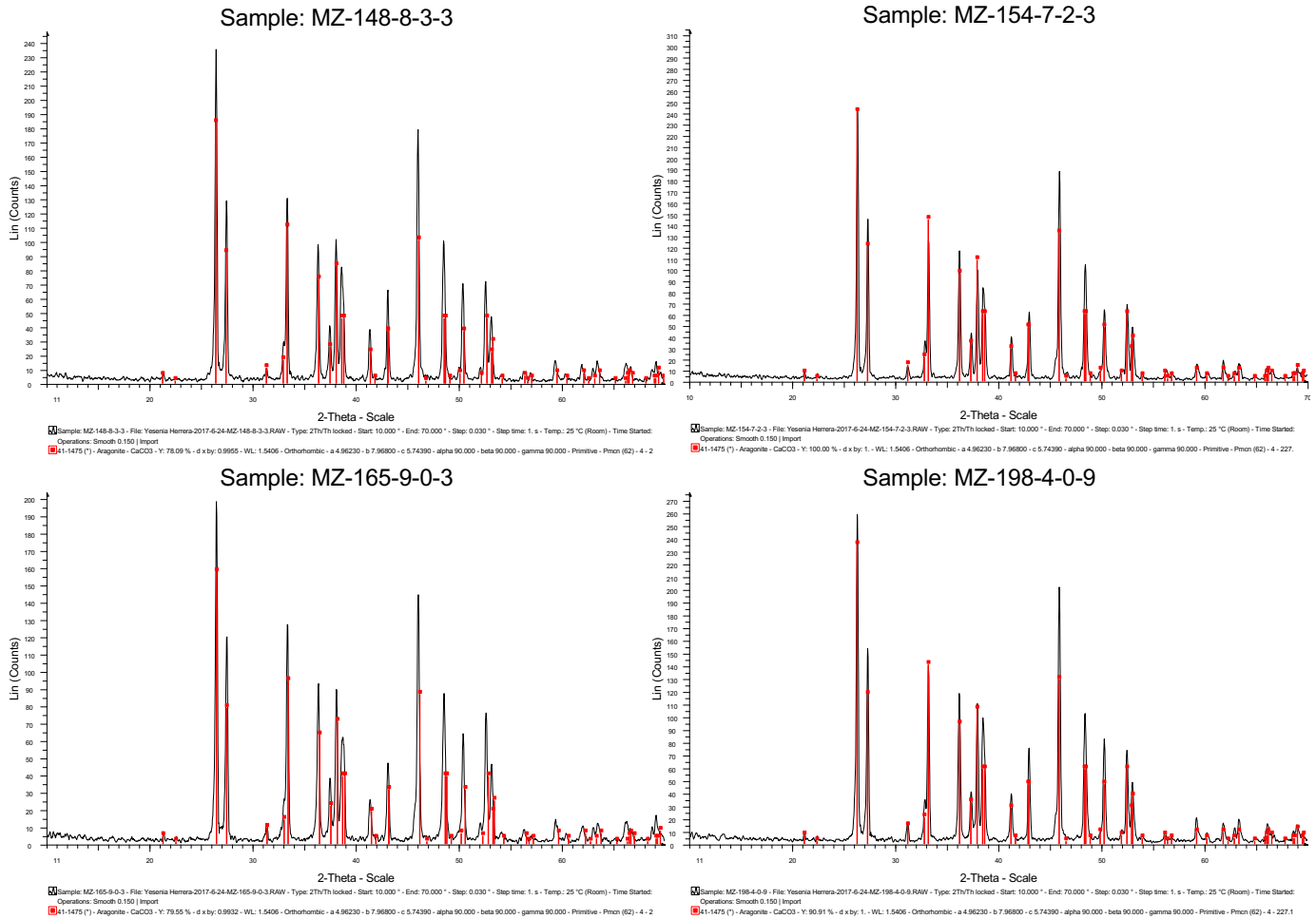


Figure 17: XRD analysis for samples MZ 148.8-3.3, MZ 165.9-0.3, MZ 154.7-2.3, and MZ 198.4-0.9. Aragonite peaks are marked in red. Calcite was not detected in the analysis.

5.2.2 Scanning Electron Microscope (SEM) Analysis

Scanning Electron Microscope (SEM) Analysis was performed to assess the presence of secondary aragonite in the samples since it can affect the Sr/Ca and $\delta^{18}\text{O}$ analysis (Fig. 18). Sample MZ 148.8-3.3 showed a small amount of secondary aragonite presented in the sample (Fig 18a). Coral samples MZ 165.9-0.3, MZ 198.4-0.9 and MZ 154.7-2.3 did not show any secondary aragonite present in the SEM images. Based on the SEM images the coral samples selected have the original structure, no recrystallization is evidence.

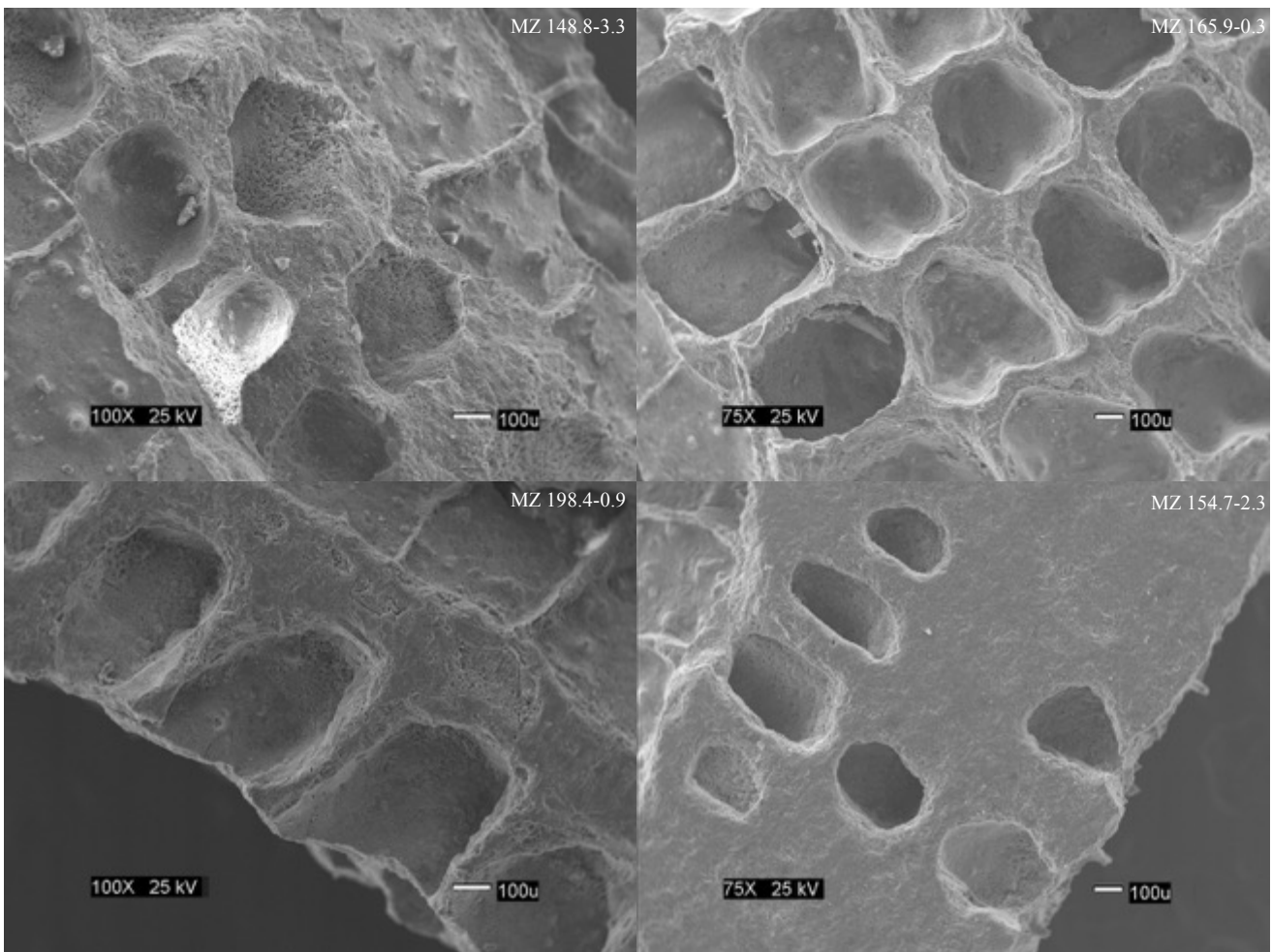


Figure 18: SEM images of coral samples MZ 148.8-3.3, MZ 165.9-0.3, MZ 154.7-2.3, and MZ 198.4-0.9. Sample name is on the upper right corner.

5.3 Growth Rate Estimates

Average growth rates were calculated for MZ 148.8-3.3, MZ 165.9-0.3, MZ 198.4-0.9, MZ 154.7-2.3, MZ 118.6-2.1, MZ 202.4-2.7 and MZ 164.1-1.2 and are shown in table 1. The average growth rate obtained for all MZ coral facies zone ranges from 4.43 ± 0.03 to 5.18 ± 0.04 mm/yr with an average value of 4.73 ± 0.03 mm/yr (n from 21 to 32 years). Different extension variation can be observe from this table and the given annual extension rate since Coral XDS software has the possibility of not analyzing a single band that could have been in the end of the transect.

Table 1: Average growth rate measurements for the coral samples selected.

<i>Sample ID</i>	<i>Years (n)</i>	<i>Extension (mm)</i>	<i>Average Growth Rate (mm/yr)</i>
<i>MZ 165.9-0.3</i>	<i>22</i>	<i>103.81</i>	<i>4.72 ± 0.03</i>
<i>MZ 198.4-0.9</i>	<i>21</i>	<i>103.18</i>	<i>4.91 ± 0.04</i>
<i>MZ 164.1-1.2</i>	<i>21</i>	<i>108.87</i>	<i>5.18 ± 0.04</i>
<i>MZ 118.6-2.1</i>	<i>25</i>	<i>117.78</i>	<i>4.71 ± 0.02</i>
<i>MZ 154.7-2.3</i>	<i>24</i>	<i>111.2</i>	<i>4.63 ± 0.04</i>
<i>MZ 202.4-2.7</i>	<i>32</i>	<i>144.9</i>	<i>4.53 ± 0.02</i>
<i>MZ 148.8-3.3</i>	<i>25</i>	<i>110.75</i>	<i>4.43 ± 0.03</i>

5.4 Sedimentation Rate estimates

Only two samples, MZ 118.6-2.1 and MZ 154.7-2.3, were selected for calculating the estimated sedimentation rate and the results are summarized in table 2. Based on the measurements of the two corals the estimated sedimentation rate in the reef at the time of accretion was 6.29 ± 0.15 to 5.76 ± 0.15 mm/yr with an average value of 6.03 ± 0.15 mm/yr ($n = 1$ to 3 years). To compare the estimated sedimentation rate from this study to sedimentation rate from other studies equation 3 was used. The obtained values in millimeter per year were converted to milligram per square centimeter per day. The converted estimated sedimentation rate obtained were values of 4.28 ± 0.15 to 4.67 ± 0.15 mg/cm²d.

Table 2: Estimated sedimentation rate calculations for the coral samples selected.

<i>Sample ID</i>	<i>Years (n)</i>	<i>Extension (mm)</i>	<i>Sedimentation Rate (mm/yr)</i>
<i>MZ 118.6-2.1</i>	<i>1</i>	<i>5.76</i>	<i>5.76 ± 0.15</i>
<i>MZ 154.7-2.3</i>	<i>3</i>	<i>18.86</i>	<i>6.29 ± 0.15</i>

Table 3: Estimated sedimentation rate calculations for the coral samples selected using equation 3 to compare to modern corals.

<i>Sample ID</i>	<i>Sedimentation Rate</i> <i>(cm/d)</i>	<i>Sedimentation Density</i> <i>(mg/cm³)</i>	<i>Sedimentation Rate</i> <i>(mg/cm²d)</i>
<i>MZ 118.6-2.1</i>	<i>0.0016</i>	<i>2710</i>	<i>4.28 ± 0.15</i>
<i>MZ 154.7-2.3</i>	<i>0.0017</i>	<i>2710</i>	<i>4.67 ± 0.15</i>

5.5 U/Th Radiogenic Dating

The U/Th dates of the four coral samples analyzed (MZ 148.8-3.3, MZ 165.9-0.3, MZ 154.7-2.3 and MZ 198.4-0.9) are present in table 4. The U/Th dates range from 5152 ± 30 to 6833 ± 31 yr B.P (Fig. 19). As anticipated, the oldest coral is MZ 165.9-0.3 since it is the closest coral to the base of the facie (in stratigraphic height) and the youngest is MZ 154.7-2.3 because it is one of the further coral from the base of the facie (in stratigraphic height). As the corals move vertically in stratigraphic height position in the column they get younger. However, MZ 154.7-2.3 is the exception since is younger than MZ 148.8-3.3.

Table 4: Summary of U/Th dates analysis for samples selected.

Sample Name	Mz-148.8	Mz-154.7	Mz-165.9	Mz-198.4
Age CORRECTED	5545	5152	6833	6431
\pm (95% CI = (Q97.5- Q2.5)/2 from MC var.)	62	30	31	36
Activity ratio 234U/238U initial	1.147	1.146	1.150	1.150
\pm (95% CI = (Q97.5- Q2.5)/2 from MC var.)	0.004	0.003	0.004	0.004
Age UNCORRECTED	5550	5159	6836	6434
\pm (95% CI = (Q97.5- Q2.5)/2 from MC var.)	62	30	31	36
Activity ratio 234U/238U initial	1.147	1.146	1.150	1.150
\pm (95% CI = (Q97.5- Q2.5)/2 from MC var.)	0.004	0.003	0.004	0.004

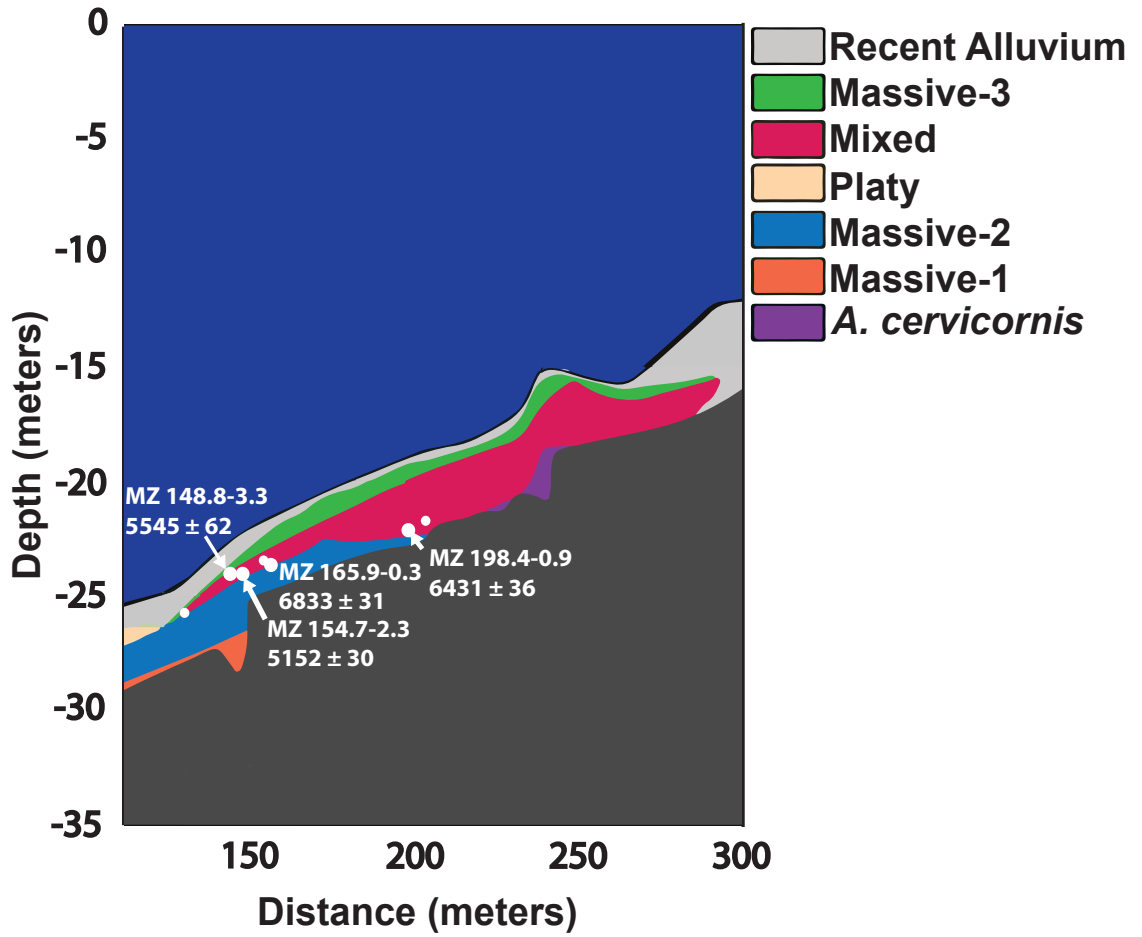


Figure 19: Cañada Honda reef facies map with the location of samples selected (MZ 148.8-3.3, MZ 165.9-0.3, MZ 154.7-2.3, and MZ 198.4-0.9) and the U/Th ages of each coral. Modified from Hubbard (2004).

5.6 Paleoenvironmental Measurements

5.6.1 Sr/Ca Elemental Analysis

Sr/Ca results for the two samples (MZ 148.8-3.3 and MZ 165.9-0.3) analyzed are presented in table 5 and plotted along with $\delta^{18}\text{O}$ values for comparisons. Sample MZ 148.8-3.3 ranges from 9.16 to 9.44 mmol/mol of Sr/Ca. Sample MZ 165.9-0.3 ranges from 9.22 to 9.52 mmol/mol of Sr/Ca. As expected the graph show a similar pattern between Sr/Ca variation and $\delta^{18}\text{O}$ variations (Fig. 20).

Table 5: Summary of Sr/Ca ratio calculations for samples selected.

Sample ID	Concentration (μg) in 1 mL solution		Sr/Ca	Sr/Ca (mmol/mol)
	Ca	Sr		
MZ148.8-3.3_05	634.70	12.87	0.02028	9.275415328
MZ148.8-3.3_06	652.34	13.07	0.02003	9.162107349
MZ148.8-3.3_11	610.29	12.48	0.02045	9.308050138
MZ148.8-3.3_19	615.74	12.49	0.02029	9.40522769
MZ148.8-3.3_29	821.44	16.76	0.02040	9.353653074
MZ148.8-3.3_36	403.12	8.18	0.02030	9.280903127
MZ148.8-3.3_47	592.38	12.18	0.02057	9.33014694
MZ148.8-3.3_62	442.53	8.97	0.02028	9.285675332
MZ148.8-3.3_69	577.61	11.87	0.02055	9.406911592
MZ148.8-3.3_76	442.93	8.92	0.02015	9.274303798
MZ148.8-3.3_87	621.80	12.84	0.02064	9.401051299
MZ148.8-3.3_96	654.11	13.41	0.02050	9.214891906
MZ148.8-3.3_106	628.78	12.80	0.02035	9.441980573
MZ148.8-3.3_116	494.04	10.16	0.02056	9.376235548

Sample ID	Concentration (μg) in 1 mL solution		Sr/Ca	Sr/Ca (mmol/mol)
	Ca	Sr		
M2165.9-0.3B_05	371.72	7.62	0.02049	9.370525917
M2165.9-0.3B_06	440.72	9.02	0.02046	9.35802411
M2165.9-0.3B_13	333.76	6.94	0.02078	9.504431223
M2165.9-0.3B_17	443.56	9.18	0.02070	9.466739186
M2165.9-0.3B_23	558.34	11.58	0.02074	9.487216175
M2165.9-0.3B_36	328.81	6.77	0.02059	9.416792977
M2165.9-0.3B_37	427.08	8.77	0.02053	9.392135311
M2165.9-0.3B_43	438.89	8.85	0.02018	9.228230894
M2165.9-0.3B_48	399.74	8.18	0.02047	9.364452559
M2165.9-0.3B_54	375.70	7.75	0.02062	9.430631112
M2165.9-0.3B_61	375.92	7.83	0.02082	9.522254206
M2165.9-0.3B_65	303.27	6.23	0.02056	9.403717958
M2165.9-0.3B_69	242.34	5.04	0.02078	9.504873452
M2165.9-0.3B_70	268.44	5.57	0.02077	9.498778242
M2165.9-0.3B_74	420.69	8.68	0.02064	9.441524351

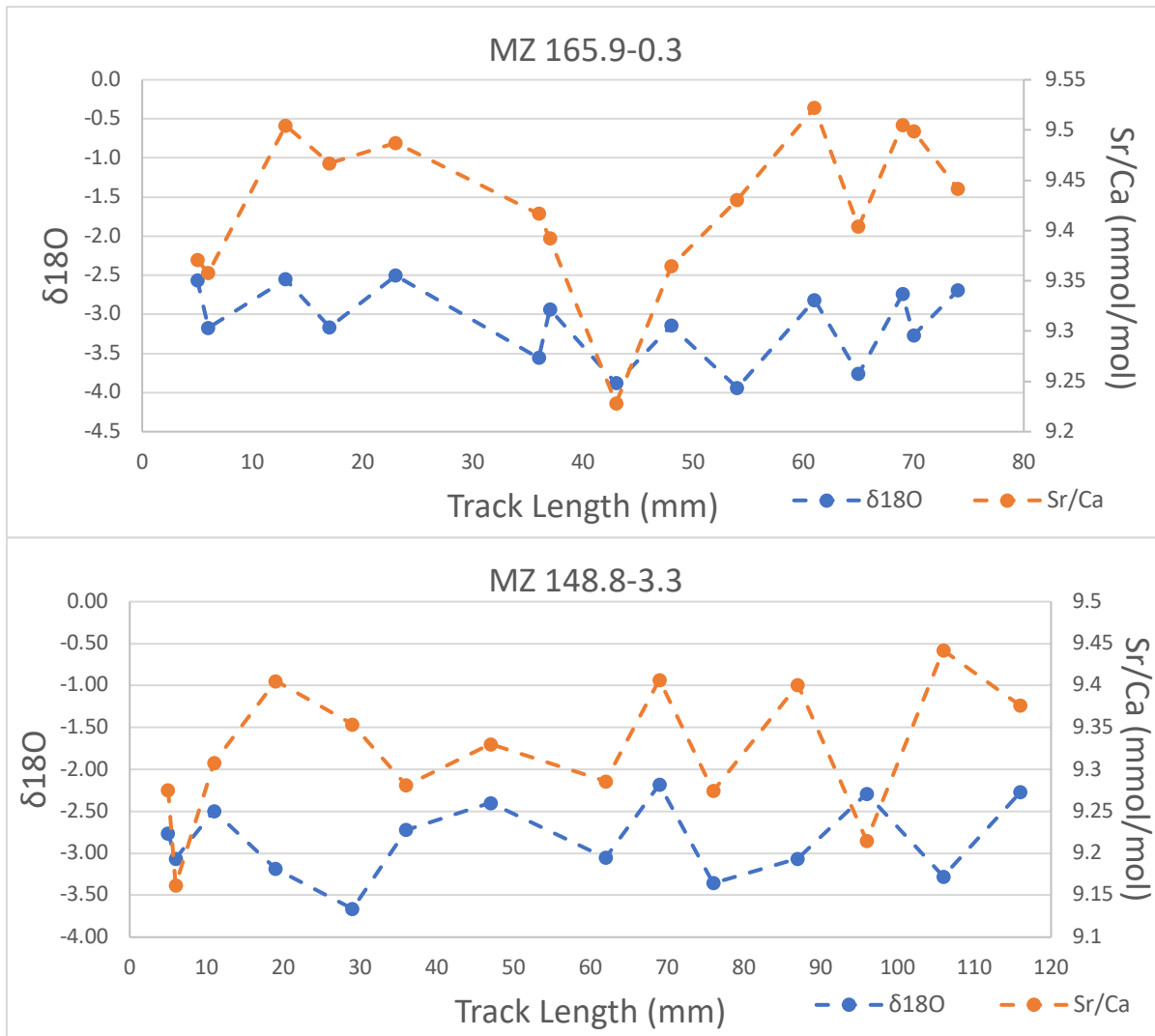


Figure 20: Sr/Ca and $\delta^{18}\text{O}$ values vs. track length of the sample in the selected coral samples MZ 148.8-3.3 and MZ 165.9-0.3 demonstrating the inverse relationship between Sr/Ca and $\delta^{18}\text{O}$ variations..

5.6.2 Stable Isotope Analysis

$\delta^{18}\text{O}$ and $\delta^{13}\text{C}$ results for the two samples (MZ 148.8-3.3 and MZ 165.9-0.3) selected are summarized in table 6 and plotted to be compared (Figure 21, a&b). $\delta^{18}\text{O}$ from sample MZ 148.8-3.3 range from -2.18 to -4.12 ‰ and $\delta^{13}\text{C}$ range from -2.45 to -4.12 ‰. The average isotopic values for $\delta^{18}\text{O}$ is -2.84 ‰ and $\delta^{13}\text{C}$ is -3.07 ‰. $\delta^{13}\text{C}$ from sample MZ 165.9-0.3 range from -2.73 to -4.12 ‰ and $\delta^{18}\text{O}$ range from -2.18 to -3.94 ‰. The average isotopic values for $\delta^{13}\text{C}$ is -3.33 ‰ and $\delta^{18}\text{O}$ is -3.11‰. The values for both $\delta^{18}\text{O}$ and $\delta^{13}\text{C}$ are very similar in sample MZ 148.8-3.3.

Table 6: Summary of $\delta^{18}\text{O}$ and $\delta^{13}\text{C}$ calculations for samples selected.

MZ 165.9-0.3		Raw	Raw	Raw Values		Average SST
Sample	Name	13C	18O	SST (+0.19)	SST (-0.19)	Raw
5	5.raw	-3.23	-2.56	11.459279	15.8601707	13.6597249
6	6.raw	-3.11	-3.18	14.1970648	19.6493925	16.9232286
13	13.raw	-3.46	-2.55	11.4074689	15.7884631	13.597966
17	17.raw	-3.86	-3.17	14.1568846	19.5937812	16.8753329
23	23.raw	-3.15	-2.51	11.2012069	15.502987	13.3520969
36	36.raw	-3.44	-3.56	15.8966754	22.001732	18.9492037
37	37.raw	-2.73	-2.94	13.1247927	18.1653185	15.6450556
43	43.raw	-3.01	-3.88	17.3605235	24.0277653	20.6941444
48	48.raw	-3.55	-3.15	14.0712025	19.4751933	16.7731979
54	54.raw	-4.12	-3.94	17.6184645	24.3847675	21.001616
61	61.raw	-2.92	-2.82	12.6063842	17.4478172	15.0271007
65	65.raw	-3.13	-3.76	16.8261412	23.2881555	20.0571483
69	69.raw	-3.43	-2.74	12.2558319	16.9626366	14.6092342
70	70.raw	-3.40	-3.27	14.6222232	20.2378314	17.4300273
74	74.raw	-3.32	-2.69	12.0438921	16.6693022	14.3565972

MZ 148.8-3.3		Raw	Raw	Raw Values		Average SST
Sample	Name	13C	18O	SST(+0.19)	SST(-0.19)	Raw
5	5.raw	-2.45	-2.76	12.3426057	17.0827355	14.7126706
6	6.raw	-3.21	-3.06	13.6917364	18.9499946	16.3208655
11	11.raw	-2.60	-2.49	11.1508076	15.433232	13.2920198
19	19.raw	-3.55	-3.19	14.2432295	19.7132865	16.978258
29	29.raw	-3.04	-3.66	16.3726452	22.6604961	19.5165706
36	36.raw	-2.81	-2.72	12.1576176	16.8267035	14.4921605
47	47.raw	-2.82	-2.40	10.7244753	14.8431685	12.7838219
62	62.raw	-3.43	-3.05	13.6483565	18.8899549	16.2691557
69	69.raw	-2.52	-2.18	9.74624111	13.4892472	11.6177442
76	76.raw	-4.12	-3.35	14.9974224	20.7571243	17.8772733
87	87.raw	-3.18	-3.06	13.6990192	18.9600744	16.3295468
96	96.raw	-3.41	-2.29	10.2293824	14.1579371	12.1936598
106	106.raw	-2.80	-3.28	14.6464068	20.2713025	17.4588546
116	116.raw	-3.02	-2.27	10.1554809	14.055654	12.1055675

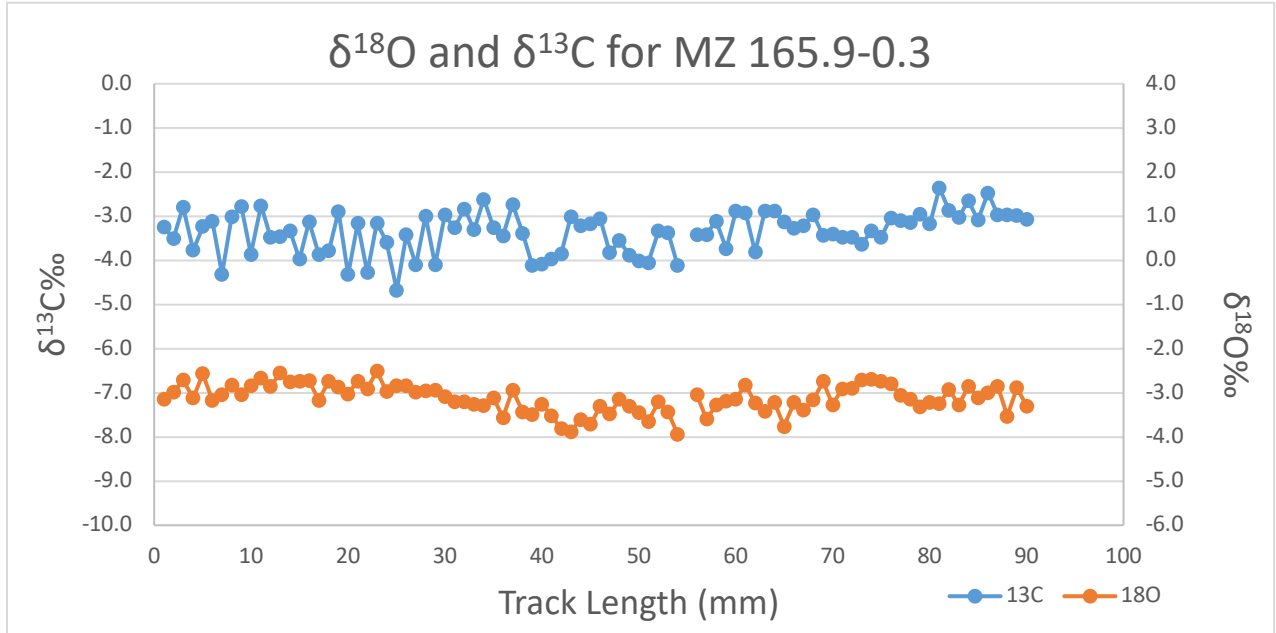


Figure 21a: $\delta^{18}\text{O}$ and $\delta^{13}\text{C}$ record for sample MZ 165.9-0.3 plotted vs. track length. The correlation between $\delta^{18}\text{O}$ and $\delta^{13}\text{C}$ is 0.09.

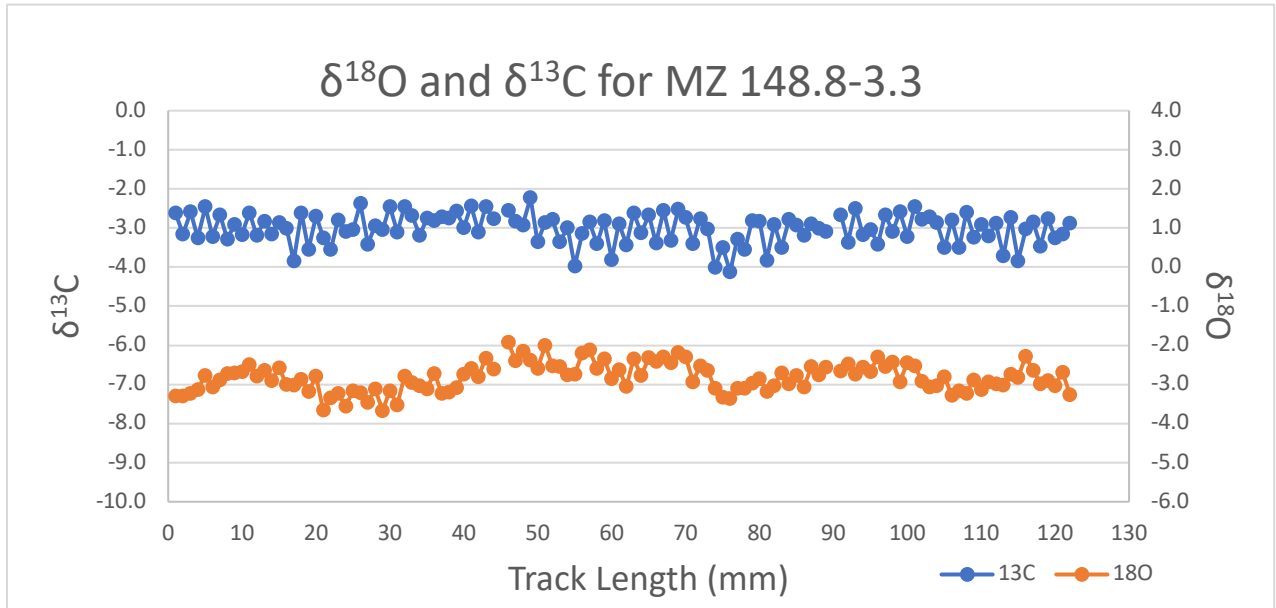


Figure 21b: $\delta^{18}\text{O}$ and $\delta^{13}\text{C}$ values for coral sample MZ 148.8-3.3 vs. track length. The correlation between $\delta^{18}\text{O}$ and $\delta^{13}\text{C}$ is 0.4.

6. Discussion

6.1 Mineralogy Analysis

The XRD results obtained from coral samples MZ 148.8-3.3, MZ 165.9-0.3, MZ 1547-2.3 and MZ 198.4-0.9 show a similar 2 theta and intensity peaks patterns as the calibration presented by Downs (2006) for the mineral aragonite. The presence of the expected aragonite XRD spectra and absence of all the possible calcite peaks in the diffractograms indicates the coral samples studied have retained the original aragonitic mineralogical composition. The detection limit of the analysis is 1-2% (Sayani et al., 2011; Reuter et al, 2005). Although minimal amounts of calcite could be present and not detected (1-2%) this quantity of calcite is not expected to have altered the results of this study analysis and for all practical purposes it is assumed that the XRD analysis performed is indication that the corals are in their pristine aragonite mineralogical composition. Nevertheless, the SEM images showed a small amount of secondary aragonite in some of the coral samples. Still, it is not consider to be an amount that would affect the analysis of the sample from Cañada Honda Reef in a drastic way (Greer and Swart, 2006) .

6.2 Growth Rate Measurements

The average growth rate obtained from the coral samples selected (MZ 148.8-3.3, MZ 165.9-0.3, MZ 154.7-2.3 and MZ 198.4-0.9) ranges from 4.43 ± 0.03 to 5.18 ± 0.04 . As a whole these numbers represent the average coral growth rates of *Orbicella sp.* coral along the MZ coral facies zone. It is well known that depth affects the growth rate of corals (Hubbard, 2005). Differences in depth could be definitively a factor that influenced the changes in average growth rate of the coral samples studied. The coral samples that are lower in vertical depth (stratigraphic height) (MZ 165.9-0.3, MZ 198.4-0.9, MZ 164.1-1.2) showed a faster average growth rate. Sample MZ 164.1-1.2 has the fastest growth rate value (5.18 ± 0.04 mm/yr), located at a stratigraphic height of 1.2. As the samples were in a higher stratigraphic position, the growth rate of the corals started to decrease, where MZ 148.8-3.3 is the highest sample in the stratigraphic position and has the slowest growth rate (4.43 ± 0.03 mm/yr)(Fig. 22). When comparing the growth rates with ages, they follow the same trend as with stratigraphic height. Meaning that as the corals get younger the growth rates decrease (Fig. 23). Coral samples MZ 148.8-3.3 and MZ 154.7-2.3 are the younger corals and they have the slower growth rates. Cuevas et al (2005), reported lower average growth rates for the mixed coral zone facies relative to the numbers produced by this study. Specifically Cuevas et al. (2005) reported average coral growth rates of 2.2 to 3.8 mm/yr while this study obtained average coral growth rates of 4.43 to 5.18 mm/yr for the same facies. When the growth rate measurements of MZ are compared with the other Cañada Honda Reef facies, the MZ facies has the highest average growth rates (Fig. 24). Abundant discussed evidence indicates that Cañada Honda Reef accreted in a high sedimentation environment. High sedimentation has been demonstrated to affect coral growth rates and reef health (Greer and Swart, 2006). High sedimentation is most definitively a factor that affected the growth of the MZ corals. It is clear

that the Cañada Honda Reef was able to accrete in this high sedimentation environment (Cuevas et al., 2005). It is also possible that high sedimentation episodes occurred periodically allowing time for the corals to react to the event and grow back, keeping-up with sedimentation (Hubbard et al., 2008). Around 5.0 to 4.0 kyr BP the large open bay started to close until it was completely separated from the Caribbean Sea creating the Enriquillo Lake and Valley (Mann et al., 1984) which is confirmed by the growth rates obtain in this study. The growth rates for the MZ facie corals starts to decrease as they get younger, indicating that a higher sedimentation input was entering the reef. Facies MZ (end of facies) and M3 are evidence of the closing of the bay with the decreasing of the corals growth rates.

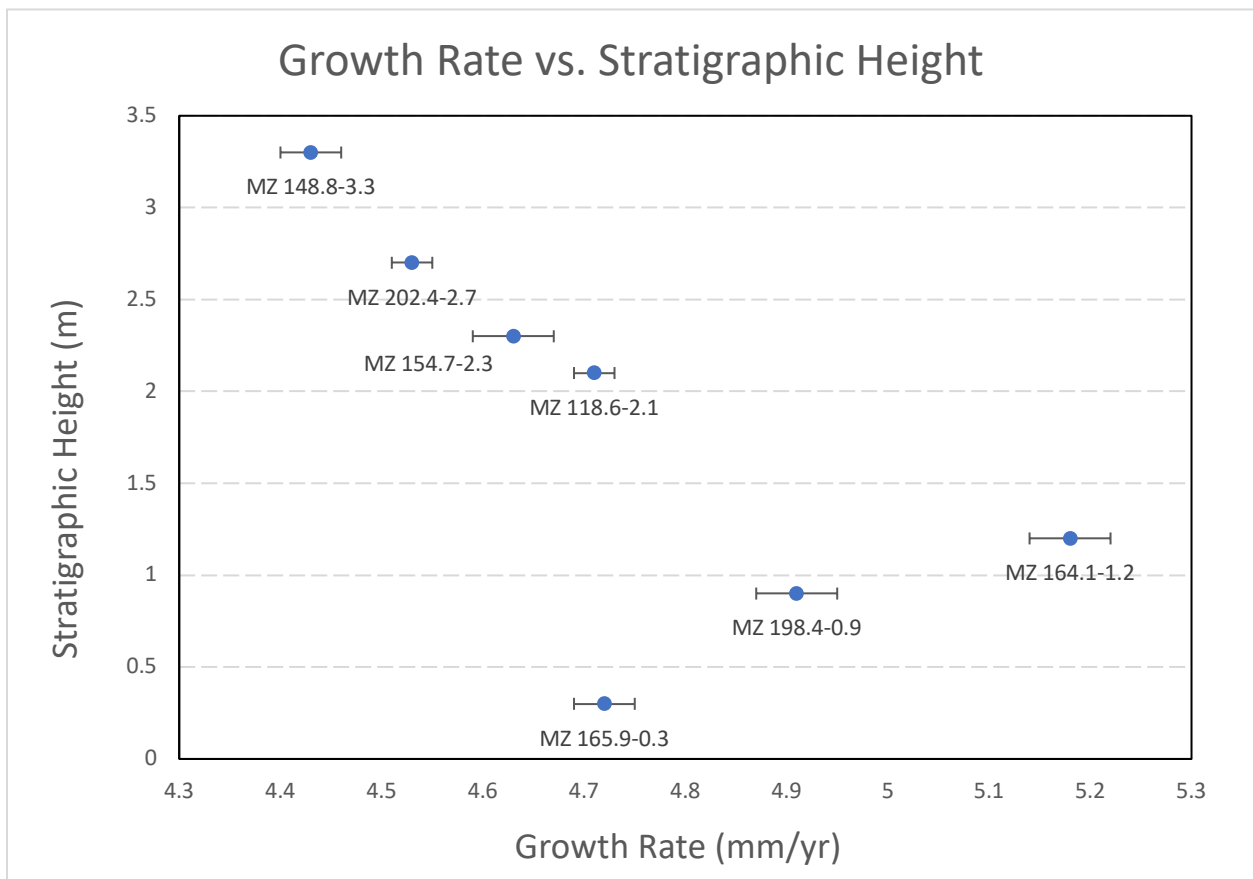


Figure 22: Growth Rare vs Stratigraphic Height for the seven coral samples selected in this study.

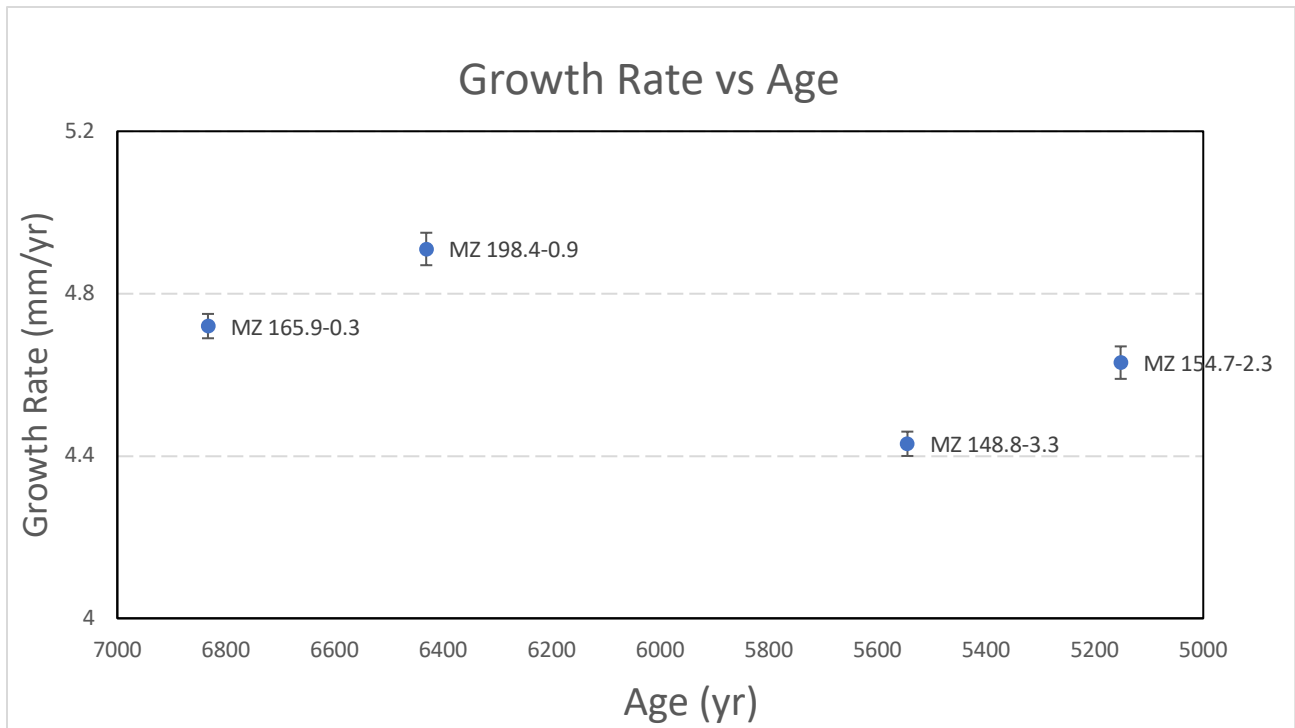


Figure 23: Growth Rate vs. Age for coral samples MZ 148.8-3.3, MZ 165.9-0.3, MZ 154.7-2.3 and MZ 198.4-0.9.

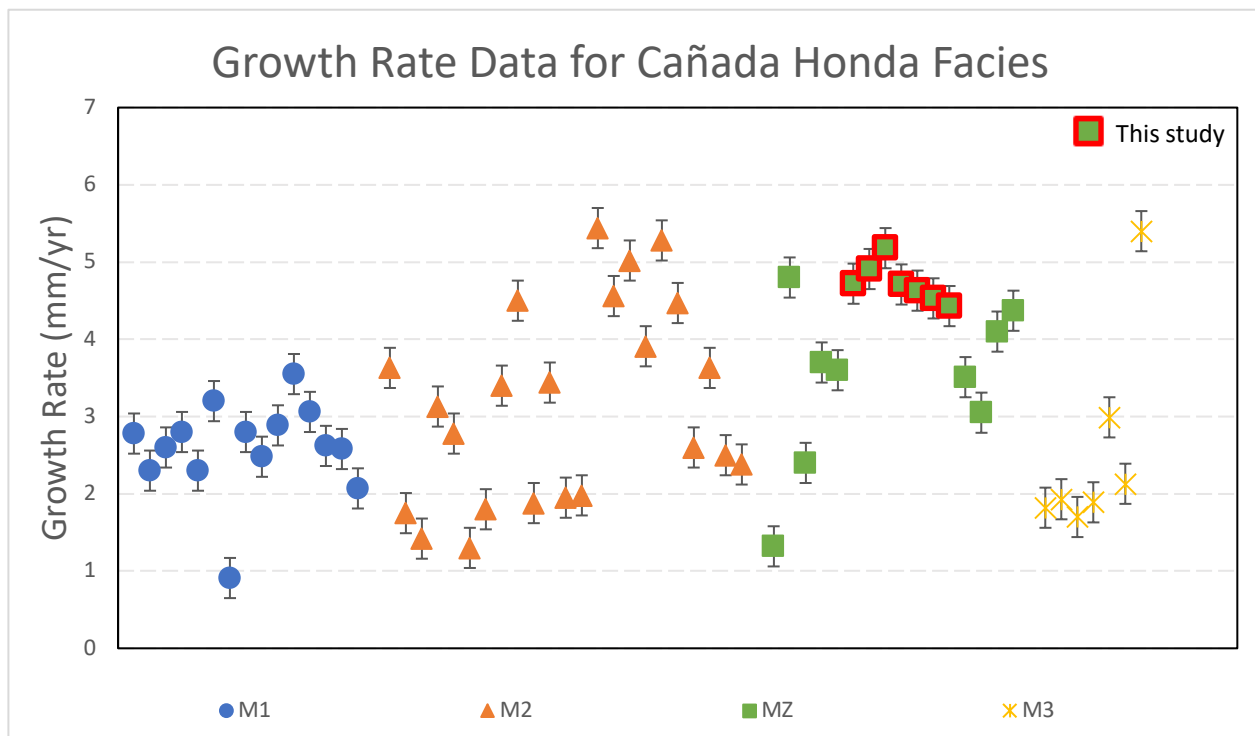


Figure 24: Growth Rate data for all Cañada Honda facies from Cuevas (2005), Diaz (2005), Cuevas (2009), Morales (2015) Jimenez (2018), Rodriguez (2018), and Herrera (2018).

6.3 Sedimentation Rate

The measurements on sedimentation rates obtained from coral samples MZ 118.6-2.1 and MZ 154.7-2.3 produced average values of 6.03 ± 0.15 mm/ yr ($n = 2$)(Fig. 25). Hubbard et al. (2004) used the same technique applied here in the same coral species and reported average sedimentation rate values of 1.67 ± 0.05 mm/yr for the M2 facie. Morales (2015) reported values of 2.06 ± 0.30 mm/yr for the M1 facie. Both average sedimentation rates from these studies are lower values than the ones reported by this study (Fig. 26). Based from the average sedimentation rates obtained from previous studies and this study, M2 facie has the lower sedimentation rate while MZ facie has the highest sedimentation rate. This means that as the corals were located in a higher stratigraphic position, a higher sedimentation influx was affecting them. In other words, younger corals were growing in a more adverse conditions. Based on Cuevas et al (2005) most of the sedimentation composition reaching the Cañada Honda reef was carbonate material. Non-carbonate material in Cañada Honda reef was measured by Cuevas (2005) to be lower than 10%. By making a simple conversion (equation 3) the sedimentation obtained from the corals (mm/yr) can be compared to sedimentations rates measured in modern marine environments ($\text{mg}/\text{cm}^2\text{d}$). When the conversion is applied the values obtain in this study range between 4.48 ± 0.15 $\text{mg}/\text{cm}^2\text{d}$. These values are significantly higher than modern sedimentation rate estimates Rogers (1990) that reported sedimentation rate values ranging from 0.5-1.1 $\text{mg}/\text{cm}^2\text{d}$ in Discovery Bay, Jamaica and 2.5-2.6 $\text{mg}/\text{cm}^2\text{d}$ in Puerto Rico. The estimate sedimentation rate average values obtained by this study are different to sedimentation rates produced by Morales (2015) 1.52 $\text{mg}/\text{cm}^2\text{d}$ and Hubbard et al. (2004) 1.24 $\text{mg}/\text{cm}^2\text{d}$. Based on this analysis, it can be confirmed that the sedimentation rates in Cañada Honda were higher than the other coral reef compared in this study. Still, the coral

reef was able to accrete, but it is observe in the morphology of the coral and bioturbation that they were heavily impacted.

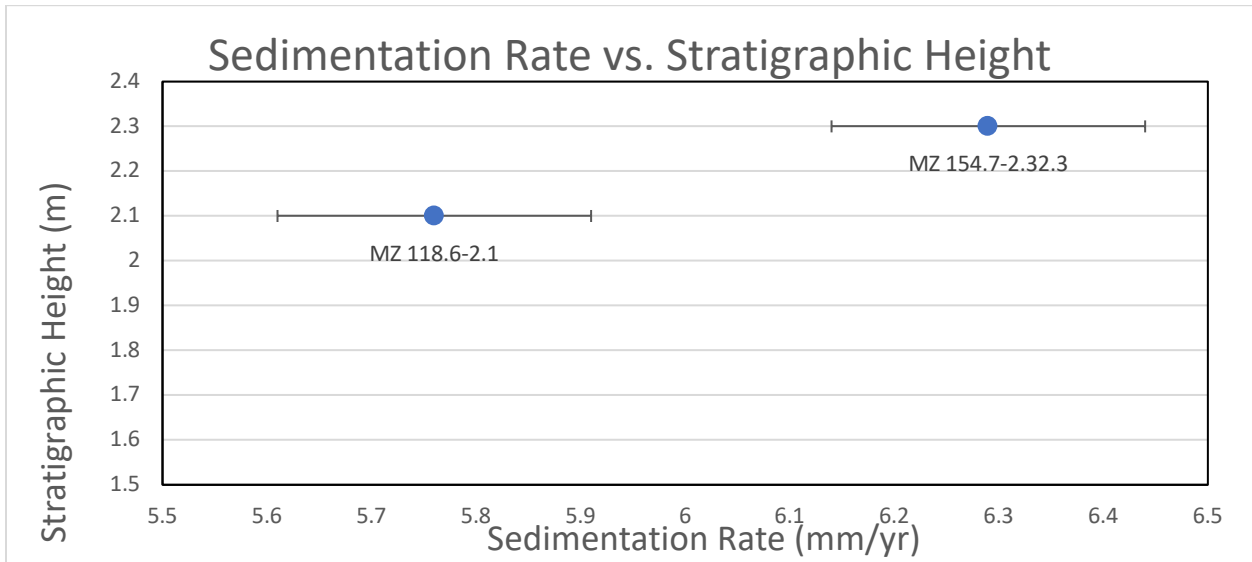


Figure 25: Sedimentation Rare vs Stratigraphic Height for two coral samples selected in this study.

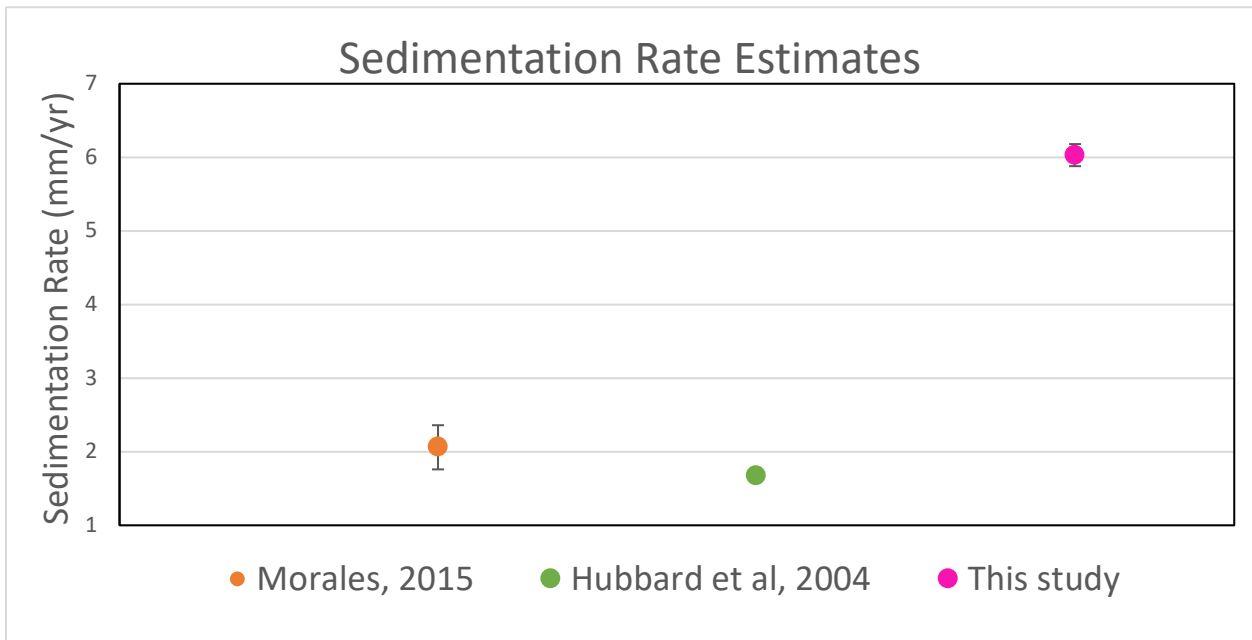


Figure 26: Compared sedimentation rates from Morales, 2015, Hubbard et al., 2004 and this study

6.4 Age of the Coral

The U/Th dates acquired from coral samples MZ 148.8-3.3, MZ 154.7-2.3, MZ 165.9-0.3, MZ 198.4-0.9 are in the mid Holocene Epoch from 5152 ± 30 to 6833 ± 31 yr B.P. and consistent with the MZ coral facies zone age proposed by Hubbard et al. (2004) that reported dates for the mixed coral zone facie to be around 6.2 to 5.7 yr B.P. As projected, as the corals moved up in a vertical direction (stratigraphic height) they had younger dates (Fig. 27). Even though, the corals that are further away from the Enriquillo Lake (lateral position) are the oldest samples, in the stratigraphic position they are located closer to the beginning (base) of the mixed zone facies. However, sample MZ 148.8-3.3 was expected to be the oldest sample, since is the heights sample located in vertical depth (stratigraphic height), but that was not the case, sample MZ 154.7-2.3 was the oldest one.

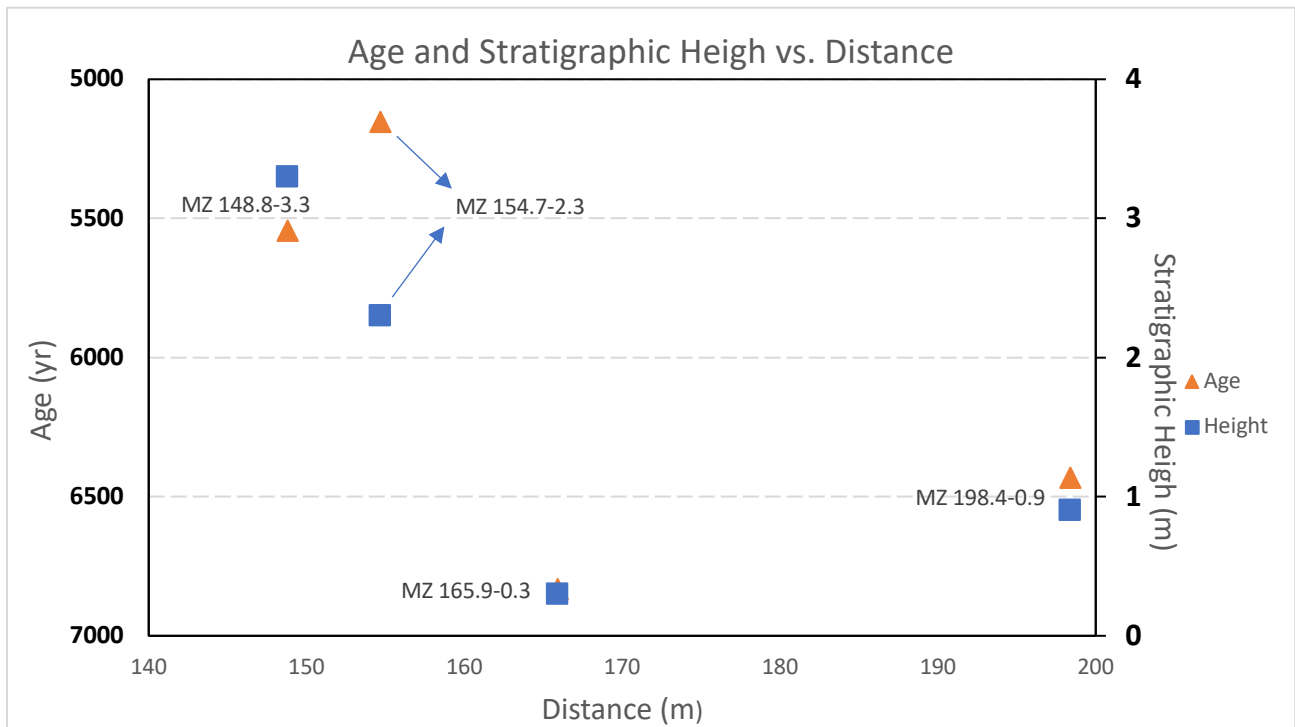


Figure 27: Age and Stratigraphic Height vs. Distance for coral samples MZ 148.8-3.3, MZ 165.9-0.3, MZ 154.7-2.3 and MZ 198.4-0.9.

6.5 Paleoenvironmental Parameters

6.5.1 Element analysis

The Sr/Ca values obtained from coral samples MZ 148.8-3.3 and MZ 165.9-0.3 range from 9.1 to 9.5 mmol/mol. The ratios obtained are slightly higher compared to *Montastraea faveolata* samples (6 kya B.P. to modern) from Dry Tortugas National park, Florida (Flannery and Poore, 2013), *Montastraea sp.* (5 kya B.P. to modern) from Dry Tortugas, Florida (Smith, 2006), and a modern *Montastraea annularis* from Ball Buoy Reef, south Florida (Swart et al., 2002). The best analogs are fossil corals that grew in an similar environment but that is difficult (Giry et al., 2011). The average Sr/Ca record from this study is 9.1-9.4 mmol/mol similar to the Holocene samples (6 kya B.P.) from Flannery et al. (2013) (9.0-9.4 mmol/mol), Smith (2006) (5 kya B.P.) (9.1-9.2 mmol/mol). The Sr/Ca values obtained in this study from corals MZ 148.8-3.3 and MZ 165.9-0.3 are relatively higher than modern coral examples reported by Swart et al (2002) (8.6-9.1 mmol/mol). In general, the Sr/Ca obtained from the MZ corals are similar to the previous studies Flannery et al. (2013) and Smith (2006). Besides the variations produced by temperatures changes, other possible factors that could have cause the high Sr/Ca ratio in the MZ coral analyzed are the presence of secondary aragonite (Sayani et al., 2011), the input of strontium into de bay in sediments and/or groundwater influx, and human error (contamination sample collection and/or processing and sampling in a non-corallite section) (Rosenthal and Linsley, 2006). The mouth of Rio Yaque del Sur was at ~20 km inside the paleo-Enriquillo Bay during the time period the corals in Cañada Honda reef were growing. The water discharge from el Rio Yaque del Sur into the bay was probably creating estuaries conditions which brought a high amount of sediment input into the bay. This could have contributed to the amount of Sr in the water, and probably, diluted the uranium which was already in small quantities.

6.5.2 Stable Isotope Analysis

The $\delta^{18}\text{O}$ values obtained from *Orbicella sp.* in this study are compared to the $\delta^{18}\text{O}$ values obtained from *Orbicella sp.* fossil corals from Enriquillo Lake, Dominican Republic (Greer and Swart, 2006) and $\delta^{18}\text{O}$ values obtained from modern *Orbicella sp.* corals from Looe Key, Florida and *Orbicella sp.* fossil corals from Dry Tortugas, Florida (Smith, 2006). The $\delta^{18}\text{O}$ values obtained from the MZ *Orbicella sp.* in this study (6 kya B.P) range from -2.84 to -3.11 ‰. These values are similar to the values obtained from fossil corals of the same species in Greer and Swart (2006) study (-1.94 to -4.94 ‰) but heavier than the values obtain from fossil corals of the same species in Smith (2006) study (-3.37 to -4.11 ‰) and modern corals of the same species in Smith (2006) study (-3.90 to -3.94‰). The $\delta^{18}\text{O}$ values reported in Greer and Swart (2006) study were obtained from Enriquillo Valley agreeing with the values obtain in this study. Greer and Swart (2006) concluded that by having a more positive $\delta^{18}\text{O}$ from the fossil corals than modern corals is a result of the corals being exposed to a salinity environment. The samples that were selected in Greer and Swart (2006) had a similar age (5.8 - 6.0 kya B.P) that the ones use in this study (5.1 – 6.8 kya B.P.). However, the samples in Greer and Swart (2006) were collected in shallower depths (15.57 m below sea level) than the coral samples collected in this study (17 a 20 m below sea level). $\delta^{18}\text{O}$ can have variations cause by precipitation (depletion in ^{18}O), evaporation (enrichment in ^{18}O) or runoff (depletion in ^{18}O) (Felis et al., 2000; Greer and Swart, 2006). High evaporation result in higher salinity, thus, an increase in $\delta^{18}\text{O}$ (Felis et al., 2000). The $\delta^{18}\text{O}$ of the coral skeleton may reflect salinity fluctuations, especially in extreme precipitation events since tropical temperature variations are minimal on decadal to interdecadal scales (Greer and Swart , 2006). In the eastern seabord, Fairbanks (1982) reported that a change of one salinity unit (ppt) translates to a change in $\delta^{18}\text{O}$ of ~0.6‰ and 0.3‰. For water in the Caribbean, a change of ~0.2‰ per salinity

unit was measured for the $\delta^{18}\text{O}$ /salinity relationship (Swart et al., 2003) where in a closed basin the relationship can be more varied and extreme (Greer and Swart, 2006). In the paleo-Enriquillo Valley estimates of the maximum salinity change allowed by the Holocene $\delta^{18}\text{O}$ coincide with a change of 2-3 ppt to 15 ppt (Greer and Swart, 2006). Even though, a change of 15 ppt is extreme, is still possible for certain coral species to survive this salinity variations. This salinity variations can affect the growth of the coral but would not result in the suspension of the growth effect (Greer and Swart, 2006). Mendez-Tejeda et al. (2016), reported that the salinity gradient of the lake increases eastward suggesting that rainfall conditions in the past were similar to today's conditions. Enriquillo Lake has a highly variable salinity ranging from 98 ppt to 44 ppt (from 1998 to 2004) (Greer and Swart, 2006). The hypersaline Enriquillo Lake had salinity concentration of 70‰ – 101.4‰ until 2003. During 2009 and 2010, slightly lower concentrations were measured, ranging from 26.06‰ to 25.41‰ (Mendez-Tejeda et al., 2016). Another indication that $\delta^{18}\text{O}$ is not only responding to temperature is the covariance of $\delta^{18}\text{O}$ and $\delta^{13}\text{C}$ in corals (Greer and Swart, 2006). By having similar patterns in geochemical variability and a positive correlation between $\delta^{18}\text{O}$ and $\delta^{13}\text{C}$ provides indirect evidence that temperature is not the main factor controlling $\delta^{18}\text{O}$ (Greer and Swart, 2006). When calculating the correlation between $\delta^{18}\text{O}$ and $\delta^{13}\text{C}$ in the coral samples selected, it is notice that the younger coral (MZ 148.8-3.3) has a higher correlation between $\delta^{18}\text{O}$ and $\delta^{13}\text{C}$ than the older coral (MZ 165.9-0.3)(Fig. 21 a&b). This could mean that the older coral (MZ 165.9-0.3) grew in a similar environment to open marine conditions while the younger coral (MZ 165.9-0.3) grew in more unstable conditions.

6.5.3 SST from Sr/Ca

The obtain Sr/Ca ratios in this study were slightly higher than the ratios reported in other studies comparatively to *Montastraea faveolata* samples (6 kya B.P. to modern) from Dry Tortugas National park, Florida (Flannery and Poore, 2013), *Montastraea sp.* (5 kya B.P. to modern) from Dry Tortugas, Florida (Smith, 2006), and a modern *Montastraea annularis* from Ball Buoy Reef, south Florida (Swart et al., 2002). Thus, by having higher Sr/Ca ratios, temperatures are expected to be colder (Rosenthal and Linsley, 2006). To calculate the SST from the Sr/Ca, four equations, based on the same species (*Orbicella sp.*) from different authors and different locations were use (equation 4-7)(Fig. 28). A Sr/Ca-T equation from the paleo-Enriquillo Valley would have been preferred to calculated SST from Sr/Ca derived temperatures since the calculation it is highly dependent on the location (Saenger et al. 2008). However, the environment where the corals grew no longer exist. The alternative used is to use equations that have been produced in similar modern environments as Barahona (Jimenez, 2018). These areas have similar SST but are open marine environments as Dry Tortugas (Flannery and Poore, 2013) contrary to the paleo-Enriquillo Bay where the large embayment and riverine input probably created an estuarine environment. When the calculations from the different equations obtained from MZ 148.8-3.3 are compared the SST calculated with the equation 5 (Smith, 2006)(18-28 °C), equation 6 (Flannery et al., 2013)(19-26 °C) and equation 7 (Jimenez, 2018)(19-24 °C) resulted in similar temperatures, while the SST calculated with equation 4 (Swart et al., 2002) resulted in colder temperatures (15-21°C). When the calculations from the different equations obtained from MZ 165.9-0.3 are compared the SST calculated with the equation 5 (Smith, 2006)(15-26 °C), equation 6 (Flannery et al., 2013)(17-27 °C) and equation 7 (Jimenez, 2018)(18-23 °C) resulted in similar temperatures, while the SST calculated with equation 4 (Swart et al., 2002) resulted in colder temperatures (13-19°C). The

majority of corals are found in regions where mean annual temperatures are not below 24 °C (Felis and Pätzold, 2004). The wide range in temperature is caused by the high variability in Sr/Ca ratio, which could be caused by different factors. Possible factors that could cause the high Sr/Ca ratio in the MZ coral analyzed are the presence of secondary aragonite (Sayani et al., 2011), the input of strontium into the bay in sediments and/or groundwater influx, and human error (contamination sample collection and/or processing and sampling in a non-corallite section) (Rosenthal and Linsley, 2006). High amount of sediment input were entering the paleo-Enriquillo Bay as a result of el Rio Yaque del Sur contributing to the amount of Sr in the water. The normal temperatures tolerance for corals to live are between 18 to 30 °C, where the optimal temperature is 27°C (Felis and Pätzold, 2004). If SST from other facies from Cañada Honda (M1 and M2) are compared with the SST obtained in this study, it can be noticed that the majority of the temperatures are in the temperatures tolerance for corals with the exception of a few from M1 facies (Fig. 29). However, other studies have used different proxies to record the SST around the world. One proxy used to calculate the SST in the Caribbean was the Alkenones. These Alkenones were measured from Grenada in the Lesser Antilles (Rühlemann et al., 1999). The SST-Anomaly obtained with this proxy gave SST-Anomaly that are becoming higher with time, and if the SST-Anomaly from the corals in Cañada Honda are compared with this proxy, a similar trend is observed (Fig. 30).

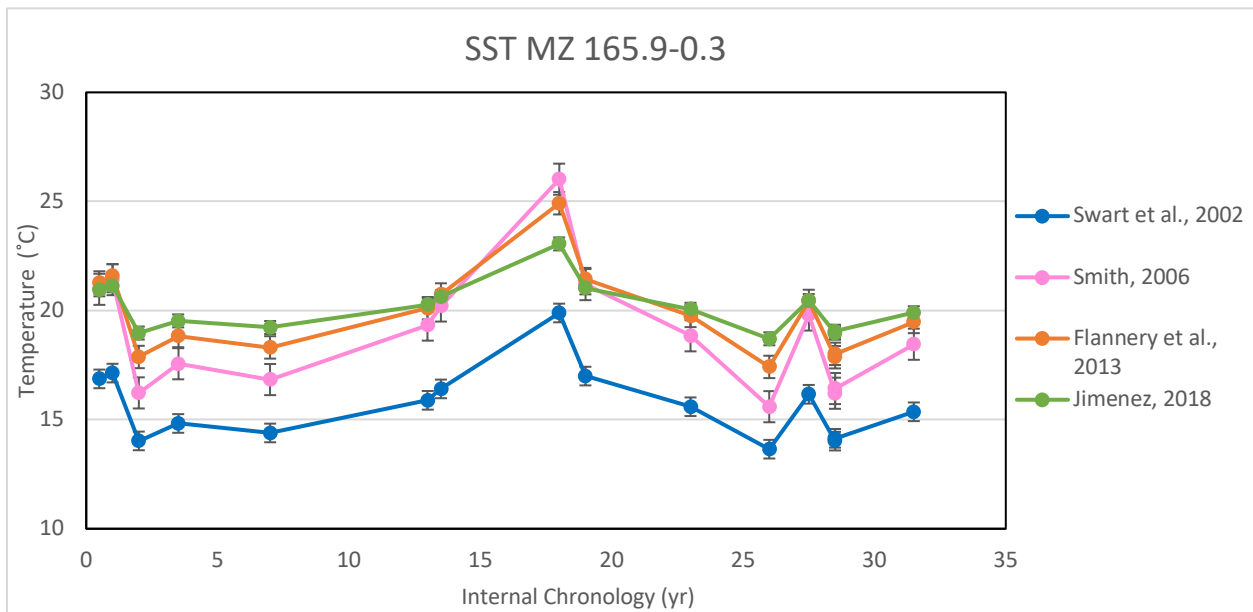
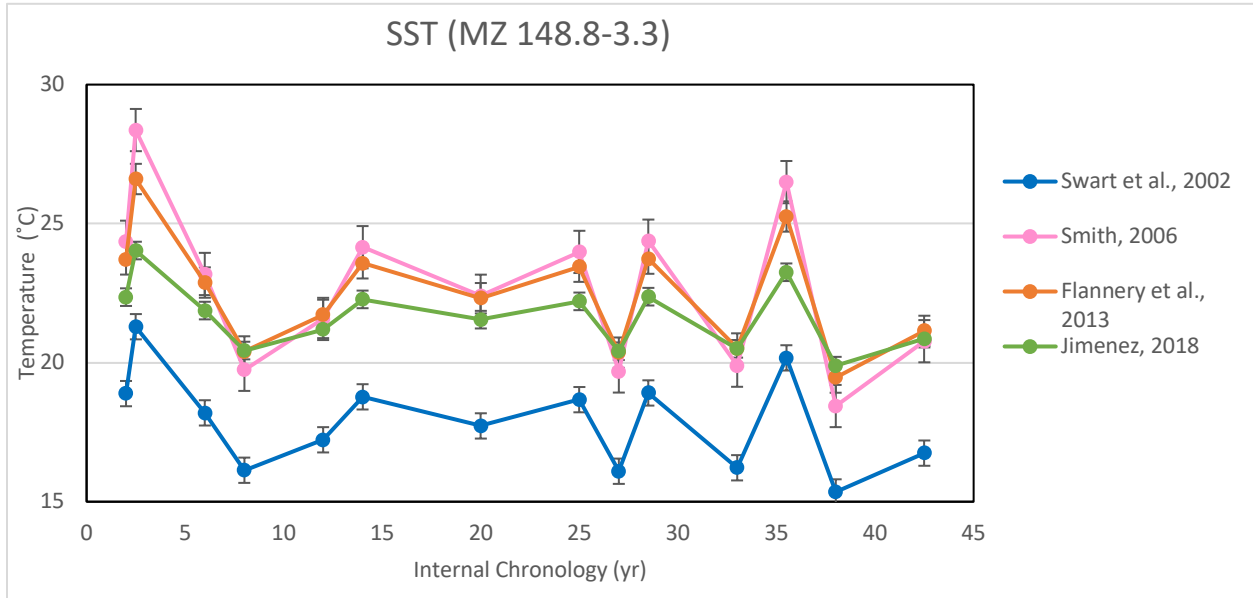


Figure 28: SST from Sr/Ca for coral samples MZ 148.8-3.3 and MZ 165.9-0.3. The SST-Sr/Ca calibration equations reported by different authors are presented in different color.

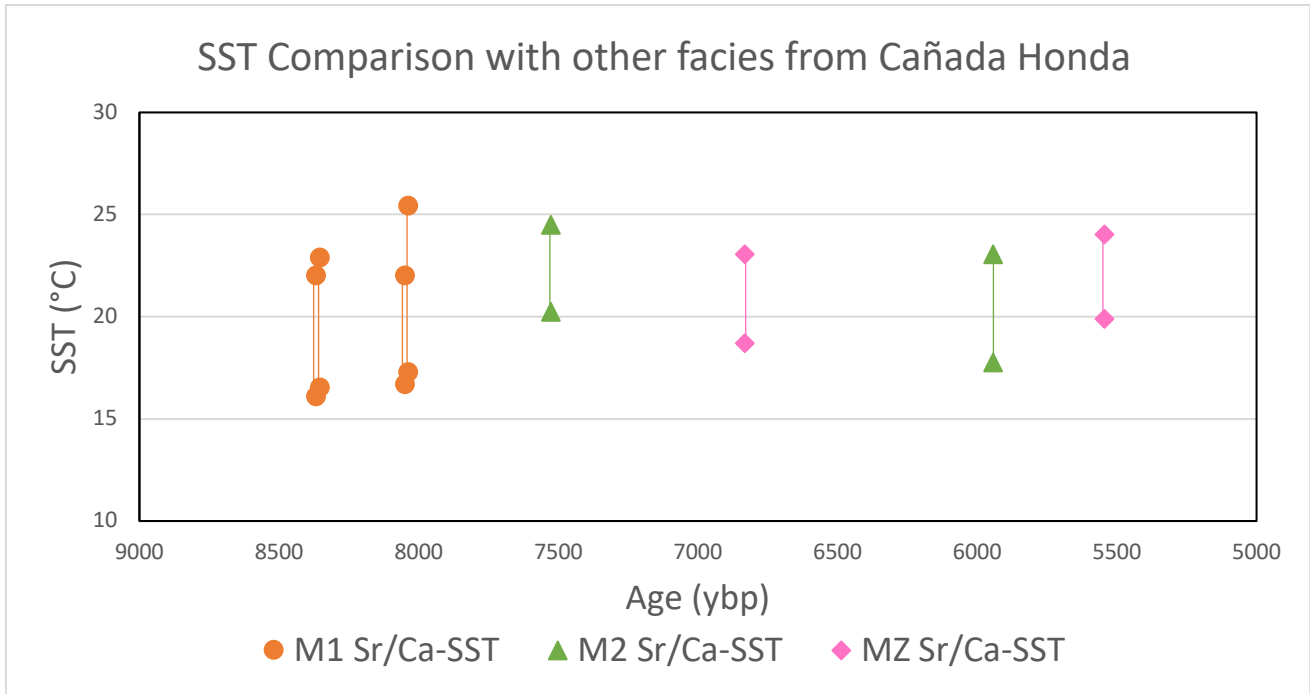


Figure 29: Sr/Ca-SST comparison from M1 (Morales, 2015), M2 (Herrera, 2018) and this study.

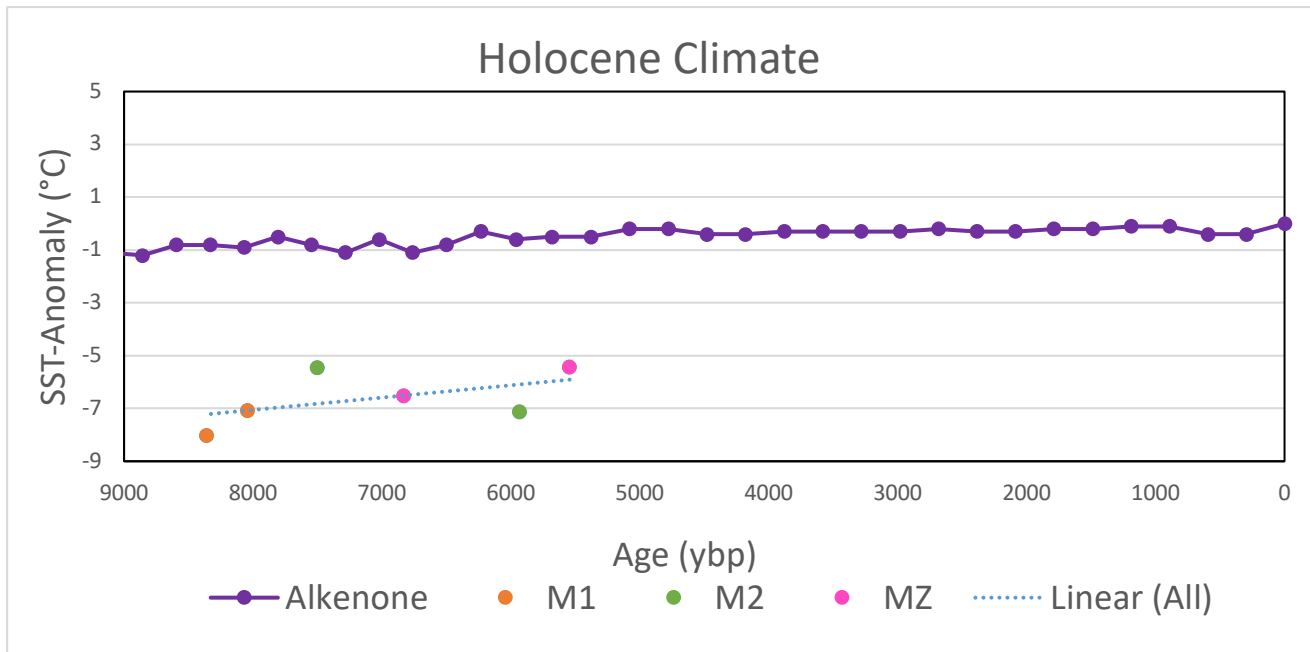


Figure 30: SST-Anomaly from Sr/Ca from Alkenones (Rühlemann et al., 1999) compared to M1 (Morales, 2015), M2 (Herrera, 2018) and this study.

6.5.4 SST from Stable Isotopes

To calculate the SST from the $\delta^{18}\text{O}$ derived for corals MZ 148.8-3.3 and MZ 165.9-0.3, equation 10 reported by Leder et al (1996) was used (Fig. 31). The SST values obtained from coral $\delta^{18}\text{O}$ reported for corals in the Caribbean vary from 18-30°C (Felis and Pätzold, 2004). The upper range (range = 12) of the SST values are 1 degree higher than the SST values from $\delta^{18}\text{O}$ reported by this study (10-21°C, range = 11). Greer and Swart (2006), reported temperatures ranging from 7 to 13 °C from *Orbicella sp.* coral samples in Enriquillo Valley. Smith (2006) reported SST values from $\delta^{18}\text{O}$ using modern corals of *Orbicella sp.* from Looe Key, Florida ranging from 23 to 30°C. Smith (2006) reported temperature changes from -1.9 to +1.5 at 5.1 kya B.P. from *Orbicella sp.* fossil corals from Dry Tortuga, Florida relative to modern samples from the same location. Thus, SST no colder than 21°C were reported in Smith (2006) from Dry Tortugas, Florida. The SST- $\delta^{18}\text{O}$ values obtained from the selected samples in this study are similar to the Greer and Swart (2006) values (Fig. 32). This could indicate that $\delta^{18}\text{O}$ has been affected more by salinity variations than temperatures variation in the water (Greer and Swart, 2006). Temperature fluctuations in the paleo-Enriquillo Bay were possibly greater than at present, a range of 7 – 13 °C in temperature average at 6 ka is highly unlikely, not being recorded evidence to indicate Holocene changes in SST of this scale (Greer and Swart, 2006).

Effective evaporation will increase when annual SST is high, which will create more moisture (Yu et al., 2005). This results in the distill of isotopic lighter oxygen isotope into the water vapor that is transported by atmosphere producing higher $\delta^{18}\text{O}$ and SSS. The residual variation $\delta^{18}\text{O}$ should represent a measure of change ineffective evaporation or moisture by extracting the SST component of the $\delta^{18}\text{O}$ variation based on the difference between coral Sr/Ca and $\delta^{18}\text{O}$ (Yu et al., 2005)(Fig. 33). Obtaining more negative values (negative $\Delta \delta^{18}\text{O}$) results in

having precipitation periods where SSS are lower. Thus, by obtaining less negative values (positive $\Delta \delta^{18}\text{O}$) results in periods of low precipitation where SSS are higher.

The $\delta^{18}\text{O}$ records of the corals from Cañada Honda were influenced by temperature, salinity and rising sea level since they were growing during the mid-Holocene sea level rise, which created the Enriquillo paleo-bay. The $\delta^{18}\text{O}$ values for four of the corals used in this study (MZ 165.9-0.3, MZ 198.4-0.9, MZ 154.7-2.3 and MZ 148.8-3.3) varied between -1.83 to -3.94 giving a range of 2.11‰. Sea level was approximately 6 meters below present sea level at the time the MZ corals were growing, hence 0.06‰ of the oxygen isotope range can be explained by sea level (Chappell and Shackleton, 1986). Enriquillo Valley had an annual temperature range of approximately 4°C over the last century based on temperatures found near the area (Greer, 2001). If the annual temperature range is assumed to be similar during the mid-Holocene, 1.0‰ of the oxygen isotope range from the selected fossil corals in this study can be explained by the 4°C annual range (Dansgaard, 1964; Leder et al., 1996), which means that the remaining 1.05‰ corresponds to salinity. A 1.0‰ change in $\delta^{18}\text{O}$ corresponds to a 4‰ (PSU) change in salinity (Craig, 1966). Therefore, Enriquillo paleo-bay could have had salinity as high as 41 PSU. Another method that can be used to determine salinity is from average Sr-U SST and $\delta^{18}\text{O}$ -SST. Rodriguez (2018) analyzed SST using Sr-U paleothermometer in two corals from Cañada Honda and found an average of 26.3°C SST. The fossil corals used in this study gave a $\delta^{18}\text{O}$ -SST average of 15.2°C. The difference between Sr-U derived SST and $\delta^{18}\text{O}$ -SST is 11.1‰, which corresponds to a 2.8‰ $\delta^{18}\text{O}$ difference. If the same assumptions previously mentioned are used, 1.0‰ by the 4°C temperature range and 0.07‰ of the $\delta^{18}\text{O}$ range corresponds to sea level, which means that the remaining 1.71‰ corresponds to salinity changes. This insinuates that that salinity in the

Enriquillo paleo-bay could have been as high as 41 PSU. Therefore, it can be infer that the corals form Enriquillo Bay were subject to the limit of coral salinity tolerance.

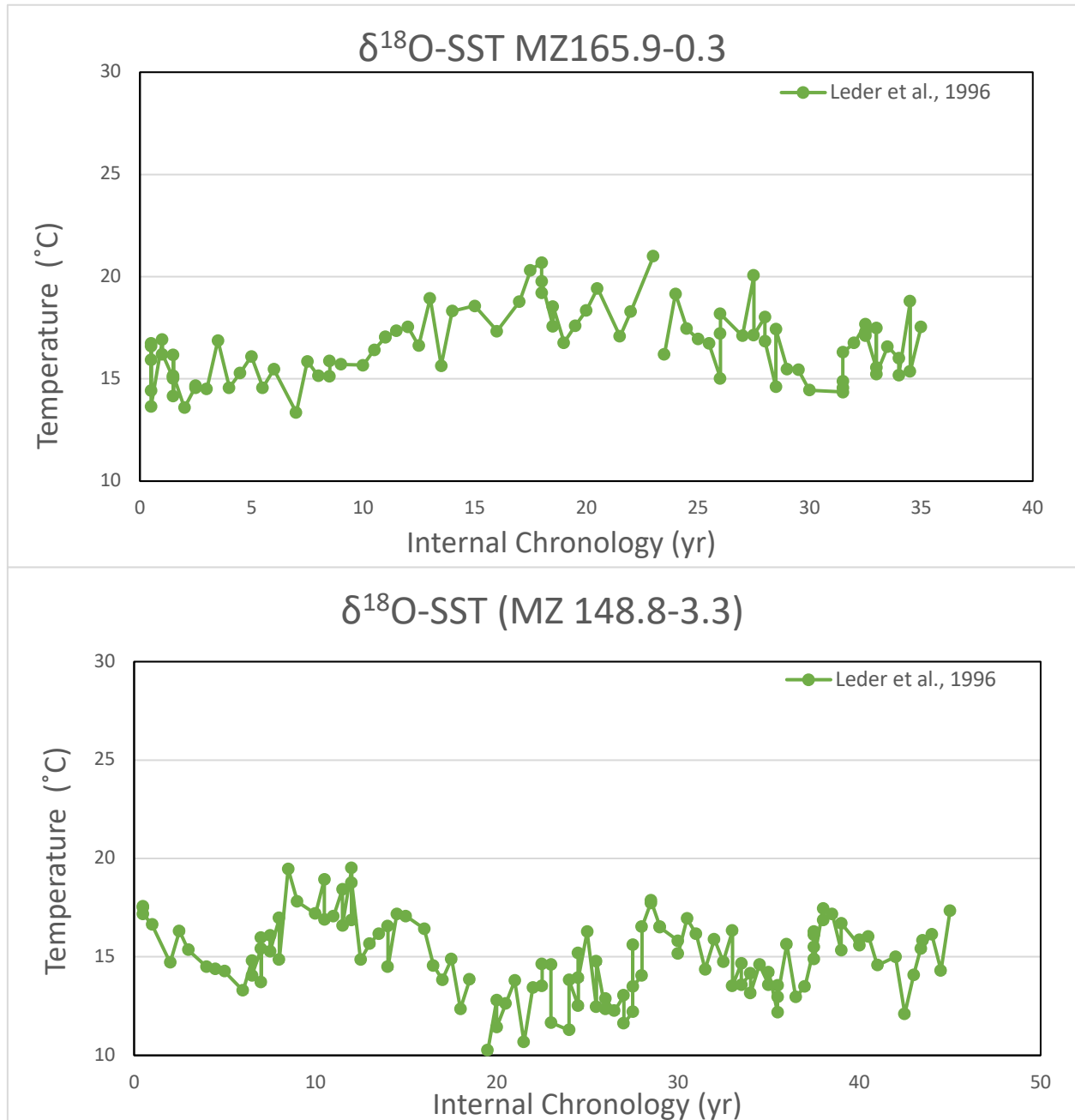


Figure 31: SST obtained from $\delta^{18}\text{O}$ for samples MZ 148.8-3.3 and MZ 165.9-0.3 using Leder et al. (1996).

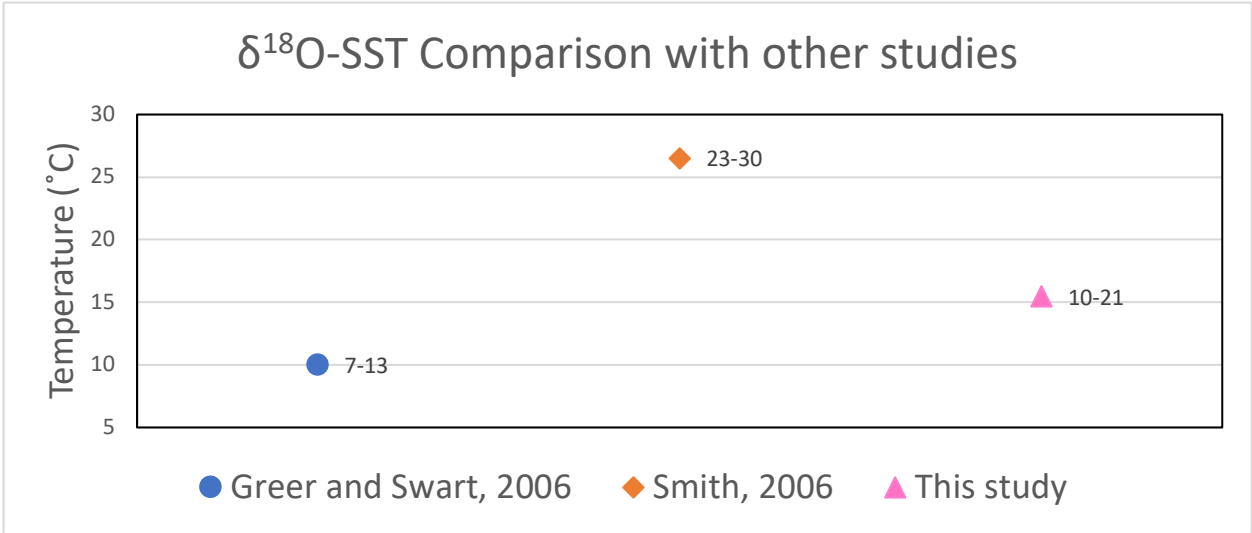


Figure 32: δ¹⁸O-SST comparison with Greer and Swart, 2006, Smith 2006 and this study.

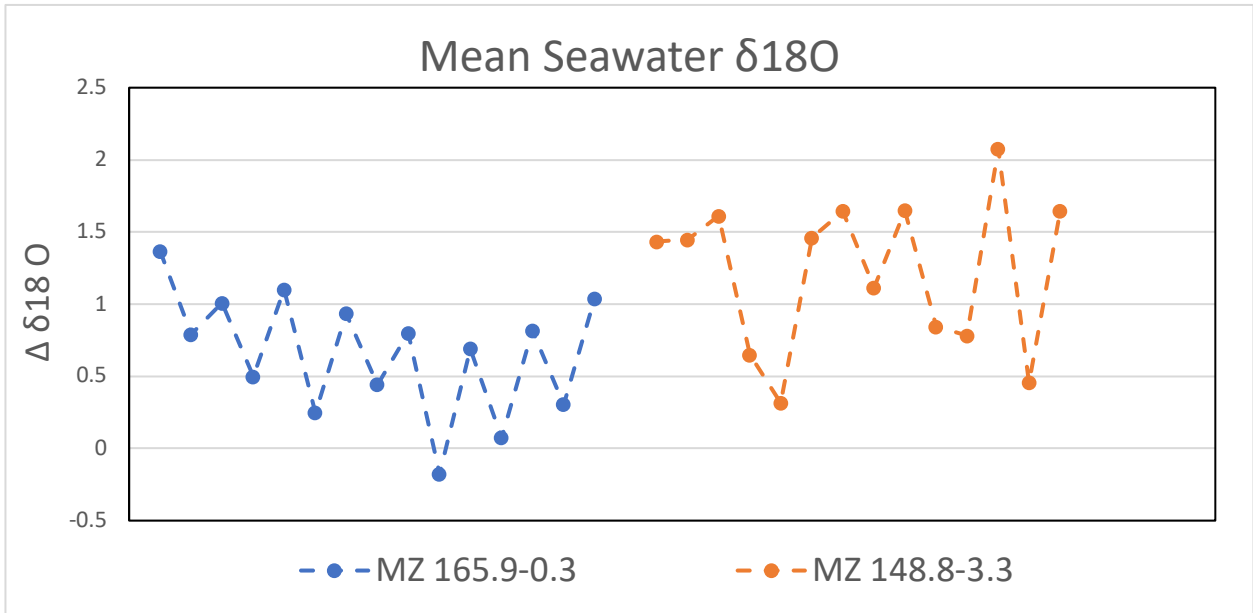


Figure 33: Mean seawater δ¹⁸O for samples MZ 165.9-0.3 and MZ 148.8-3.3. The average value for MZ 165.9-0.3 is 0.66 and for MZ 148.8-3.3 is 1.22.

7.0 Conclusion

(1) Cañada Honda fossil coral reef in Enriquillo provided remarkable well-preserved corals that lived in a shallow water reef environment during the early to middle Holocene. It is difficult to find fossil coral reefs with corals that have pristine preservation. The fast burial of the reef and the relatively dry climate resulted in an outstanding preservation of these fossil corals skeletons. The XRD analysis revealed that the four selected samples (MZ 165.9-0.3, MZ 198.4-0.9, 154.7-2.3 and MZ 148.8-3.3) are composed of at least 98-99% aragonite (detection level is 1-2%). SEM image showed a small amount of secondary aragonite in coral sample MZ 118.6-2.1 sample. This occurrence was limited in sample MZ 118.6-2.1 and not observed in the samples MZ 148.8-3.3, MZ 165.9-0.3, MZ 198.4-0.9 and 154.7-2.3. Concluding that the samples suffered little or almost no alteration. However, this sample was not use for the analysis.

(2) The Cañada Honda reef is dated to be from 9-5 kya B.P. based on the radiocarbon ages from fossil corals sampled at various stratigraphic levels (Cuevas, 2010) and the mixed zone facies is between 5.1-6.8 kya B.P based on the uranium thorium radiogenic date results. The dates obtained in this study are consistent with the dates obtained in Hubbard et al (2004) study (5.7-6.2 kya B.P.) from the same facies. Samples MZ 165.9-0.3 and MZ 198.4-0.9 were between 5.1-5.5 kya B.P. while the other samples MZ 154.7-2.3 and MZ 148.8-3.3 were near 6.4-6.8 kya B.P., representing a 900 yr gap. The corals sample in this study (MZ 165.9-0.3, MZ 198.4-0.9, 154.7-2.3 and MZ 148.8-3.3) based on their stratigraphic height, move from older to younger.

(3) The growth rates produced in this study from corals MZ 165.9-0.3, MZ 198.4-0.9, 154.7-2.3 and MZ 148.8-3.3 (4.37 mm/yr) resulted lower than the growth rates reported in Smith (2006) (6.5 mm/yr) which was measured in open marine environments. This confirms the theory of the presence of high sediment conditions reflecting stress conditions on the corals (Greer and Swart, 2006). Having high sedimentation influx makes the water turbid causing a decrease in the

coral growth. The younger corals represent a slower growth rate, while the older corals have faster growth rates. Coral samples 154.7-2.3 and MZ 148.8-3.3 with age of 5152 and 5545 yr. respectively, had the lower growth rates (4.63 and 4.34 mm/yr). Coral samples MZ 165.9-0.3 and MZ 198.4-0.9 with ages of 6833 and 6441 yr. respectively, had the faster growth rates 4.42 and 4.91 mm/yr). This can implied that in the begging of the formation of the facies more suitable conditions were present and as vertical depth increase the sedimentation input started to be higher. This supports the idea that around 5.0 to 4.0 kyr BP the large open bay was starting to get restricted until it was completely separated from the Caribbean Sea creating the Enriquillo Lake and Valley (Mann et al., 1984). Sedimentation rates can confirm this since the heights sample had a higher value of sedimentation.

(4) By observing the foliated morphology in some of the MZ corals it can be said that stress conditions were affecting the development of the coral. The foliated and columnar morphology combined with the presence of bioerosion, mainly cause by *Lithophaga sp.* is a clear indicator that the environment conditions were not favorable. However, by obtaining close values in growth rate and sedimentation rate it can indicate that the corals were able to keep up with the reef development.

(5) The high $\delta^{18}\text{O}$ values (2.18 to -3.94 ‰) obtained from corals MZ 165.9-0.3, MZ 198.4-0.9, 154.7-2.3 and MZ 148.8-3.3 in the MZ facies suggest a high salinity environment. This indicates that de $\delta^{18}\text{O}$ composition of water is influence by local evaporation and fresh water contribution. For this reason, the $\delta^{18}\text{O}$ of the fossil coral can reflect changes in salinity, especially significant precipitation events (Greer and Swart, 2006). Cañada Honda is surrounded by Sierra de Bahoruco in the south and Sierra Neiba to the north, increasing the precipitation and flooding effect. The mouth of Rio Yaque del Sur was at ~20 km inside the paleo-Enriquillo Bay during the

time period the corals in Cañada Honda reef were growing. The water discharge from el Rio Yaque del Sur into the bay was probably creating estuaries conditions which brought a high amount of sediment input into the bay. It is reported that the salinity gradient of the lake increases eastward which suggest that rainfall conditions in the past were similar to today's conditions (Mendez-Tejeda et al., 2016). Enriquillo Lake has a highly variable salinity ranging from 98 ppt to 44 ppt (from 1998 to 2004) (Greer and Swart, 2006)

(6) The SST obtained from $\delta^{18}\text{O}$ in corals MZ 165.9-0.3, MZ 198.4-0.9, 154.7-2.3 and MZ 148.8-3.3 of the facies MZ obtained (10-21°C) were slightly colder than the temperatures reported for the Caribbean region (18-30°C) by Felis and Pätzold, 2004. However, the SST obtained from $\delta^{18}\text{O}$ in corals MZ 165.9-0.3, MZ 198.4-0.9, 154.7-2.3 and MZ 148.8-3.3 of the facies MZ obtained reported in this study are similar to the temperatures reported by Greer and Swart (2006) indicating that the temperatures are not consistent in Enriquillo Valley. Thus, suggesting that SST- $\delta^{18}\text{O}$ temperatures have been affected more by salinity variations than temperatures variation in the water (Greet and Swart, 2006).

(7) The Sr/Ca ratios measured in corals MZ 165.9-0.3, MZ 198.4-0.9, 154.7-2.3 and MZ 148.8-3.3 of the facies MZ resulted relatively higher than Sr/Ca measurements reported for modern corals but similar to Holocene samples from different locations. There are various factors that can produced higher Sr/Ca ratios 1) presence of secondary aragonite; 2) the input of sediment and/or groundwater influx; 3) human error, such as, processing and sampling in a non-corallite section and/or contamination in sample collection. By measuring higher Sr/Ca ratios, the temperatures obtain were colder than anticipated. To obtain precise temperatures, a Sr/Ca calibration equation from Enriquillo Valley would have been preferred, but the environment where

the corals grew no longer exist making it difficult to complete. Sr/Ca calibrations from other studies from similar environments had to be use to obtain the SST-derived temperatures.

(8) However, a new Sr/Ca calibration equation (Jimenez, 2018) using a modern coral from Barahona Bay southeast of Enriquillo was use to obtain temperatures from the selected samples. Barahona is also surrounded by the same mountain ranges as Cañada Honda (Sierra de Neiba and Sierra Bahoruco), hence, the coral reef has the same sedimentation influx. The coral use is also influence by the discharge of Yaque del Sur River as Cañada Honda reef was. Resulting in similar temperature values than Flannery and Poore (2013) and Smith (2006). Thus, having a wide range in SST-Sr/Ca temperatures, which is cause by the variability in Sr/Ca ratio, could be produce by different factors. A more longer and continuous record of $\delta^{18}\text{O}$ and Sr/Ca values is necessary.

References

- Adkins, J.F., Griffin, S., Kashgarian, M., Cheng, H., Druffel, E.R., Boyle, E.A., Edwards, R.L., Shen, Chuan-Chou, 2002, Radiocarbon dating of deep-sea corals, *Radiocarbon*, Vol. 44, nr. 2, p. 567-580.
- Aronson, R.B. and Precht, W.F., 2001, Applied Paleocology and the Crisis on Caribbean coral reefs. *PALAIOS*, 16, p. 195-195.
- Birgmark, D., 2014, El Niño-Southern Oscillation and North Atlantic Oscillation induced sea surface temperature variability in the Caribbean Sea [M.S. thesis]: University of Gothenburg, 27 p.
- Brachert, T. C., M. Reuter, K. F. Kroeger, and J. M. Lough, 2006, Coral growth bands: A new and easy to use paleothermometer in paleoenvironment analysis and paleoceanography (late Miocene, Greece), *Paleoceanography*, 21, PA4217, doi:10.1029/2006PA001288.
- Bryson, R. A., and Goodman, B. M., 1980, Volcanic activity and climatic: *Science*, 207(4435), 1041-1044.
- Budd, A., Fukami, H., Smith, N., and Knowlton, N., 2012, Taxonomic classification of the reef coral family Mussidae (Cnidaria: Anthozoa: Scleractinia), *Zoological Journal of the Linnean Society*, Vol. 166, No. 3, p 465-529.
- Chappell, J., and Shackleton, N., 1986, Oxygen isotopes and sea level. *Nature*, 324(6093), 137.
- Cheng, H., Edwards, R.L., Shen, C.C., Polyak, V.J., Asmerom, Y., Woodhead, J., Hellstrom, J., Wang, Y., Kong, X., Spötl, C., Wang, X., Alexander, E.C., 2013, Improvements in ^{230}Th dating, ^{230}Th and ^{234}U half-life values, and U-Th isotopic measurements by a multi-collector inductively coupled plasma mass spectrometry, *Earth and Planetary Science Letters*, 371- 372, 82-91.
- Chollett, I., Müller-Karger, F. E., Heron, S. F., Skirving, W., and Mumby, P. J., 2012, Seasonal and spatial heterogeneity of recent sea surface temperature trends in the Caribbean Sea and southeast Gulf of Mexico: *Marine Pollution Bulletin*, 64(5), 956-965.
- Cohen, A.L., Layne, G.D., and Hart, S.R., 2001, Kinetic control of skeleton Sr/Ca in a symbiotic coral: Implications for the paleotemperature proxy, *Paleoceanography*, Vol. 16, No. 1, p. 20-26.
- Corrège, T., 2006, Sea surface temperature and salinity reconstruction from coral geochemical tracers, : *Palaeogeography, Palaeoclimatology, Palaeoecology*, 232, 408-428.
- Craig, H., 1966, Isotopic composition and origin of the Red Sea and Salton Sea geothermal brines. *Science*, 154(3756), 1544-1548.

- Cramer, K.L., Jackson, J.B.C., Angioletti, C.V., Leonard-Pingel, J., Guilderson, T.P., 2012, Anthropogenic mortality on coral reefs in Caribbean Panama predates coral disease and bleaching, *Ecology Letters*, 15, 561-567.
- Cuevas, D.N., Sherman, C.E., Ramirez, W., Díaz, V., Hubbard, D.K., 2005, Development of Mid-Holocene Cañada Honda fossil reef, Dominican Republic: Preliminary results and implications to modern trends of reef degradation in high sedimentation environments, 17th Caribbean Geological Conference in San Juan, Puerto Rico, 27-36.
- Cuevas, D.N., Sherman, C.E., Ramirez, W., Hubbard, D., 2009, Coral growth rates from the Holocene Cañada Honda fossil reef, Southwestern Dominican Republic: Comparisons with modern counterparts in high sedimentation settings, *Caribbean Journal of Science*, Vol. 45, No. 1, 94-109.
- Cuevas, D.N., 2010, Development of the Holocene Cañada Honda Fossil Reef, Dominican Republic: Short and long-term responses to high sedimentation [M.S. Thesis]: University of Puerto Rico, Mayagüez Campus, 80 p.
- Dansgaard, W., 1964, Stable isotopes in precipitation. *Tellus*, 16(4), 436-468.
- Delanoy, R.A., and Méndez-Tejeda, R., 2017, Hydrodynamic Study of Lake Enriquillo in Dominican Republic, *Journal of Geoscience and Environment Protection*, 5, 115-124.
- Denton, G. H., and Karlén, W., 1973, Holocene climatic variations—their pattern and possible cause: *Quaternary Research*, 3(2), 155IN1175-174IN2205.
- Diaz, V.D., 2005, The effects of terrigenous sedimentation on the growth rate and morphology of the Holocene fossil corals of Cañada Honda in Enriquillo Valley, Southern Dominican Republic, [Unpublished Undergraduate Investigation]: University of Puerto Rico, Mayagüez Campus.
- Downs, R.T., 2006, The RRUFF Project: an integrated study of the chemistry, crystallography, Raman and infrared spectroscopy of minerals. Program and Abstracts of the 19th General Meeting of the International Mineralogical Association in Kobe, Japan, 003-13.
- Edwards, R.L., Chen, J.H., Wasserburg, G.J., 1985, Precise measurements of $^{234}\text{U}/^{238}\text{U}$ in Pacific and Atlantic profiles, *Geol. Soc. Am., Abst. Prog.* 17, 572.
- Flannery, J.A., Poore, R.Z., 2013, Sr/Ca proxy sea-surface temperature reconstructions from modern and Holocene *Montastraea faveolata* specimens from the Dry Tortugas National Park, Florida, U.S.A., *Journal of coastal Research*, 63, 20-31.
- Fairbanks, R.G., 1982, The origin of continental shelf and slope water in the New York Bight and Gulf of Maine: Evidence from $\text{H}^1\text{2}^8\text{O}/\text{H}^1\text{2}^6\text{O}$ ratio measurements, *J. Geophys. Res.*, 87, 5796–5808.

- Felis, T. and Pätzold, J., 2004, Climate Reconstruction from annually banded corals, *Global Environmental Change in the Ocean and on Land*, Eds. M. Shiyomi et al., 205-227.
- Felis, T., Pätzold, J., Loya, Y., Fine, M., Nawar, A. H., and Wefer, G., 2000, A coral oxygen isotope record from the northern Red Sea documenting NAO, ENSO, and North Pacific teleconnections on Middle East climate variability since the year 1750. *Paleoceanography*, 15(6), 679-694.
- Giannini, A., Cane, M. A., and Kushnir, Y., 2001, Interdecadal changes in the ENSO teleconnection to the caribbean region and the north atlantic oscillation*: *Journal of Climate*, 14(13), 2867-2879.
- Giry, C., Felis, T., Kölling, M., Scholz, D., Wei, W., Lohmann, G., Scheffers, S., 2012, Mid- to late Holocene changes in tropical Atlantic temperature seasonality and interannual to multidecadal variability documented in southern Caribbean corals: *Earth and Planetary Science Letters*, 331-332, 187-200.
- Goudeau, M. S., Reichert, G. J., Wit, J. C., De Nooijer, L. J., Grauel, A. L., Bernasconi, S. M., and De Lange, G. J., 2015, Seasonality variations in the Central Mediterranean during climate change events in the Late Holocene: *Palaeogeography, Palaeoclimatology, Palaeoecology*, 418, 304-318.
- Greer, L. and Swart, P.K., 2006, Decadal cyclicality of regional mid-Holocene precipitation: Evidence from Dominican coral proxies, *Paleoceanography*., 21, PA2020, doi:10.1029/2005PA001166.
- Greer, L., 2001, Seasonal to Centennial Holocene and Modern Climate Variability in the Dominican Republic [Ph.D. Thesis]: Miami, University of Miami, 228 p.
- Grottoli, A.G, 2001, Climate: Past Climate from Corals, in: *Encyclopedia of Ocean Sciences* [eds. Steele, J., Thorpe, S., Turekian, K.], Academic Press, London p. 2098-2107.
- Haase-Schramm, A., Böhm, F., Eisenhauer, A., Vacelet, J., Reitner, J., Wörheide, G., Garbe-Schönberg, D., Dullo, W.-Chr., Pawlik, J., 2003, Application of Sr/Ca Ratios in Sclerosponges as Temperature Proxy, PP52A-0965.
- Haigh, J., 2011, Solar influences on Climate, Grantham Institute for Climate Change, Biefing paper No. 5, p. 20.
- Hendy, E.J., Gagan, M.K., Lough, J.M., McCulloch, M., deMenocal, P.D., 2007, Impact of skeletal dissolution and secondary aragonite on trace element and isotopic climate proxies in Porites corals, *Paleoceanography*, 22, PA4101, doi:10.1029/2007PA001462
- Herrera, Y., 2018, Middle Holocene SST record (7518 to 5944 ybp) based on corals from th Enriquillo Valley, Dominican Republic, [Unpublished M.S. Thesis]: University of Puerto Rico, Mayagüez Campus.

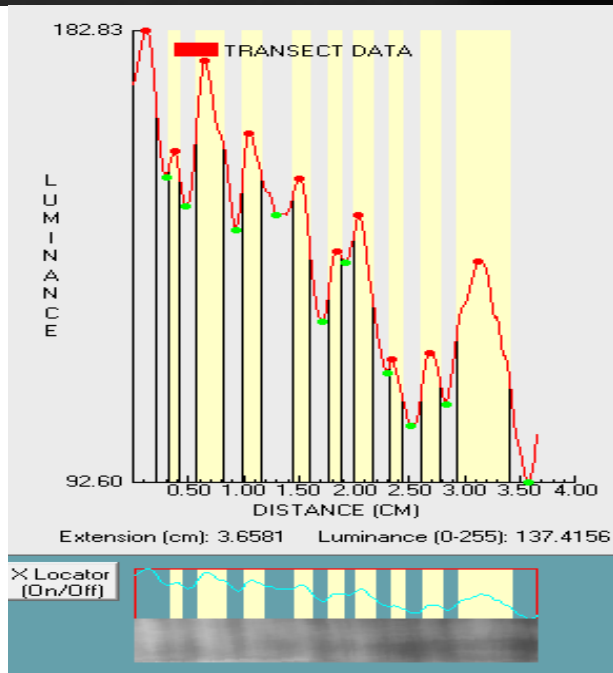
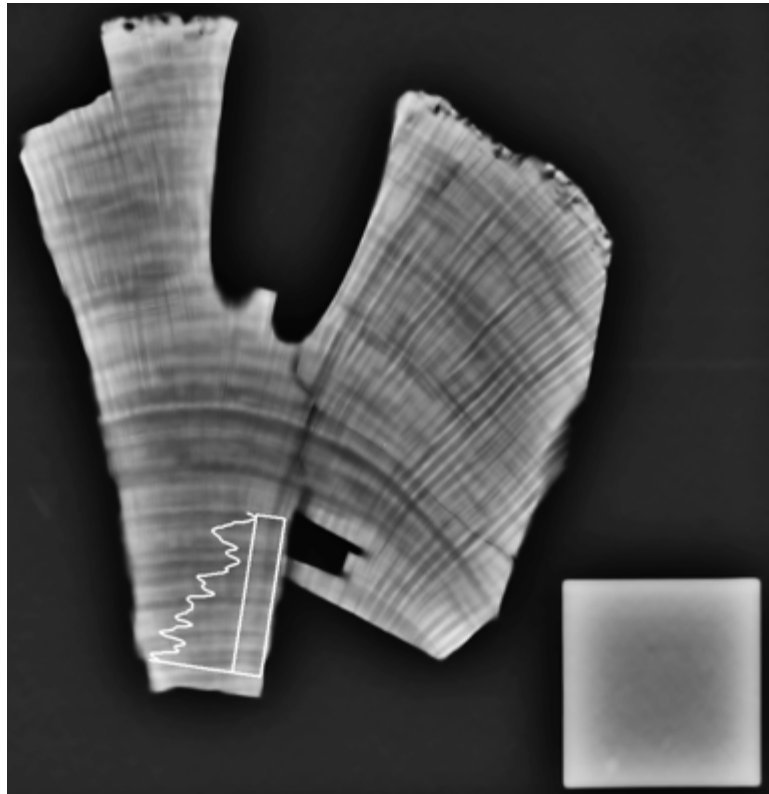
- Heubeck, C. , and P. Mann, 1991, Geologic Evaluation of Plate-kinematic Models for the North American-Caribbean Plate Boundary Zone: *Tectonophysics* , 191, p. 1-26.
- Hubbard, D.K., Ramirez, W., Cuevas, D., 2004, A preliminary model of Holocene coral-reef development in the Enriquillo Valley, SW Dominican Republic. Abstract. *GSA Abstracts with Programs*, Vol. 36, No. 5, p. 291.
- Hubbard, D.K., Ramirez, W., Cuevas D., Erickson, T., Estep, A., 2008, Holocene reef accretion along the north side of Bahia Enriquillo (western Dominican Republic): unique insights into patterns of reef development in response to sea-level rise, *Proceedings of the 11th International Coral Reef Symposium*, Ft. Lauderdale, Florida, 43-47.
- Hughes, T.P., 1994, Catastrophes, Phase Shifts, and Large-Scale Degradation of a Caribbean Coral Reef, *Science*, Vol. 265, p. 1547-1551.
- Jaffey, A.H., Flynn, K.F., Glendenin, L.E., Bentley, W.C., Essling, A.M., 1971, Precision measurement of half-lives and specific activities of ^{235}U and ^{238}U . *Phys. Rev. C4*, 1889–1906.
- Jimenez, A., 2018, Sea Surface Temperature reconstruction (Sr/Ca) from modern and fossil coral Caribbean Holocene corals [Unpublished M.S. Thesis]: University of Puerto Rico, Mayagüez Campus.
- Jimenez, I. M., Larkum, A. W., Ralph, P. J., and Kühl, M., 2012, In situ thermal dynamics of shallow water corals is affected by tidal patterns and irradiance: *Marine biology*, 159(8), 1773-1782.
- Kilpatrick, K. A., Podestá, G., Walsh, S., Williams, E., Halliwell, V., Szczodrak, M., and Evans, R., 2015, A decade of sea surface temperature from MODIS, *Remote Sensing of Environment*, 165, 27-41.
- Lane, C. S., Horn, S. P., Mora, C. I., and Orvis, K. H., 2009, Late-Holocene paleoenvironmental change at mid-elevation on the Caribbean slope of the Cordillera Central, Dominican Republic: a multi-site, multi-proxy analysis: *Quaternary Science Reviews*, 28(23), 2239-2260.
- Leder., J.J., Swart, P.K., Szmant, A., Dodge, R.E., 1996, The origin of variations in the isotopic record of Scleractinian corals; I Oxygen, *Geochim. Cosmochim. Acta*, 60, 2857-2870.
- Magny, M., Leuzinger, U. R. S., Bortenschlager, S., & Haas, J. N., 2006, Tripartite climate reversal in Central Europe 5600–5300 years ago. *Quaternary research*, 65(1), 3-19.
- Mann, P., Hernaiz, P., Ramirez, W., 2008, Stratigraphy, tectonics and subsurface petroleum geology of Ocoa, Azua, and Enriquillo basins, Dominican Republic: 18th Caribbean Geological Conference, 127p.

- Mann, P., 1999, Caribbean sedimentary basins: Classification and tectonic setting from Jurassic to present: *Sedimentary Basins of the World*, 4, 3-90.
- Mann, P., McLaughlin P., Van Den Bold, W., Lawrence, S., Lamar M., 1999, Tectonic and Eustatic Controls on Neogene Evaporitic and Siliciclastic Deposition in the Enriquillo Basin, Dominican Republic: *Sedimentary Basins of the World*, 4, 3287-342.
- Mann, P., Taylor, F.W., Edwards, R.L., Ku, T., 1995, actively evolving microplate formation by oblique collision and sideways motion along strike-slip faults: An example from the northeastern Caribbean plate margin, *Tectonophysics*, 246, 1-69.
- Mann, P., Lawrence, S., 1991, Petroleum potential of Southern Hispaniola: *Journal of Petroleum Geology*, 14, No. 3, 291-308.
- Mann, P., Taylor, F. W., Burke, K. and Kulstad, R., 1984, Subaerially exposed Holocene coral reef, Enriquillo Valley, Dominican Republic: *Geological Society of America Bulletin*, v. 95, p. 1084-1092.
- Maslin, M., Stickley, C., and Ettwein, V., 2010, Holocene climate variability: *Marine Policy & Economics: A Derivative of the Encyclopedia of Ocean Sciences*, 479.
- Mayewski, P.A., Rohling, E.E., Stager J.C., Karlé, W., Maasch, K.A., Meeker L.D., Meyerson, E.A., Gasse, F., van Kreveld, S., Holmgren, K., Lee-Thorp, J., Rosqvist, G., Rack, F., Staubwasser, M., Schneider R.R., Steig, E.J., 2004, Holocene climate variability: *Quaternary Research*, 62, 243-255.
- Mendez-Tejeda, R., Rosado, G., Rivas, D.V., Montilla, T., Hernández, S., Ortiz, A., Santos, F., 2016, Climate Variability and its effects on the increased level of lake Enriquillo in the Dominican Republic, 2000-2013, Vol. 4, No. 1, 26-36.
- Mickler, P. J., Stern, L. A., and Banner, J. L., 2006, Large kinetic isotope effects in modern speleothems: *Geological Society of America Bulletin*, 118(1-2), 65-81.
- Morales, J., 2015, Reconstructing sea surface temperatures in the Caribbean during the early-mid Holocene from a reef exposure in Cañada Honda, Enriquillo Valley, Dominican Republic [M.S. Thesis]: University of Puerto Rico, Mayagüez Campus, 105 p.
- Nurhati, I.S., Cobb, K.M., Charles, C.D., Dunbar, R.B., 2009, Late 20th century warming and freshening in the central tropical Pacific, *Geophys. Res. Lett.*, 36, L21606, doi:10.1029/2009GL040270.
- Nurhati, I. S., Cobb, K.M., and Di Lorenzo, E., 2011, Decadal-Scale SST and Salinity Variations in the Central Tropical Pacific: Signatures of Natural and Anthropogenic Climate Change, *Journal of Climate*, 24.13, 3294-3308.
- Pandolfi, J.M., 2002, Coral community dynamics at multiple scales, *Coral Reefs*, 21, 13-23.

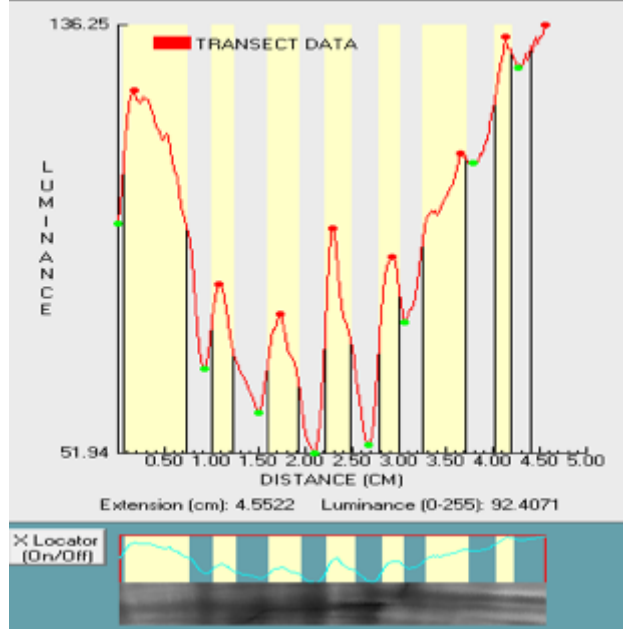
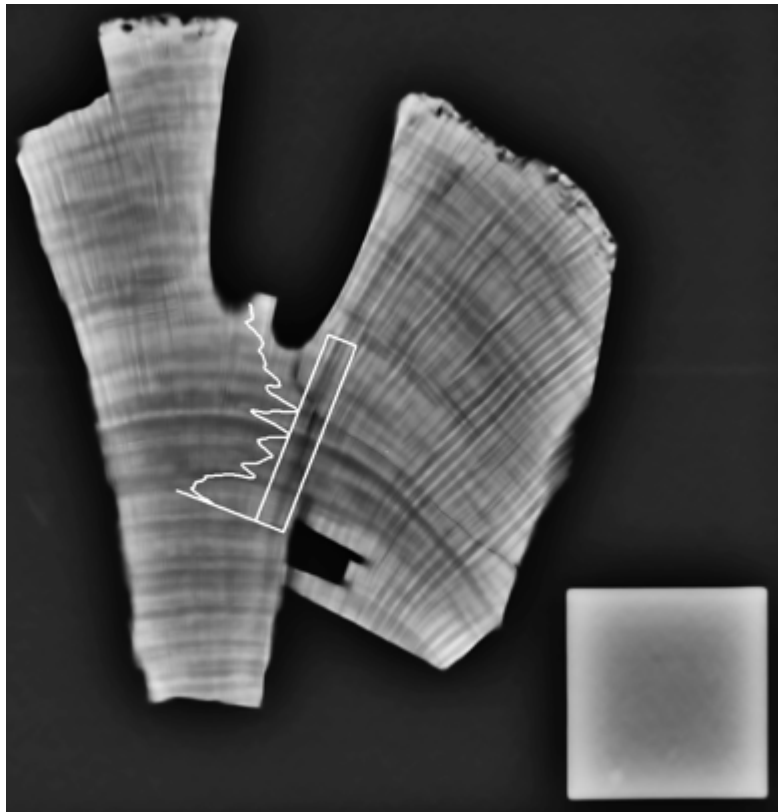
- Reuter M, Brachert TC, Kroeger KF., 2005, Diagenesis of growth bands in fossil scleractinian corals: identification and modes of preservation. *Facies* 51:146–159. doi: 10.1007/s10347-005-0064-7
- Renssen, H., Goosse, H., & Muscheler, R., 2006, Coupled climate model simulation of Holocene cooling events: solar forcing triggers oceanic feedback. *Climate of the Past Discussions*, 2(3), 209-232.
- Robinson, L.F., Belshaw, N.S., Henderson, G.M., 2004, U and Th concentrations in isotope ratios in modern carbonates and waters from the Bahamas, *Geochimica et cosmochimica Acta*, 68, No. 8, 1777-1789.
- Rodriguez, L.G., 2018, Application of the Sr-U coral paleo-thermometer to reconstruct sea surface temperatures during the Mid-Holocene using corals from Cañada Honda, Dominican Republic, [Unpublished M.S. Thesis]: University Of Puerto Rico, Mayagüez Campus.
- Roland, T. P., Daley, T. J., Caseldine, C. J., Charman, D. J., Turney, C. S. M., Amesbury, M. J., Thompson, G.J., and Woodley, E. J., 2015, The 5.2 ka climate event: Evidence from stable isotope and multi-proxy palaeoecological peatland records in Ireland. *Quaternary Science Reviews*, 124, 209-223.
- Rosado G., Rafael M.T., Rivas V.D., Infante I. M. (2016) Physicochemical analysis of Lake Enriquillo in Dominican Republic. *Open Science Journal* 1(3).
- Rosenthal, Y. and Linsley, B., 2006, Mg/Ca and Sr/Ca Paleothermometry from calcareous marine fossils, *Encyclopedia of Quaternary Sciences*, Elsevier Ltd, 20 p.
- Rühlemann, C., Mulitza, S., Müller, P.J., Wefer, G., Zahn, R., 1999, Sea surface temperature reconstruction based on alkenones of sediment core M35003-4. *PANGAEA*, <https://doi.org/10.1594/PANGAEA.734784>
- Saenger, C., Cohen, A.L., Oppo D.W., Hubbard, D, 2008, Interpreting sea surface temperature from strontium/calcium ratios in *Monstrastraea* corals: Link with growth rate and implications for proxy reconstructions, *Paleoceanography.*, 23, PA3102, doi:10.1029/2007PA001572.
- Sayani, H.R., Cobb, K.M., Cohen, A.L., Crawford, E.W., Nurhati, I.S., Dunbar, D.B., Rose, K.A., Zaunbrecher, L.K., 2011, *Geochimica et Cosmochimica Acta*, 75, 6361-6373.
- Schrag, D.P., 1999, Rapid analysis of high-precision Sr/Ca ratios in corals and the other marine carbonates. *Palaeoceanography*, 14, 97-102.
- Smith, J.M., 2006, Geochemical signatures in the coral *Monstrastrea*: Modern and mid-Holocene perspectives, *Theses and Dissertations*, paper 2706, p. 125.
- Stoll, H.M., Schrag, D.P., Clemens, C.S., 1999, Are seawater Sr/Ca ratio preserved in Quaternary foraminifera?, *Geochimica et Cosmochimica Acta*, Vol. 63, no. 21, 3535-3547.

- Swart, P.K. and Grottoli, A., 2003, Proxy indicators of climate in coral skeletons: a perspective, *Coral Reefs*, 22, 313-315.
- Swart, P.K., Elderfield, H., Greaves, M.J., 2002, A high-resolution calibration of Sr/Ca thermometry using the Caribbean coral *Montrastrea annularis*, *Geochem. Geophys. Geosyst.*, 3, 11, 8402.
- Wanner, H., Beer, J., Bütikofer, J., Crowley, T.J., Flückiger, J., Cubasch, U., Goosse, H., Grosjean, M., Joos, F., Küttel, M., Kaplan, J.O., Müller, S.A., Prentice, I.C., Solomina, O., Stocker, T.F., Tarasov, P., Wagner, M., Widmann, M., 2008, Mid- to Late Holocene climate change; an overview: *Quaternary Science Reviews*, 27, 1791-1828.
- Werner, K., Müller, J., Husum, K., Spielhagen, R. F., Kandiano, E. S., and Polyak, L., 2015, Holocene sea subsurface and surface water masses in the Fram Strait—Comparisons of temperature and sea-ice reconstructions: *Quaternary Science Reviews*.
- Winter, A., Ishioroshi, H., Watanabe, T., Oba, T., Christy, J., 2000, Caribbean sea surface temperatures: two-to-three degrees cooler than present during the Little Ice Age, *Geophysical Research Letters*, 27, No. 20, 3365-3368.
- Yu, Ke-Fu., Zhao, Jian-Xin., Wei, Gang-Jian., Cheng, Xin-Rong., and Wang, Pin-Xian., 2005, Mid-late Holocene monsoon climate retrieved from seasonal Sr/Ca and $\delta^{18}\text{O}$ records of *Porites lutea* corals at Leizhou Peninsula, northern coast of South China Sea, *Global and Planetary change*, 47, 301-316.

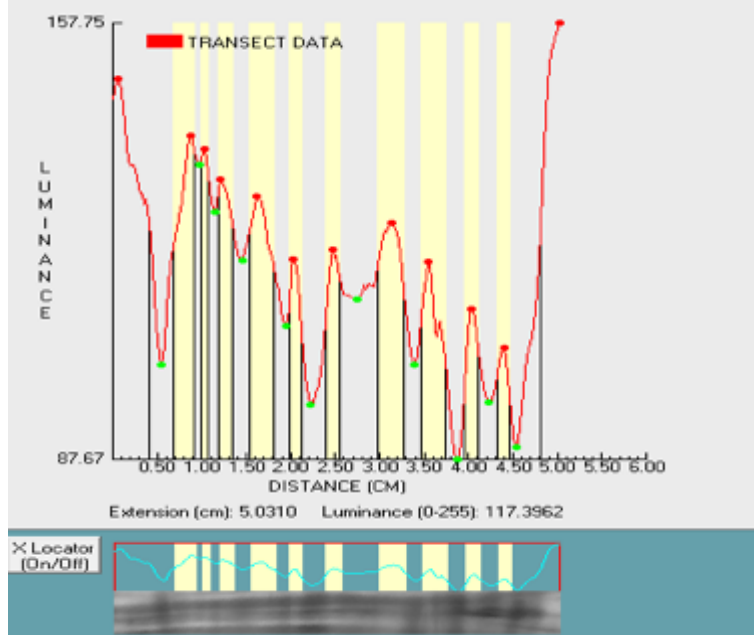
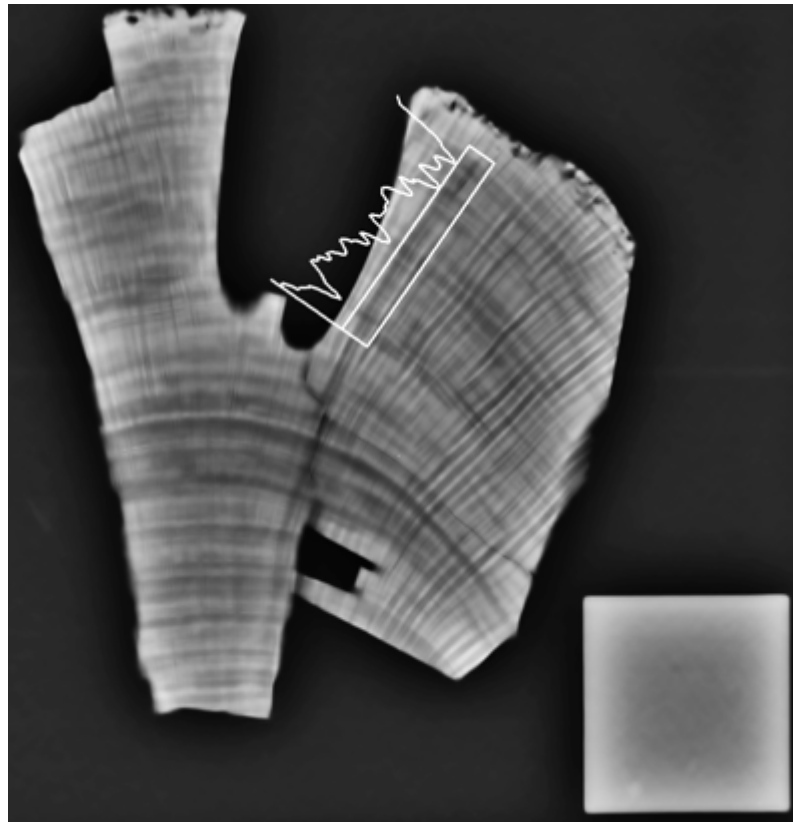
Appendix



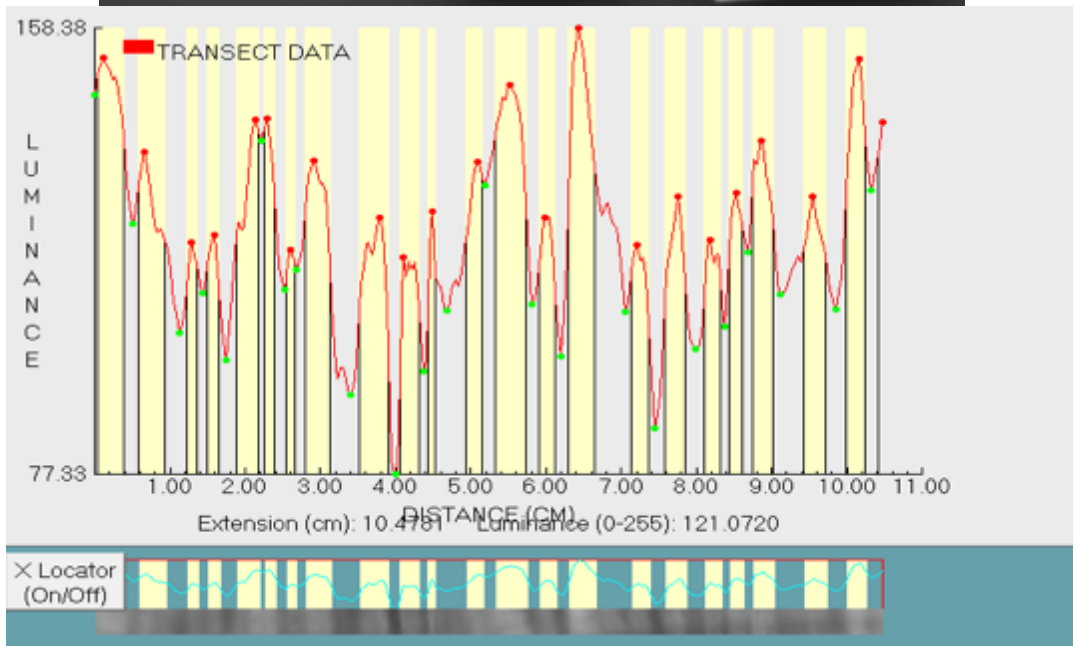
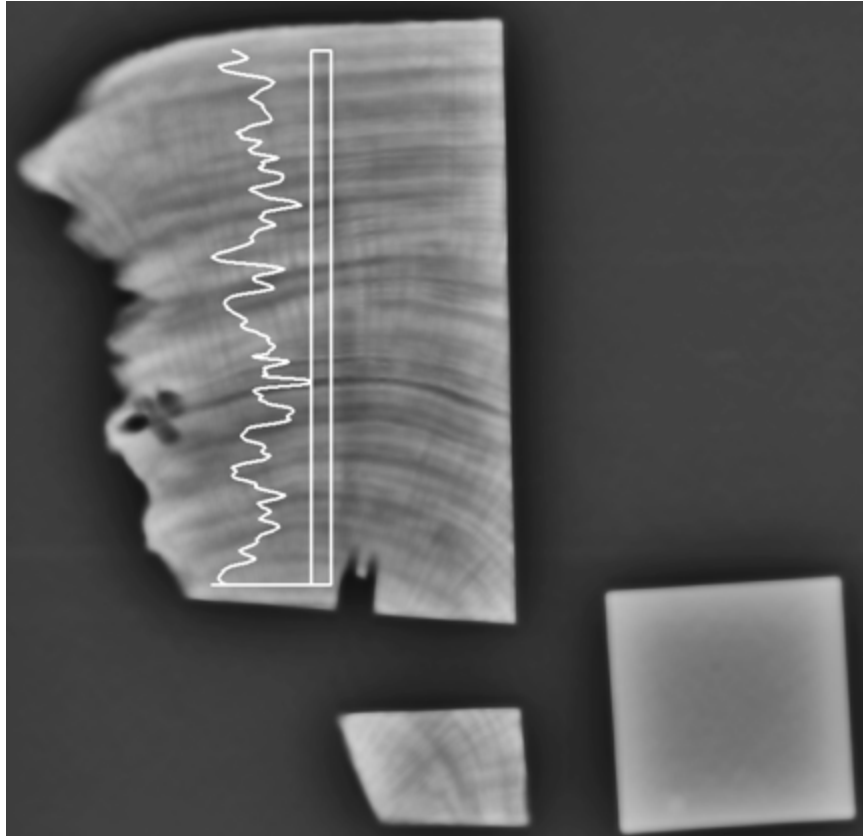
Appendix 1: Selected transect and densitometry analysis of sample MZ 148.8-3.3 part a.



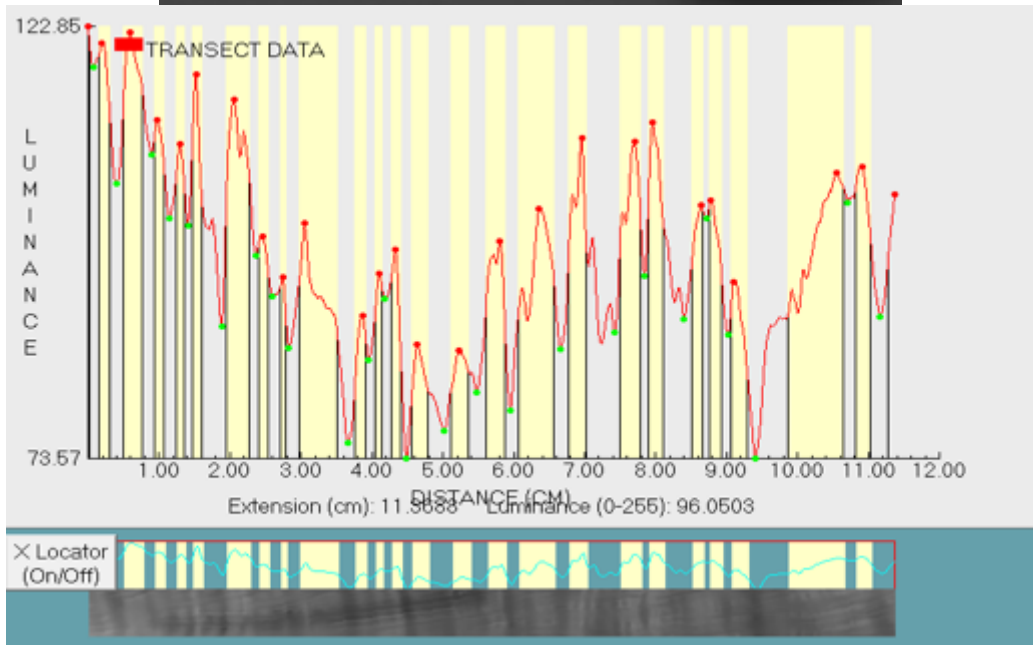
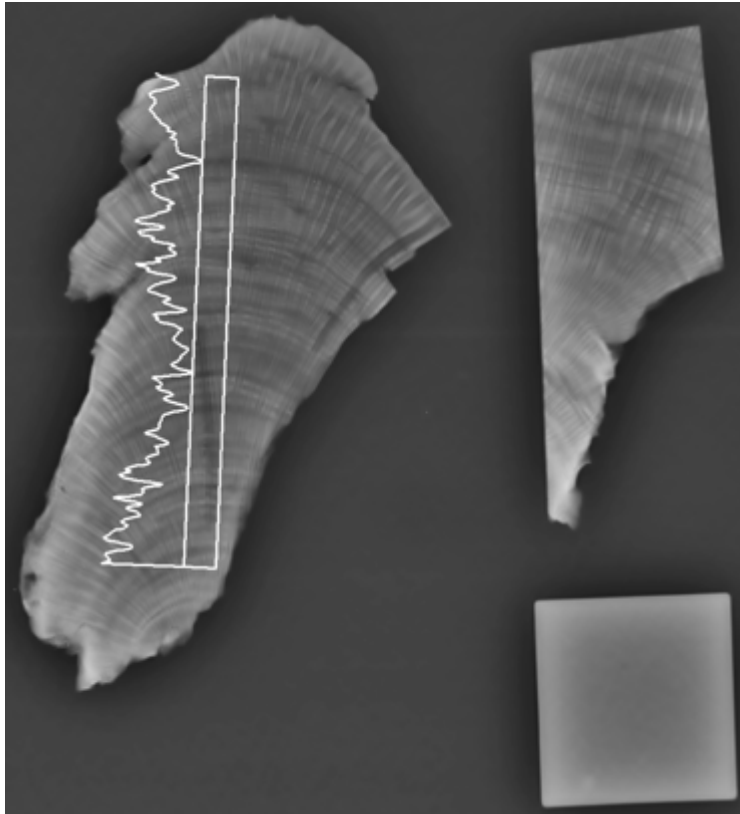
Appendix 2: Selected transect and densitometry analysis of sample MZ 148.8-3.3 part b.



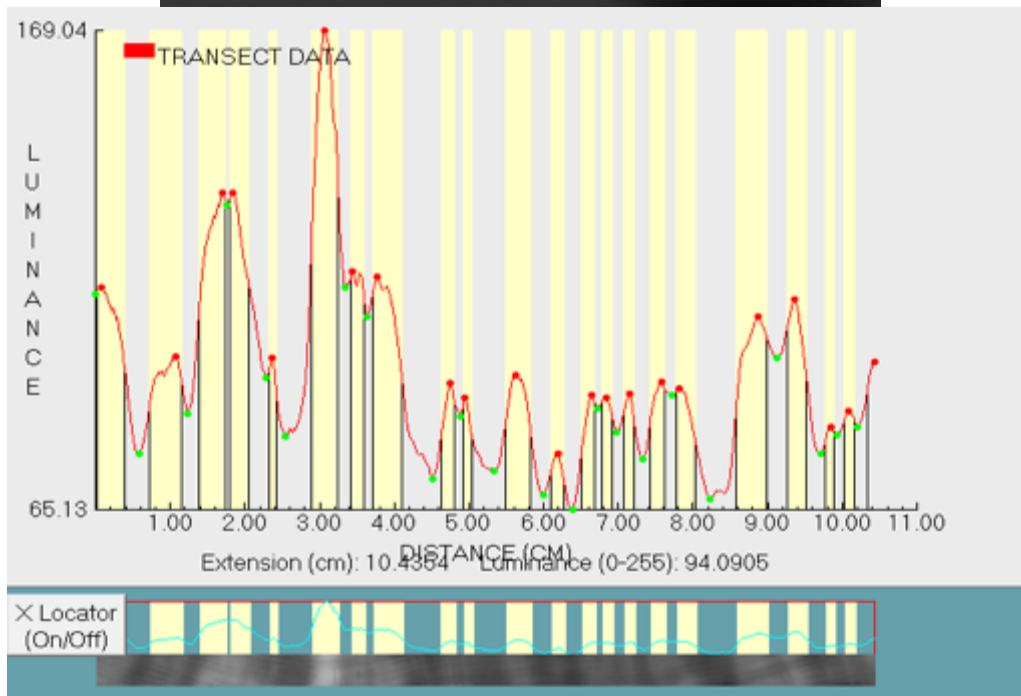
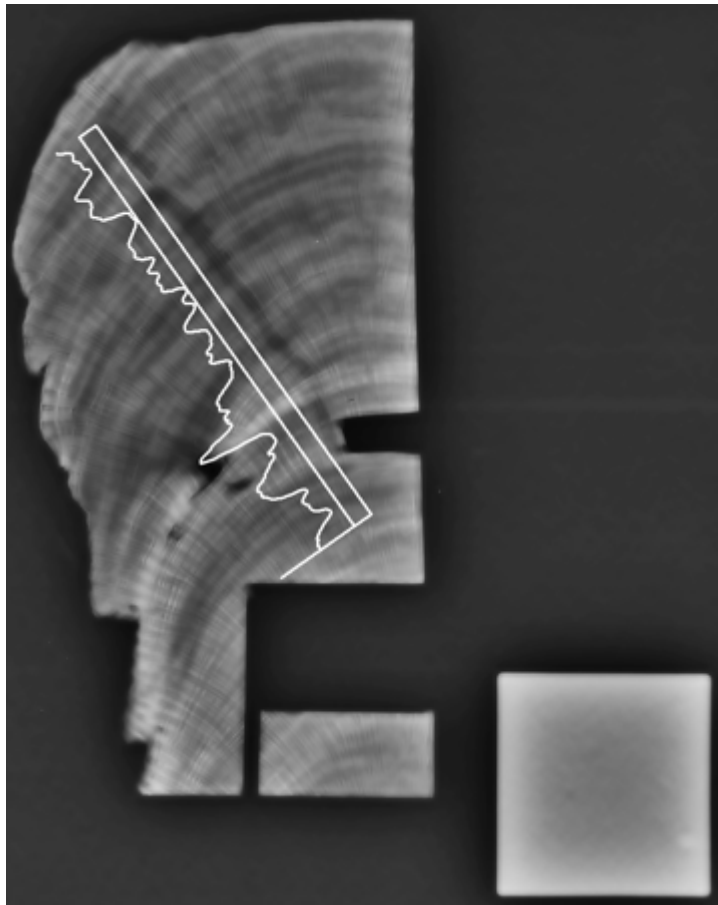
Appendix 3: Selected transect and densitometry analysis of sample MZ 148.8-3.3 part c.



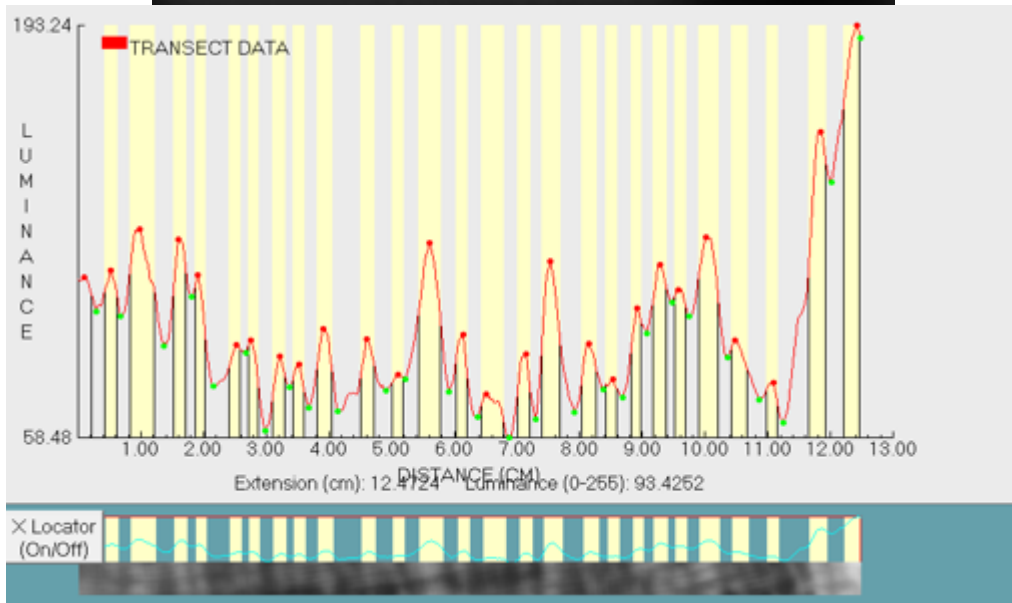
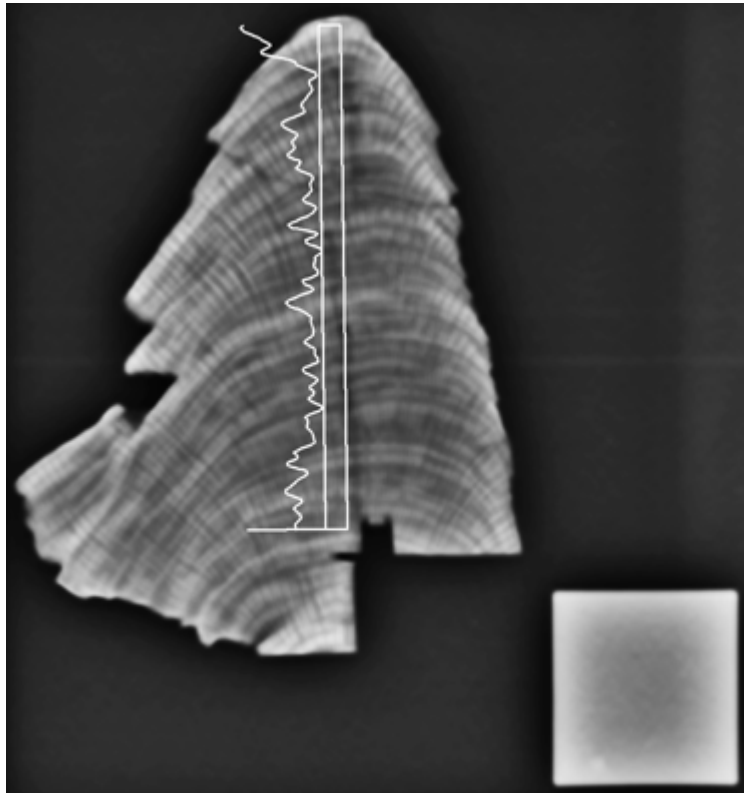
Appendix 4: Selected transect and densitometry analysis of sample MZ 165.9-0.3



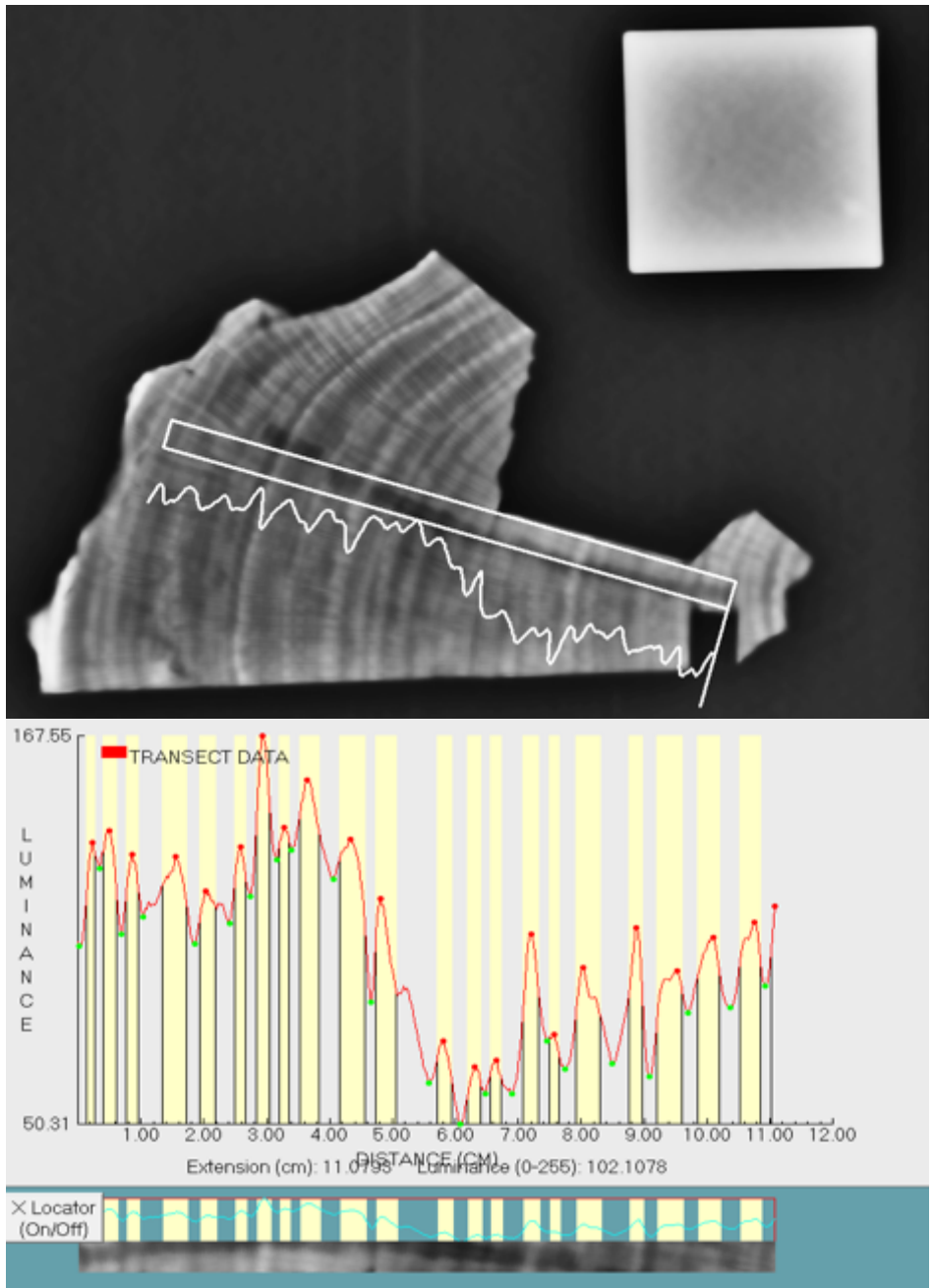
Appendix 5: Selected transect and densitometry analysis of sample MZ 154.7-2.3



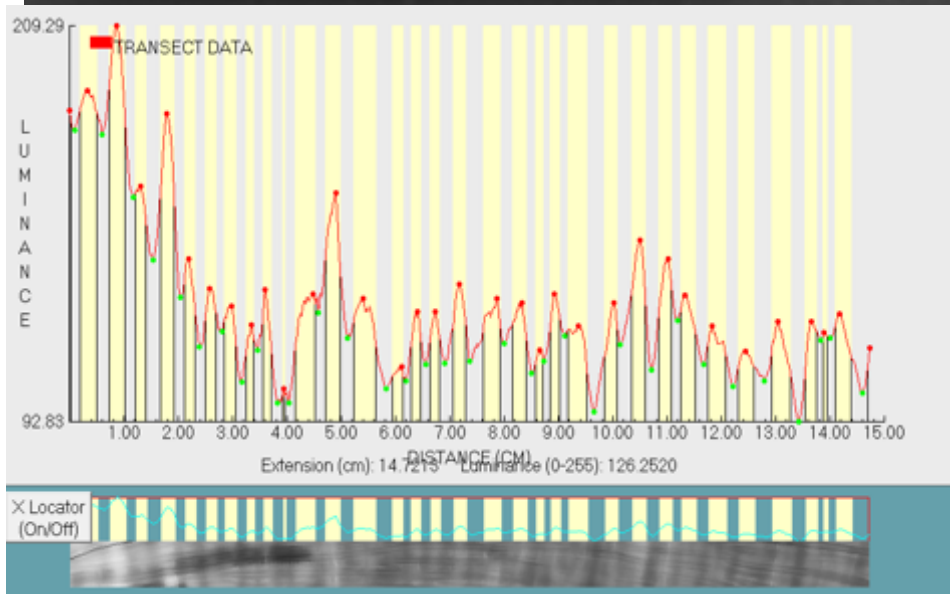
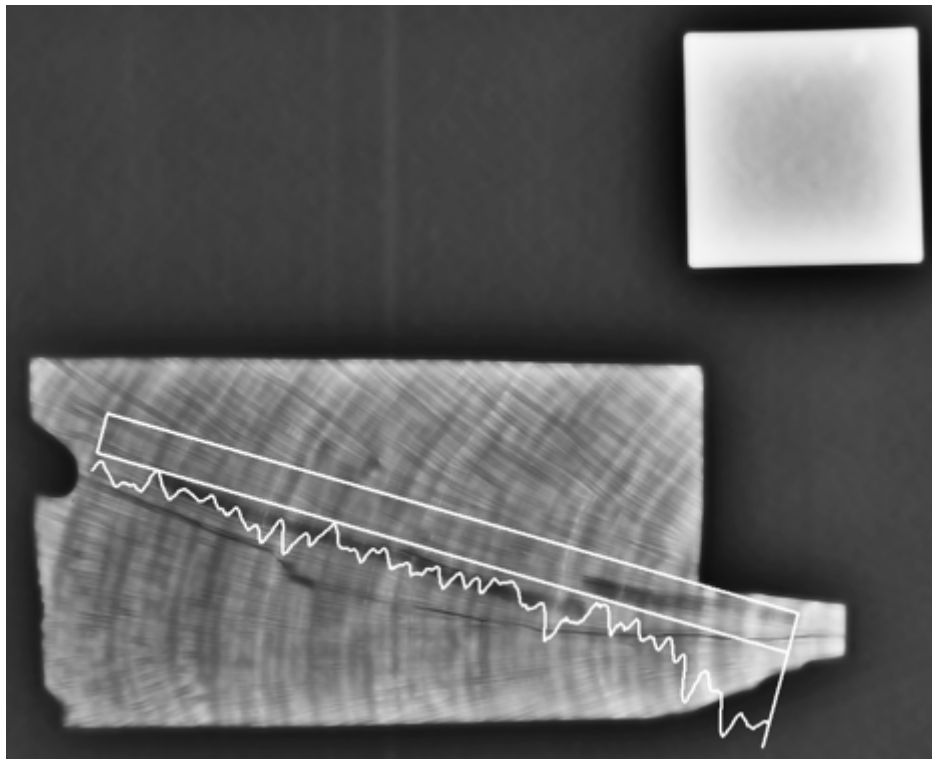
Appendix 6: Selected transect and densitometry analysis of sample MZ 198.4-0.9



Appendix 7: Selected transect and densitometry analysis of sample MZ 118.6-2.1

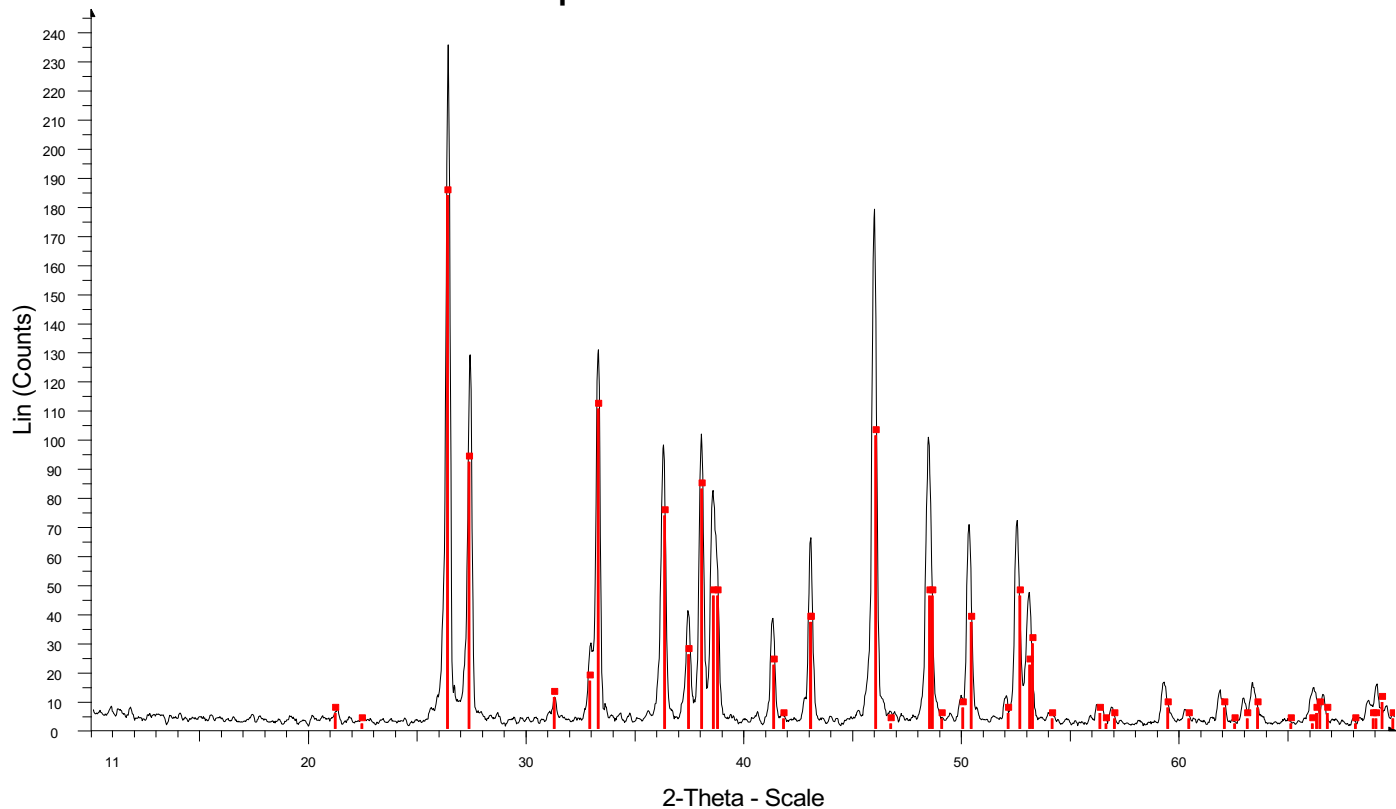


Appendix 8: Selected transect and densitometry analysis of sample MZ 164.1-1.2



Appendix 9: Selected transect and densitometry analysis of sample MZ 202.4-2.7

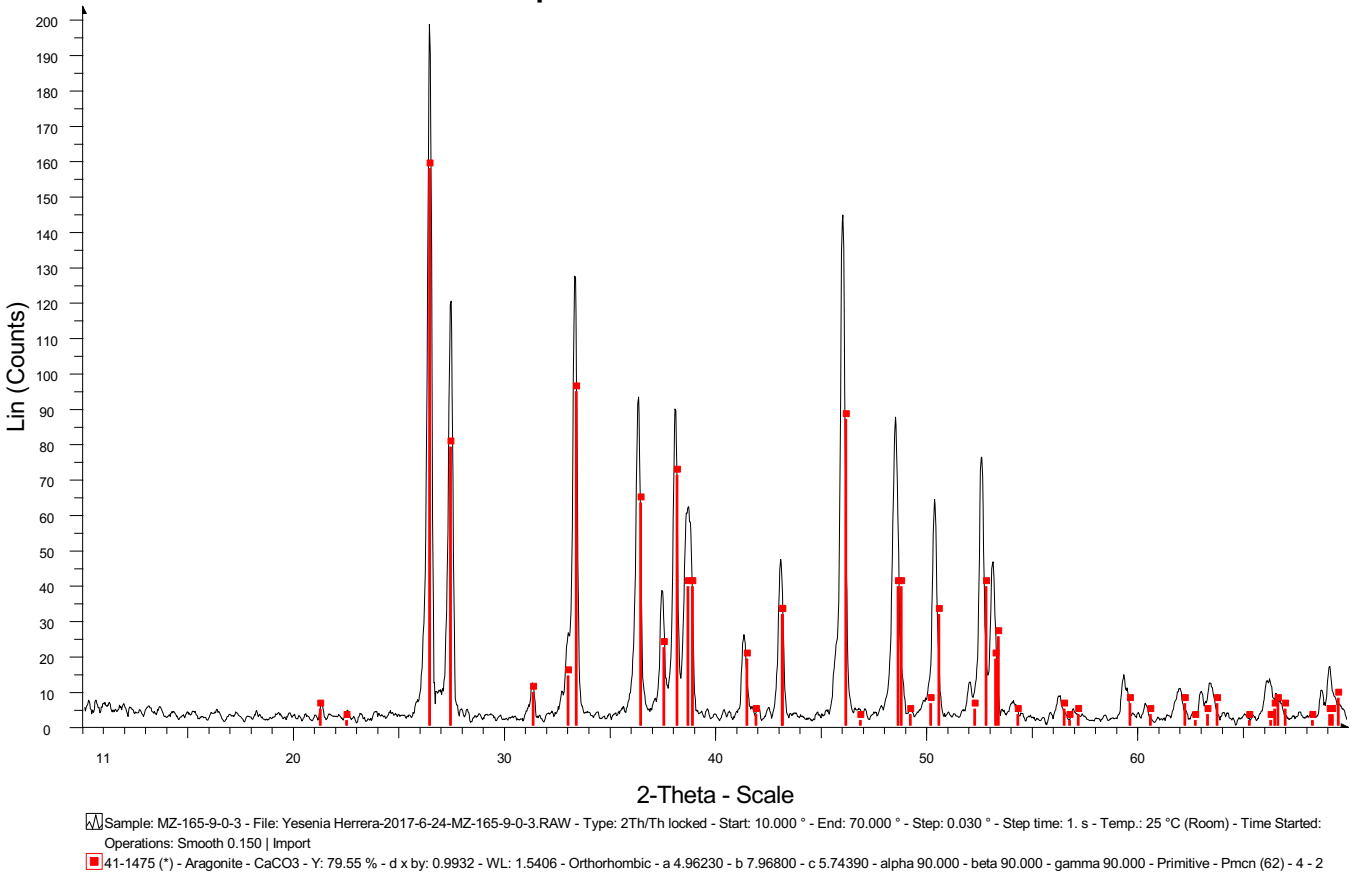
Sample: MZ-148-8-3-3



Sample: MZ-148-8-3-3 - File: Yesenia Herrera-2017-6-24-MZ-148-8-3-3.RAW - Type: 2Th/Th locked - Start: 10.000 ° - End: 70.000 ° - Step: 0.030 ° - Step time: 1. s - Temp.: 25 °C (Room) - Time Started: Operations: Smooth 0.150 | Import
41-1475 (*) - Aragonite - CaCO₃ - Y: 78.09 % - d x by: 0.9955 - WL: 1.5406 - Orthorhombic - a 4.96230 - b 7.96800 - c 5.74390 - alpha 90.000 - beta 90.000 - gamma 90.000 - Primitive - Pmcn (62) - 4 - 2

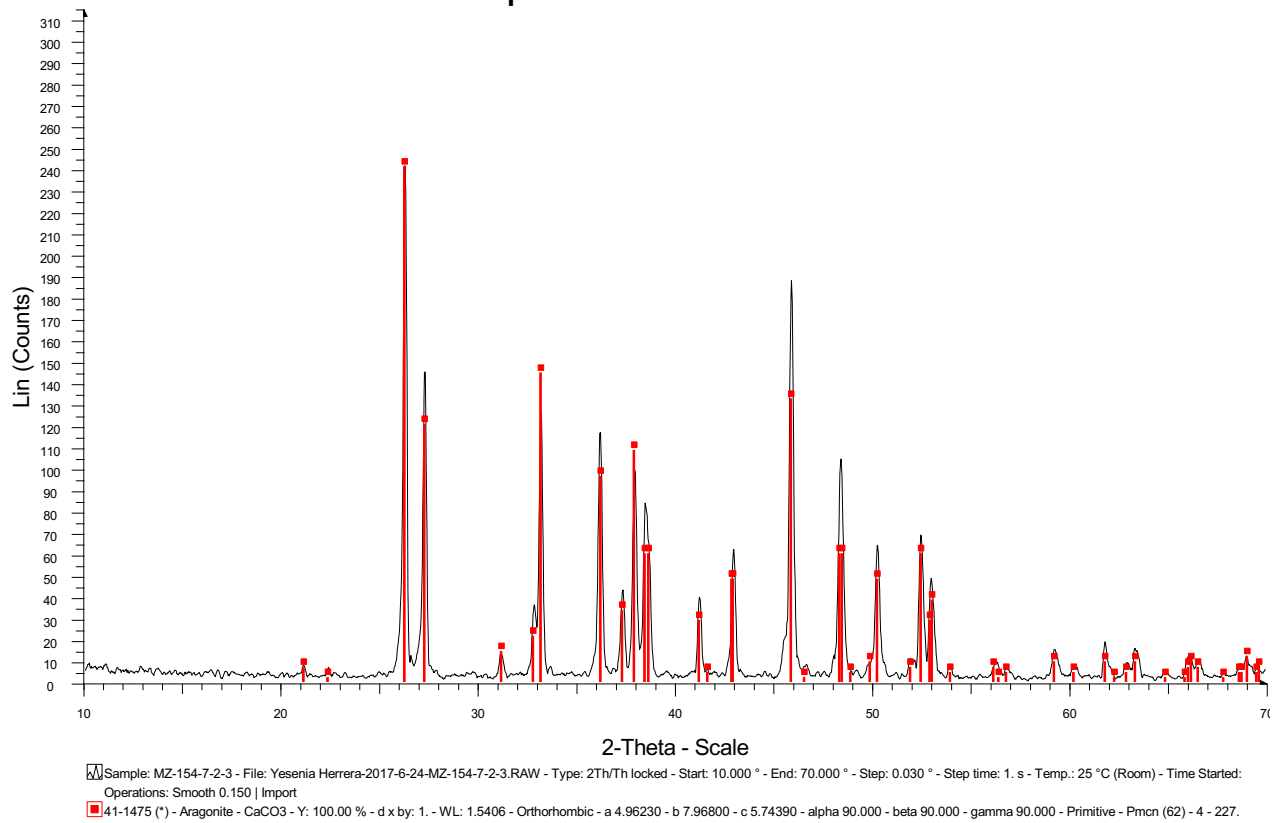
Appendix 10: XRD analysis for sample MZ 148.8-3.3.

Sample: MZ-165-9-0-3



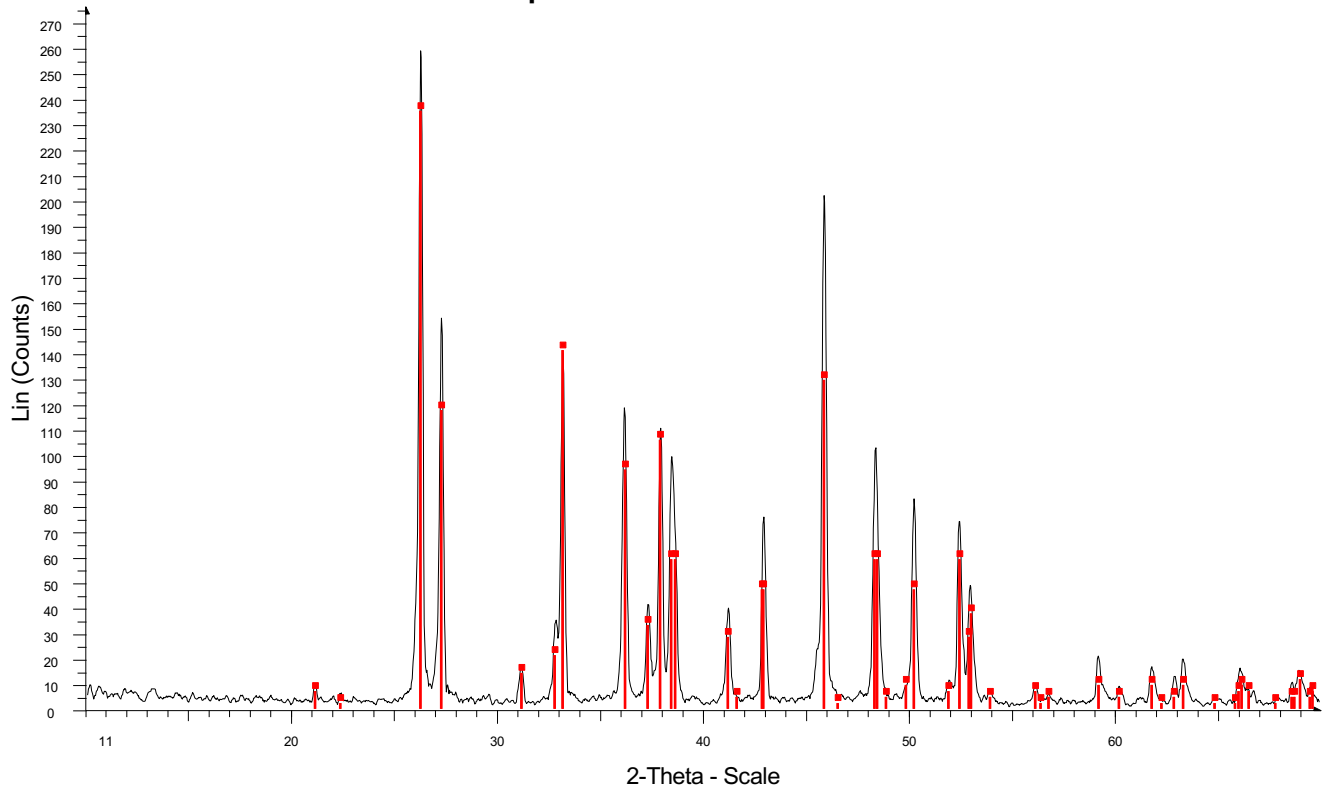
Appendix 11: XRD analysis for sample MZ 165.9-0.3

Sample: MZ-154-7-2-3



Appendix 12: XRD analysis for sample MZ 154.7-2.3

Sample: MZ-198-4-0-9

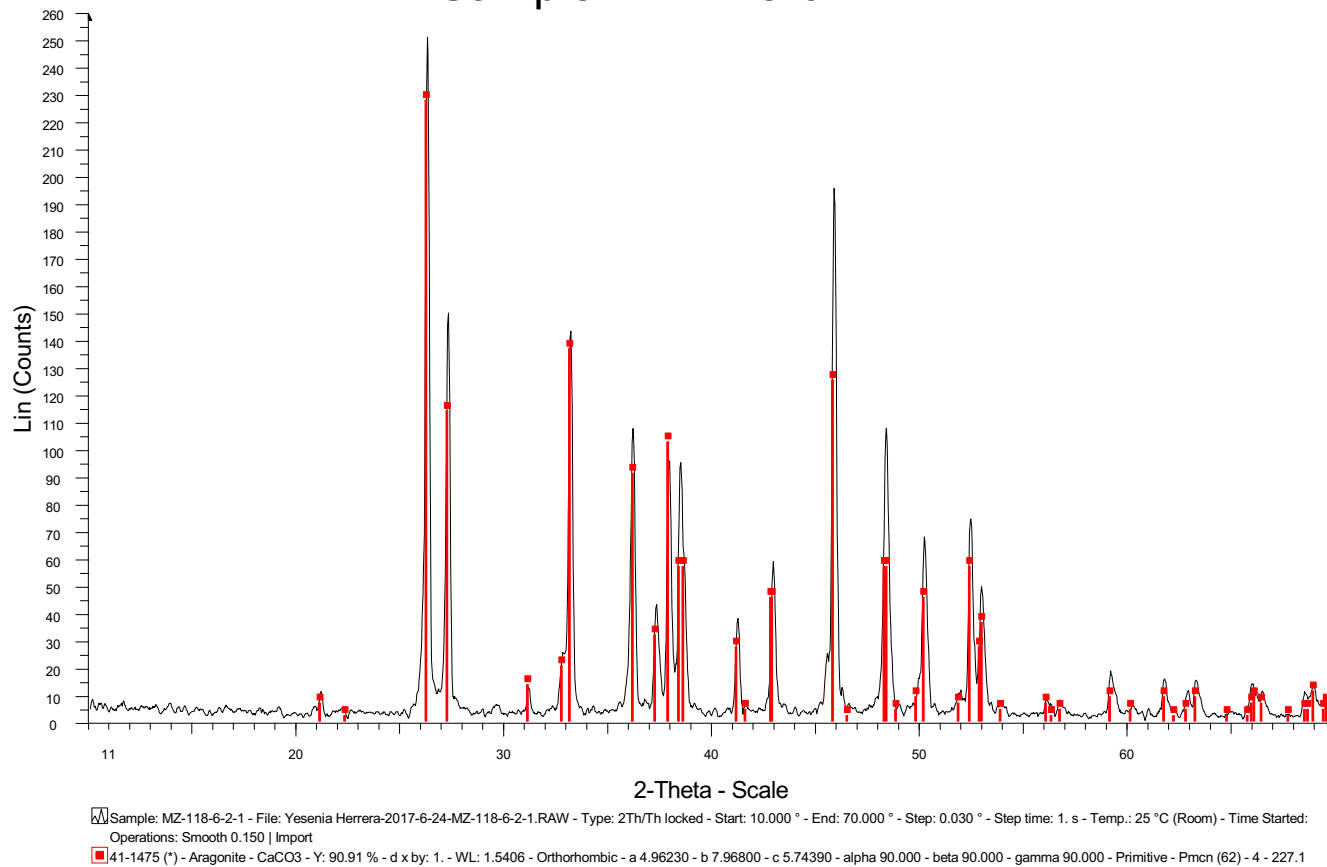


Sample: MZ-198-4-0-9 - File: Yesenia Herrera-2017-6-24-MZ-198-4-0-9.RAW - Type: 2Th/Th locked - Start: 10.000 ° - End: 70.000 ° - Step: 0.030 ° - Step time: 1. s - Temp.: 25 °C (Room) - Time Started: Operations: Smooth 0.150 | Import

41-1475 (*) - Aragonite - CaCO₃ - Y: 90.91 % - d x by: 1. - WL: 1.5406 - Orthorhombic - a 4.96230 - b 7.96800 - c 5.74390 - alpha 90.000 - beta 90.000 - gamma 90.000 - Primitive - Pmcn (62) - 4 - 227.1

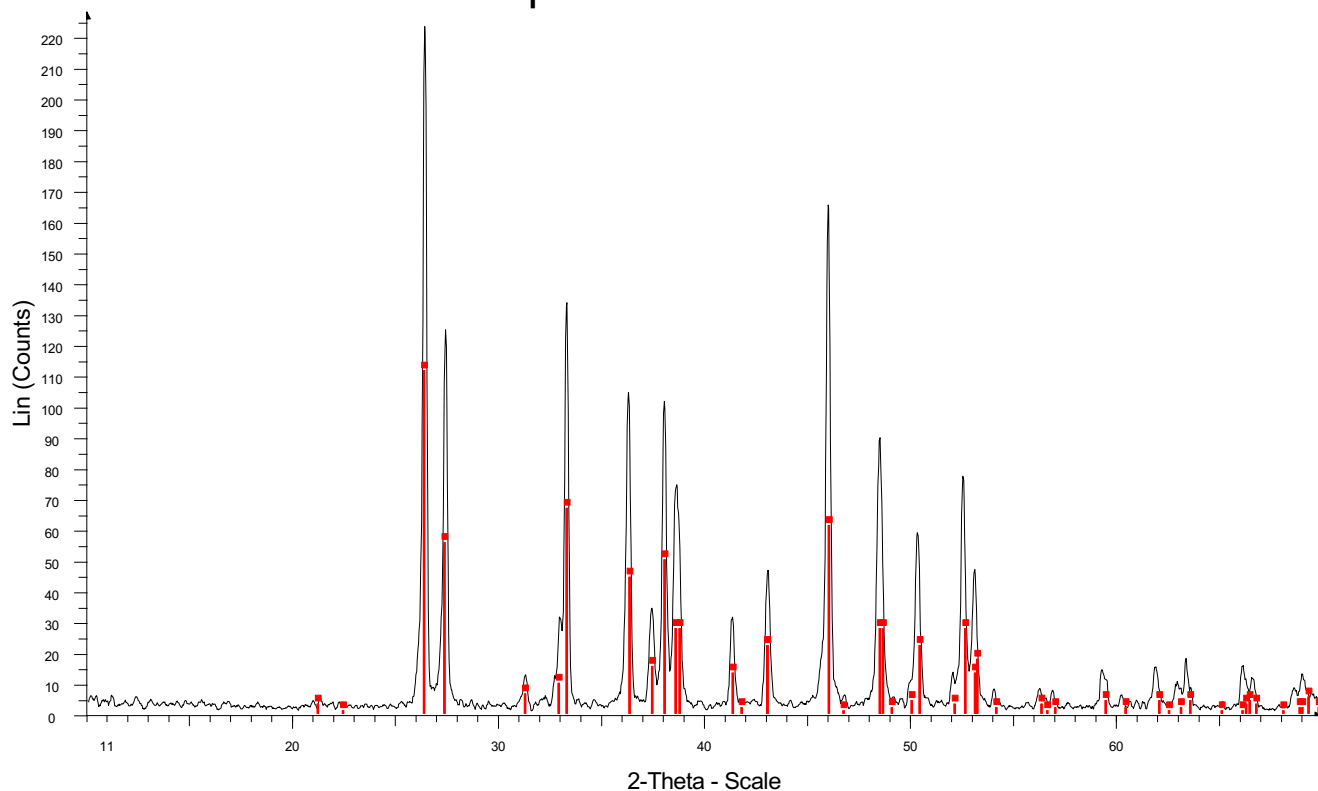
Appendix 13: XRD analysis for sample MZ 198.4-0.9

Sample: MZ-118-6-2-1



Appendix 14: XRD analysis for sample MZ 118.6-2.1

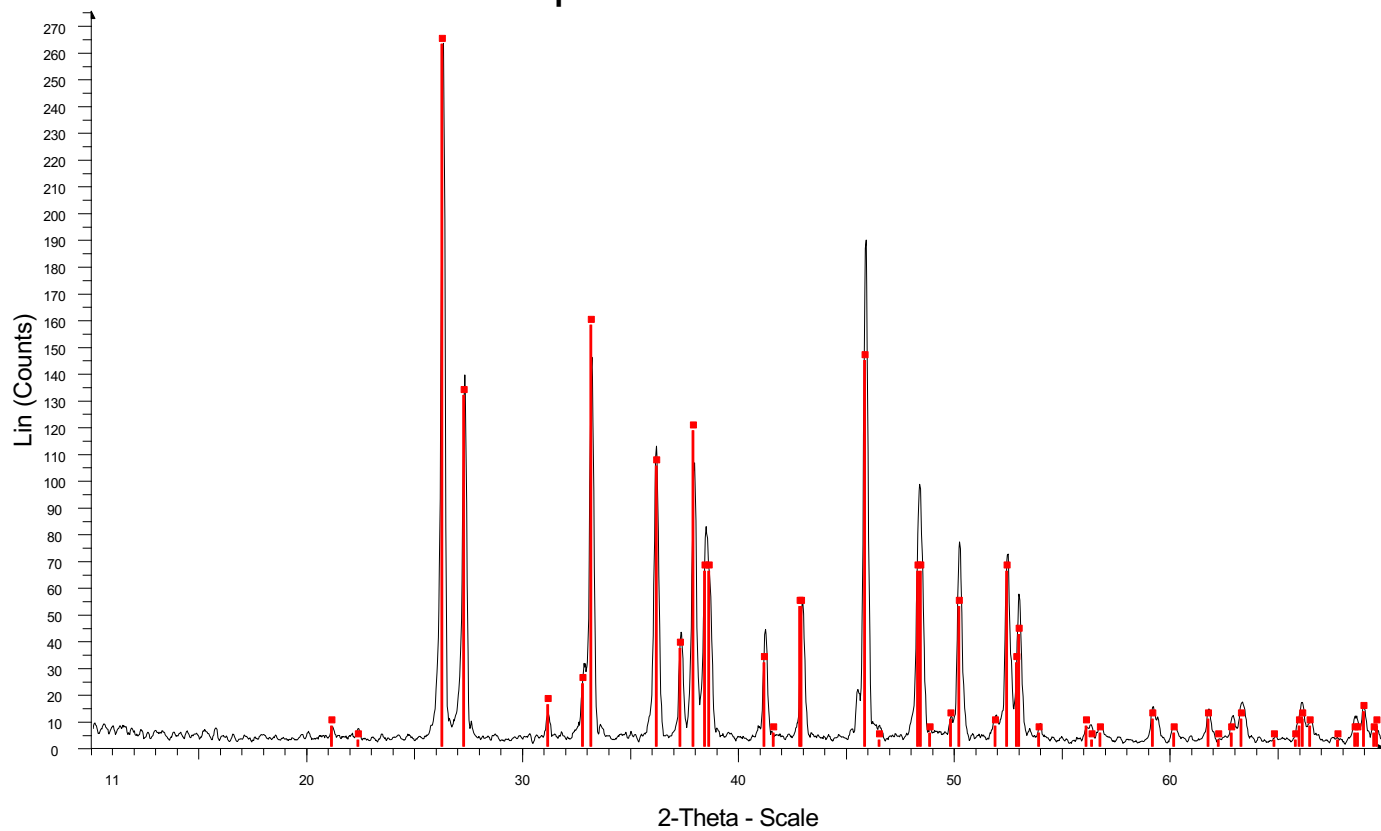
Sample: MZ-164-1-1-2



Sample: MZ-164-1-1-2 - File: Yesenia Herrera-2017-6-24-MZ-164-1-1-2.RAW - Type: 2Th/Th locked - Start: 10.000 ° - End: 70.000 ° - Step: 0.030 ° - Step time: 1. s - Temp.: 25 °C (Room) - Time Started:
Operations: Smooth 0.150 | Import
41-1475 (*) - Aragonite - CaCO₃ - Y: 50.00 % - d x by: 0.9955 - WL: 1.5406 - Orthorhombic - a 4.96230 - b 7.96800 - c 5.74390 - alpha 90.000 - beta 90.000 - gamma 90.000 - Primitive - Pmcn (62) - 4 - 2

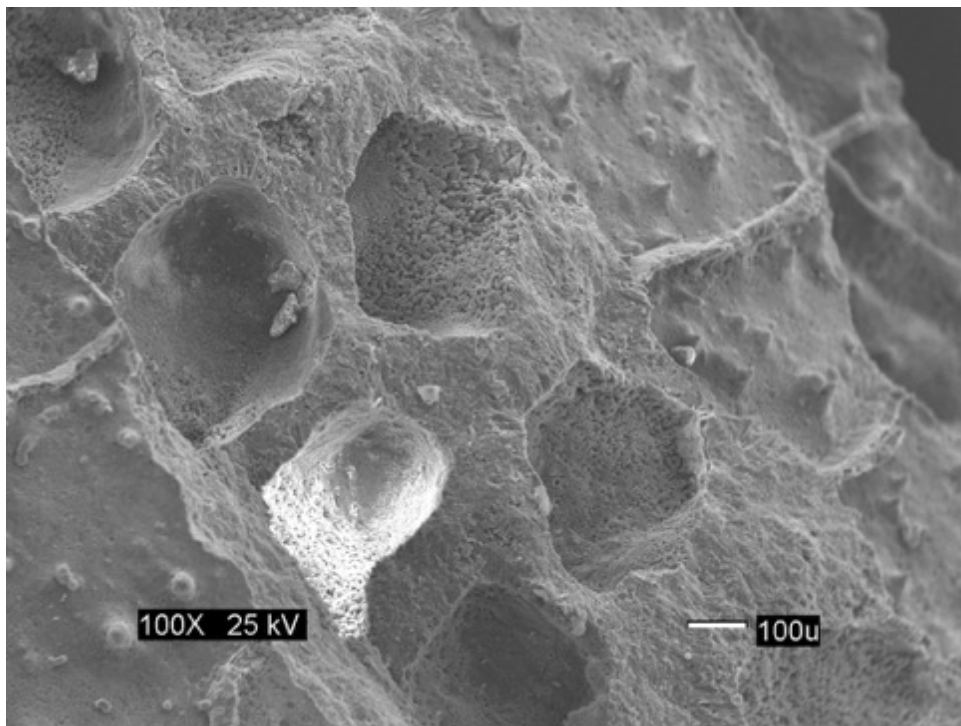
Appendix 15: XRD analysis for sample MZ 164.1-1.2

Sample: MZ-202-4-2-7

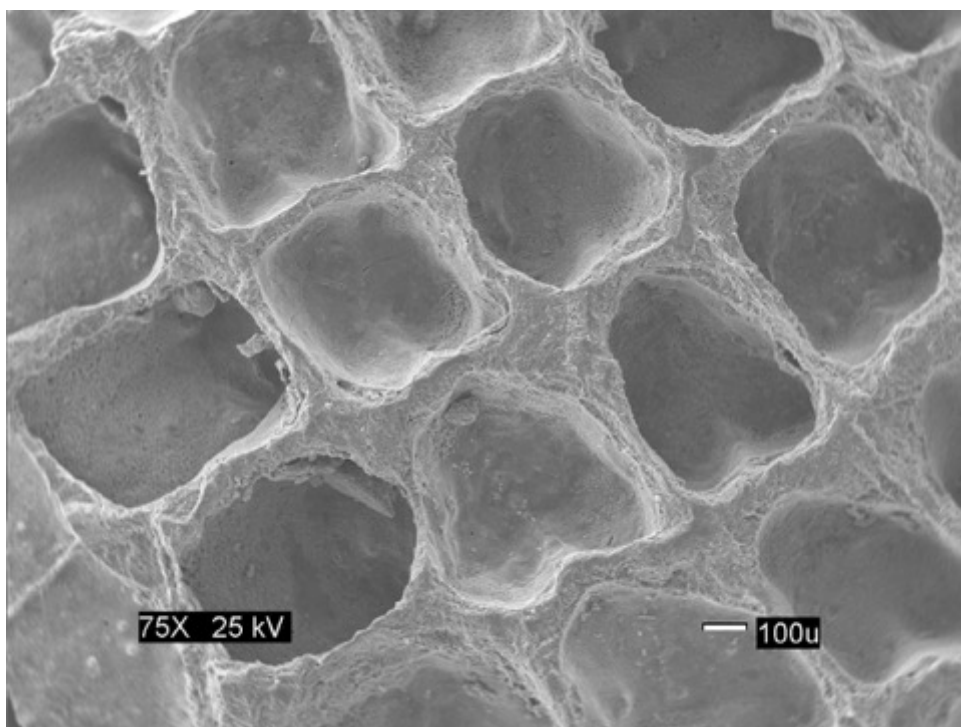


Sample: MZ-202-4-2-7 - File: Yesenia Herrera-2017-6-24-MZ-202-4-2-7.RAW - Type: 2Th/Th locked - Start: 10.000 ° - End: 70.000 ° - Step: 0.030 ° - Step time: 1. s - Temp.: 25 °C (Room) - Time Started:
Operations: Smooth 0.150 | Import
41-1475 (*) - Aragonite - CaCO₃ - Y: 100.00 % - d x by: 1. - WL: 1.5406 - Orthorhombic - a 4.96230 - b 7.96800 - c 5.74390 - alpha 90.000 - beta 90.000 - gamma 90.000 - Primitive - Pmcn (62) - 4 - 227.

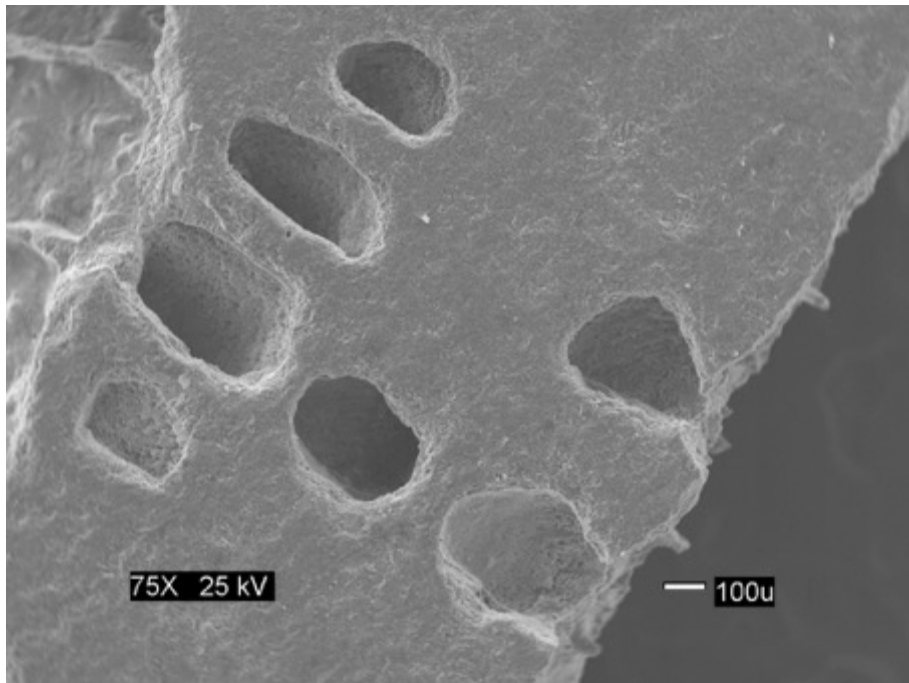
Appendix 16: XRD analysis for sample MZ 202.4-2.7



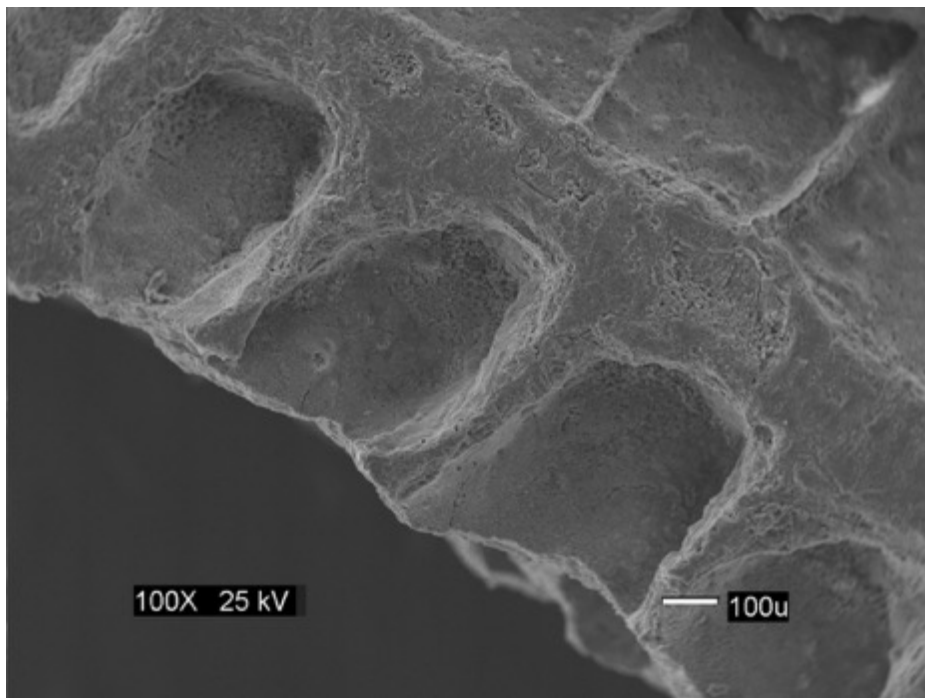
Appendix 17: SEM analysis for sample MZ 148.8-3.3



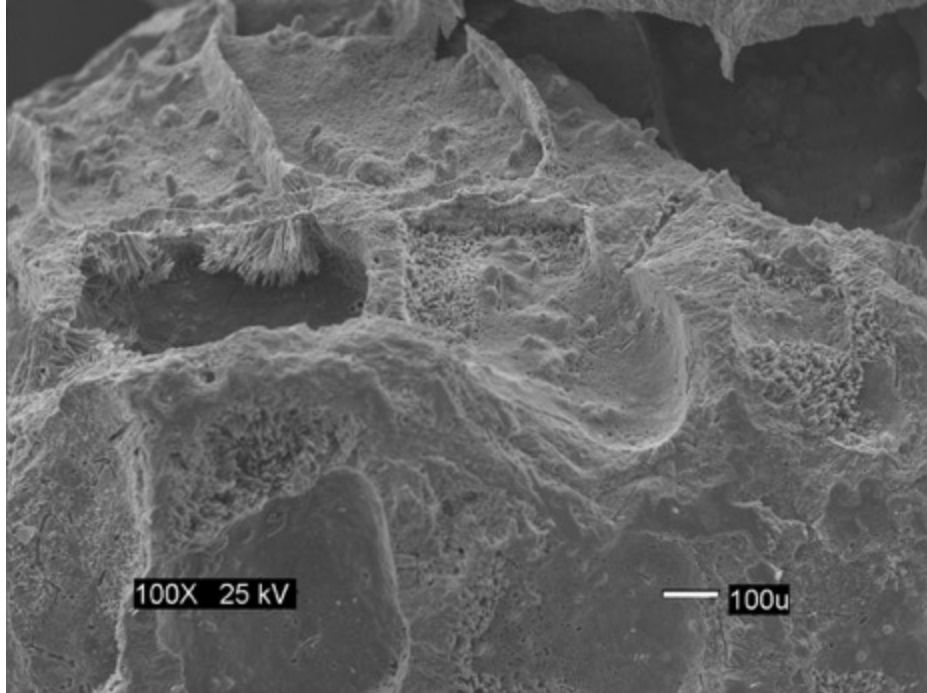
Appendix 18: SEM analysis for sample MZ 165.9-0.3



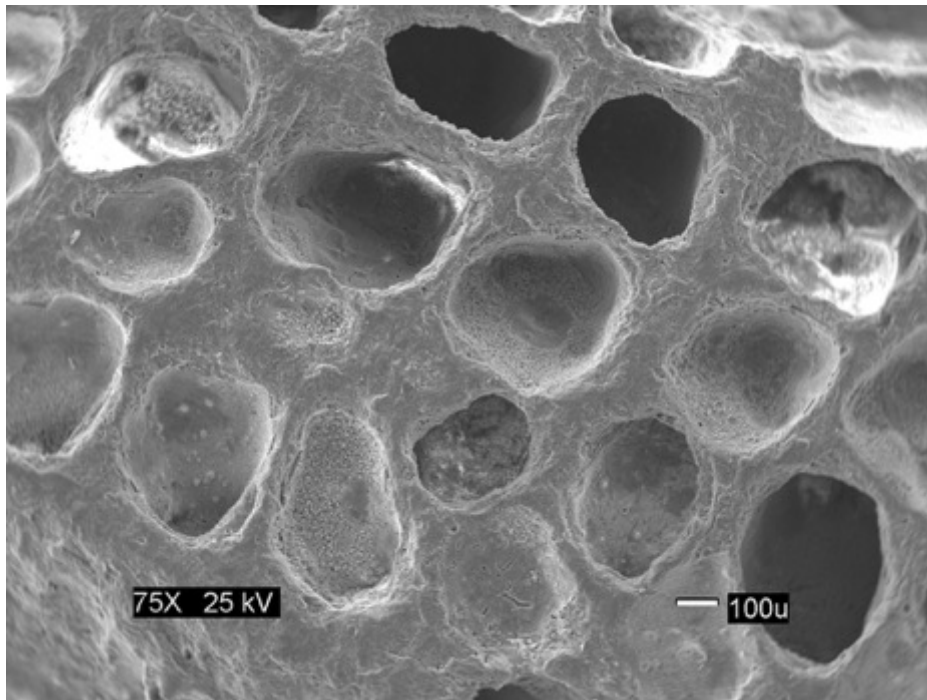
Appendix 19: SEM analysis for sample MZ 154.7-2.3



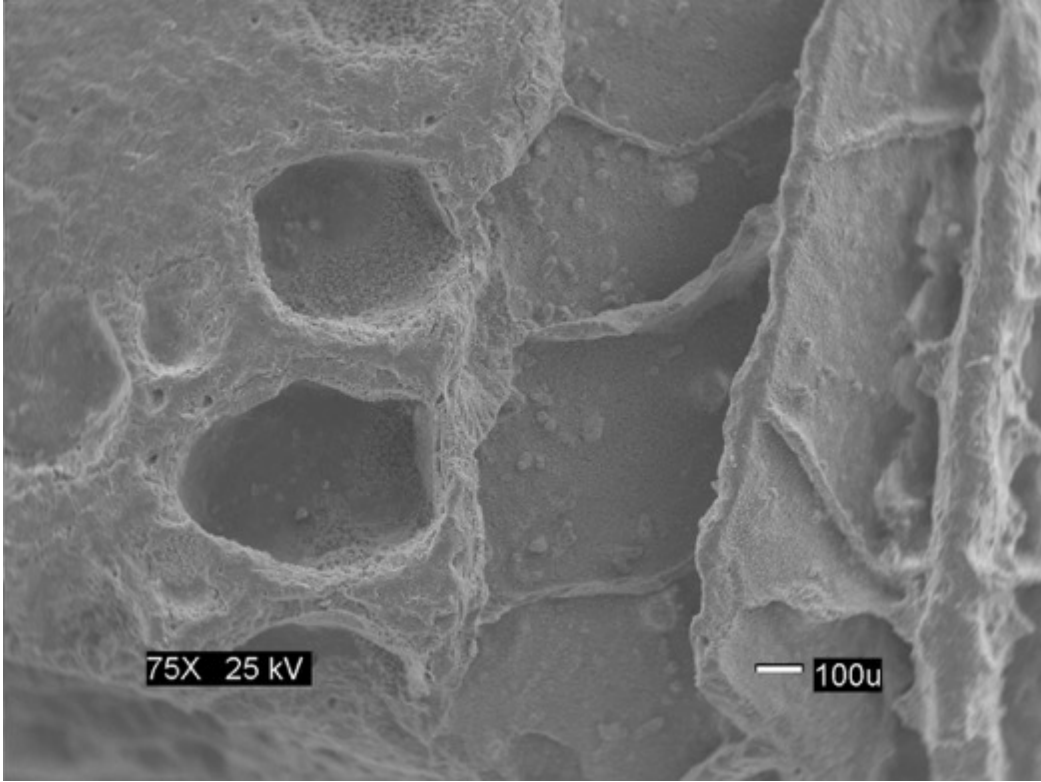
Appendix 20: SEM analysis for sample MZ 198.4-0.9



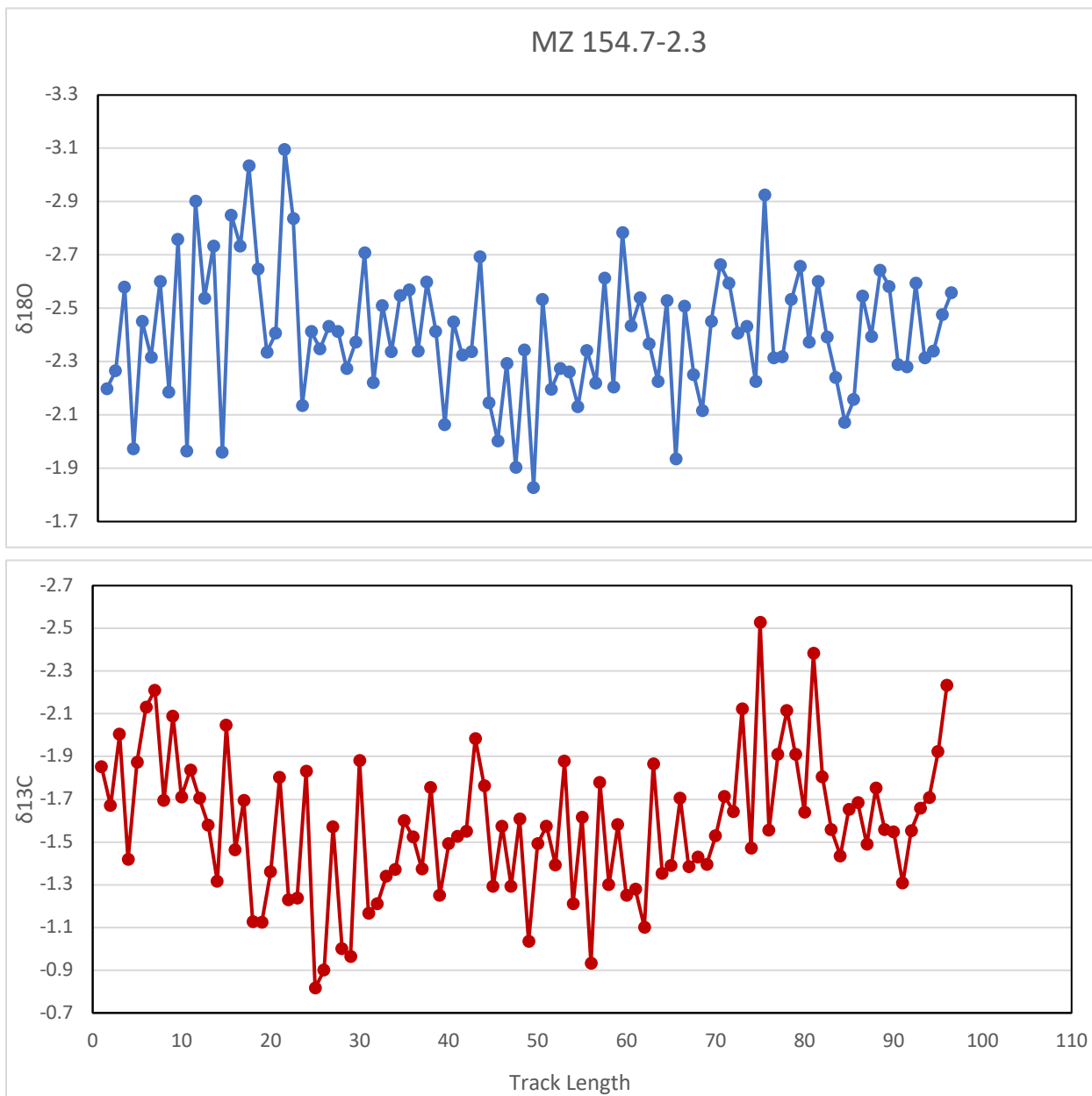
Appendix 21: SEM analysis for sample MZ 118.6-2.1



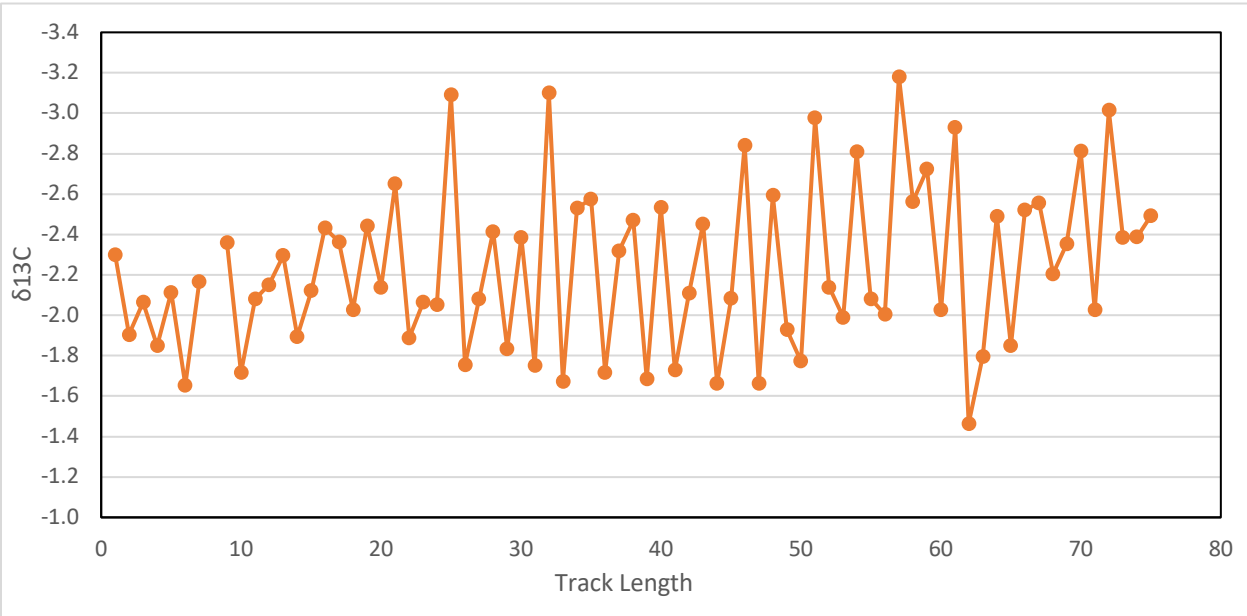
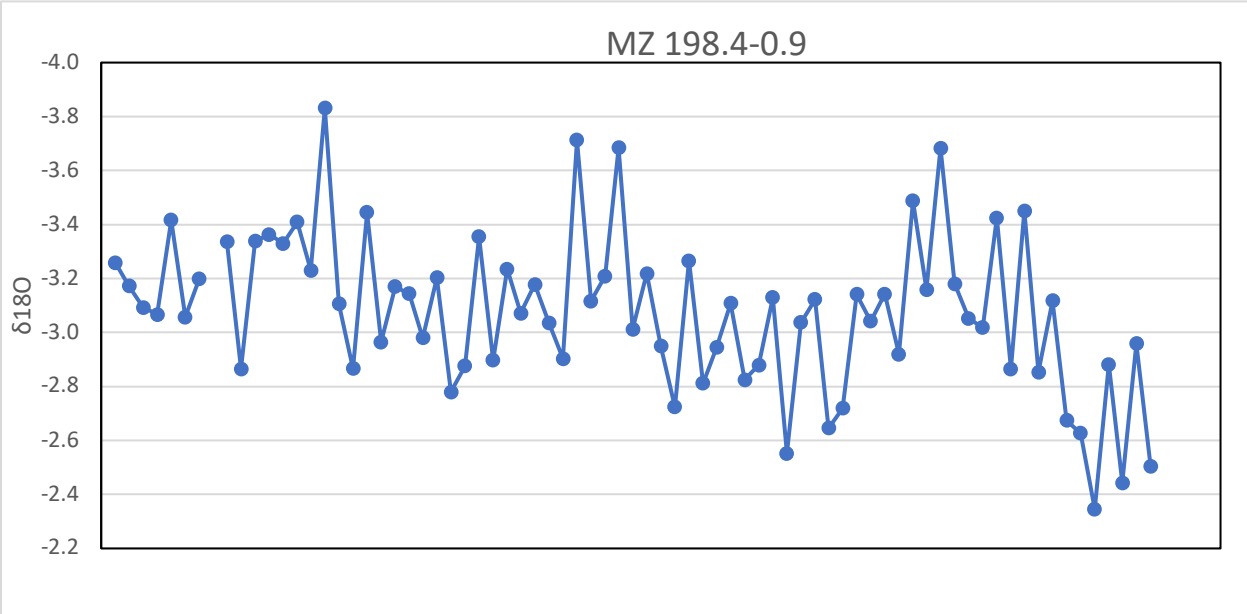
Appendix 22: SEM analysis for sample MZ 164.1-1.2



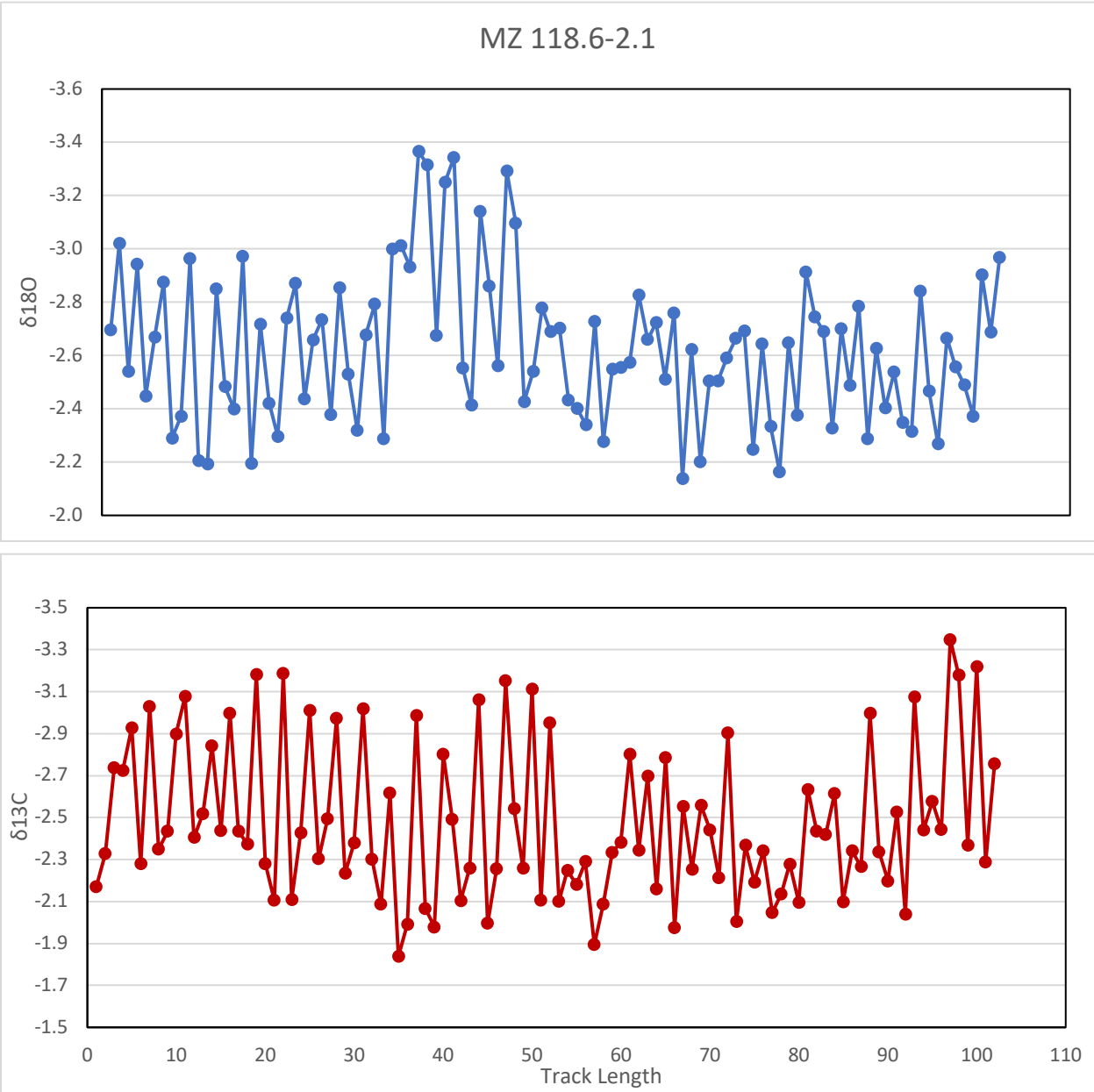
Appendix 23: SEM analysis for sample MZ 202.4-2.7



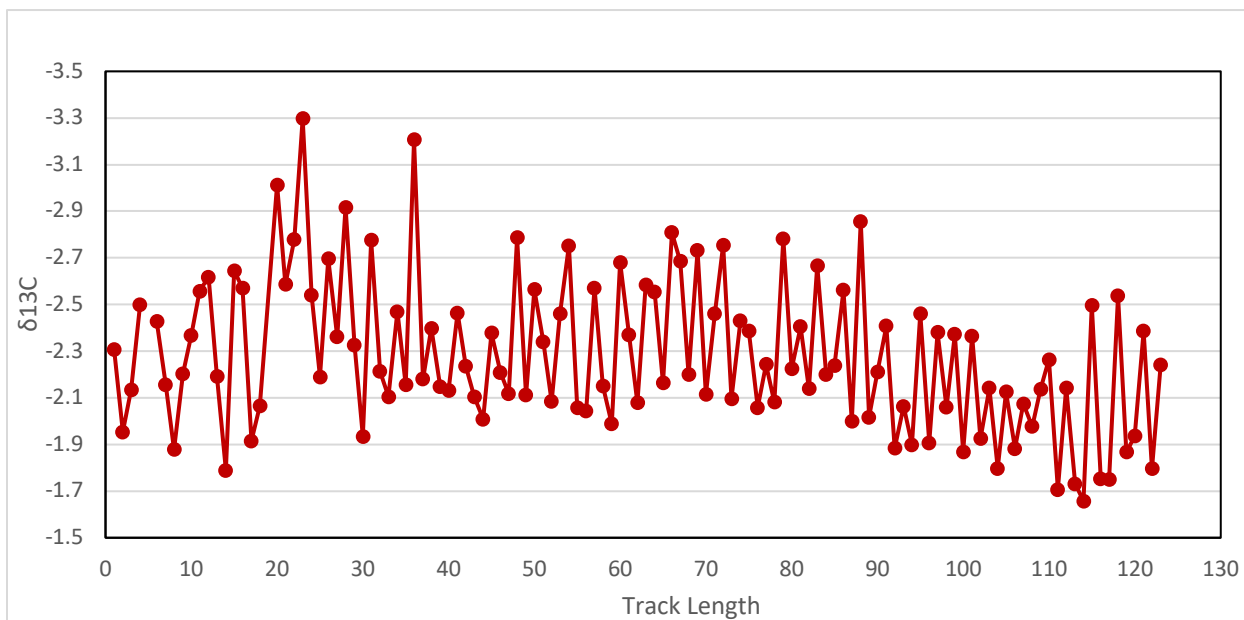
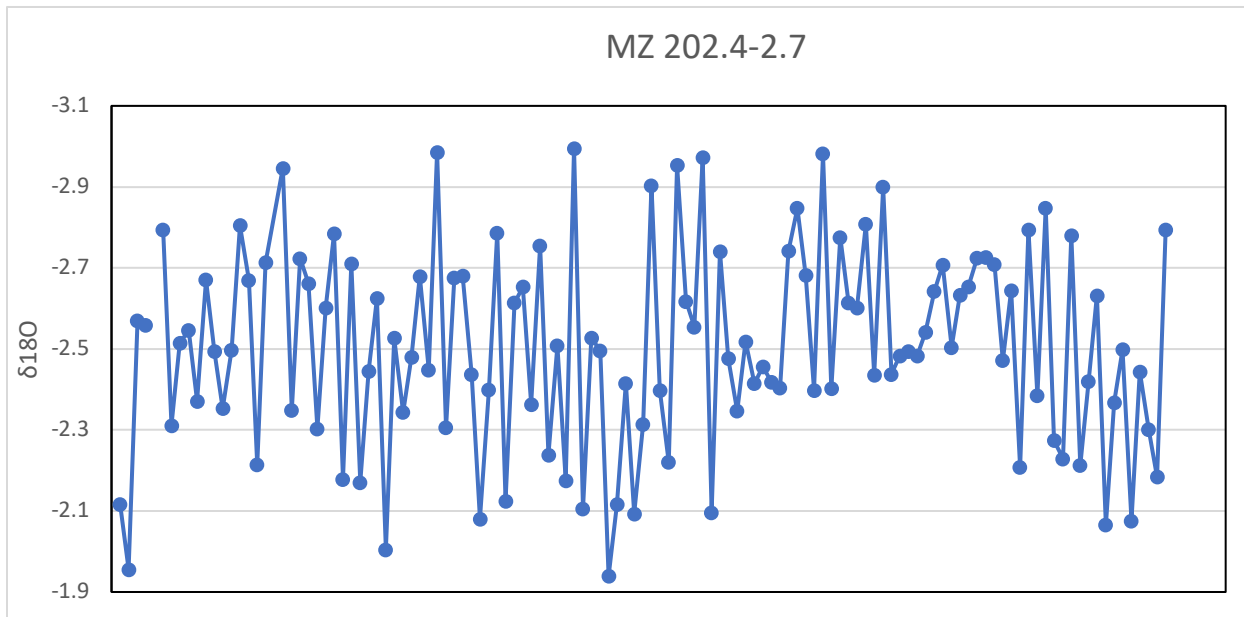
Appendix 24: $\delta^{18}\text{O}$ and $\delta^{13}\text{C}$ plot for MZ 154.7-2.3



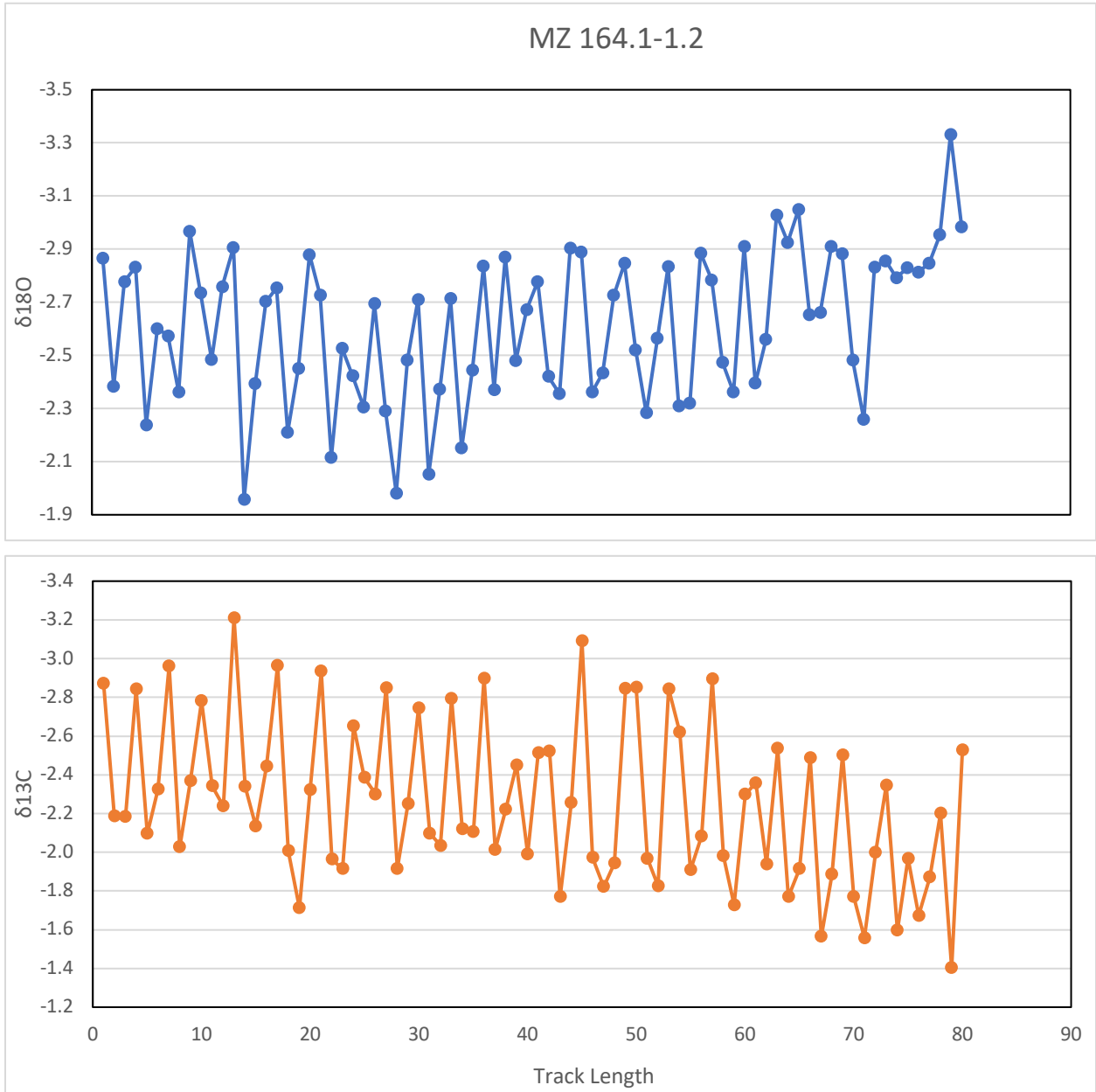
Appendix 25: $\delta^{18}\text{O}$ and $\delta^{13}\text{C}$ plot for MZ 198.4-0.9



Appendix 26: $\delta^{18}\text{O}$ and $\delta^{13}\text{C}$ plot for MZ 118.6-2.1



Appendix 27: $\delta^{18}\text{O}$ and $\delta^{13}\text{C}$ plot for MZ 202.4-2.7



Appendix 28: $\delta^{18}\text{O}$ and $\delta^{13}\text{C}$ plot for MZ 164.1-1.2

Appendix 29: Sr/Ca-SST for fossil coral MZ 165.9-0.3 using the four equations

Equation 4 Swart et al., 2002	Equation 5 Smith, 2006	Equation 6 Flannery et al., 2013	Equation 7 Jimenez, 2018
16.86781493	20.9742583	21.28760416	20.94932075
17.13324607	21.4175848	21.60652781	21.13425873
14.0248148	16.2258432	17.87165247	18.96847303
14.82507036	17.5624402	18.83318403	19.52604754
14.39031476	16.8363059	18.31081186	19.22313351
15.88549943	19.3335824	20.10732202	20.26489679
16.40901675	20.2079677	20.73634411	20.62965516
19.88894068	26.0201811	24.91757923	23.05427672
16.99676096	21.1896256	21.44253676	21.03916333
15.59169614	18.8428684	19.75430837	20.06019065
13.64640752	15.5938225	17.41698454	18.70481944
16.16310068	19.7972355	20.44086842	20.45831423
14.01542565	16.2101613	17.86037112	18.96193118
14.14483563	16.4263035	18.01586117	19.05209701
15.36041718	18.4565833	19.47641962	19.89904806

Appendix 30: Sr/Ca-SST for fossil coral MZ 148.8-3.3 using the four equations

Equation 4 Swart et al., 2002	Equation 5 Smith, 2006	Equation 6 Flannery et al., 2013	Equation 7 Jimenez, 2018
18.887148	24.3469742	23.7138947	22.3562821
21.2928376	28.3649876	26.6044044	24.0324357
18.1942646	23.1897114	22.881374	21.8735187
16.1310469	19.7436989	20.4023549	20.4359809
17.2260494	21.572586	21.7180338	21.198919
18.7706342	24.1523714	23.5738998	22.2751017
17.725118	22.4061369	22.3176801	21.5466429
18.6693135	23.9831443	23.4521599	22.2045069
16.0952953	19.6839861	20.3593982	20.4110711
18.9107474	24.3863901	23.74225	22.3727249
16.2197176	19.8917979	20.5088954	20.4977618
20.1721464	26.4931948	25.2578595	23.251599
15.3507309	18.4404052	19.4647813	19.8922992
16.7465913	20.7717891	21.1419503	20.8648588

Appendix 31: Residual variations for fossil coral MZ 165.9-0.3 and MZ 148.8-3.3

MZ 165.9-0.3	MZ 148.8-3.3
1.36752818	1.43394153
0.78998925	1.44669056
1.00750712	1.60988918
0.49727406	0.64866882
1.10140646	0.31560856
0.24682403	1.46007975
0.93511088	1.64390522
0.44276083	1.11347189
0.80029511	1.64962814
-0.1766114	0.84334671
0.68994003	0.78195714
0.07525873	2.0744694
0.81656595	0.4565142
0.30430028	1.64324305
1.03976379	